DETAILED STUDY OF SELECTED NATURAL TERRAIN LANDSLIDES AT CLOUDY HILL

GEO REPORT No. 207

HALCROW CHINA LIMITED

GEOTECHNICAL ENGINEERING OFFICE
CIVIL ENGINEERING AND DEVELOPMENT DEPARTMENT
THE GOVERNMENT OF THE HONG KONG
SPECIAL ADMINISTRATIVE REGION

DETAILED STUDY OF SELECTED NATURAL TERRAIN LANDSLIDES AT CLOUDY HILL

GEO REPORT No. 207

HALCROW CHINA LIMITED

First published, June 2007

Prepared by:

Geotechnical Engineering Office,
Civil Engineering and Development Department,
Civil Engineering and Development Building,
101 Princess Margaret Road,
Homantin, Kowloon,
Hong Kong.

Table of Contents

Table of Contents

Table of Contents

Table of Contents

PREFACE

In keeping with our policy of releasing information which may be of general interest to the geotechnical profession and the public, we make available selected internal reports in a series of publications termed the GEO Report series. The GEO Reports can be downloaded from the website of the Civil Engineering and Development Department (http://www.cedd.gov.hk) on the Internet. Printed copies are also available for some GEO Reports. For printed copies, a charge is made to cover the cost of printing.

The Geotechnical Engineering Office also produces documents specifically for publication. These include guidance documents and results of comprehensive reviews. These publications and the printed GEO Reports may be obtained from the Government's Information Services Department. Information on how to purchase these documents is given on the second last page of this report.

R.K.S. Chan
Head, Geotechnical Engineering Office
June 2007

FOREWORD

This report presents the findings of a detailed study of a cluster of over 45 natural terrain landslides that occurred in April 2000 and June 2001 in the vicinity of Cloudy Hill, Tai Po. The incidents ranged in volume from about 12 m^3 to 630 m^3 and consisted of debris slides, debris avalanches and debris flows, about 85 % of which became channelised. A high concentration of relict landslides was also identified in the Study Area.

The key objectives of the detailed study were to assess the characteristics of the landslides, mechanisms of failure and mobility of the debris following systematic collection of data. This was achieved through API study combined with engineering geological and regolith mapping and detailed inspection of selected landslides. The data have been interpreted with reference to spatial, topographical and geotechnical data, together with proposed geomorphological and landslide models of the natural terrain.

The report was prepared as part of the Landslide Investigation Consultancy, for the Geotechnical Engineering Office, Civil Engineering Department, under Agreement No. CE 86/2001 (GE). This is one of a series of reports produced during the consultancy by Halcrow China Limited.

Dr X D Pan
Project Director
Halcrow China Limited

Agreement No. CE 86/2001 (GE)
Study of Landslides Occurring in Hong Kong Island and Outlying Islands in 2002 – Feasibility Study

CONTENTS

VOLUME 1: DETAILED STUDY OF SELECTED NATURAL TERRAIN LANDSLIDES AT CLOUDY HILL

HALCROW CHINA LIMITED

This report was originally produced in July 2003 as GEO Landslide Study Report No. LSR 6/2003

CONTENTS

Page No.

1. INTRODUCTION

1.1 Background

As a result of intense rainstorms in April 2000 and June 2001, more than 45 natural terrain landslides occurred in the vicinity of Cloudy Hill, Tai Po in the northeast New Territories (Figures 1 & 2 and Plates 1 & 2). No casualties were reported as a result of the landslides. In July 2001, this detailed study was initiated to conduct a systematic examination of the characteristics and mechanisms of these natural terrain failures in order to assess the morphological, geomorphological and geological factors that affect the susceptibility and risk of similar failures in Hong Kong.

This report was prepared as part of the Landslide Investigation Consultancy, for the Geotechnical Engineering Office (GEO), Civil Engineering Department (CED), under Agreement No. CE 86/2001 (GE).

The report is presented in three volumes. Volume 1 is a factual documentation of the investigation and observations of the recent and relict landslides, together with the findings and diagnosis of the landslides and analysis of the data collected in the study. Volume 2 contains landslide record sheets prepared as part of the Aerial Photographic Interpretation (API) together with thematic maps. Volume 3 contains field sheets prepared for the landslides inspected and guidelines for site specific regolith mapping adapted from the methodology outlined in Special Project Report No. SPR 1/2002, Guidelines for Natural Terrain Hazard Studies (Ng et al, 2002).

1.2 Objectives

The key objectives of the study were:

(a) to collect factual information on both the recent and relict landslides in the vicinity of Cloudy Hill,

(b) to assess the typical characteristics and mechanisms of the failures and mobility of the debris, by field inspection and ground truthing of selected landslides,

(c) to carry out systematic analysis to investigate the controlling factors that influence the spatial distribution and susceptibility of the failures, and

(d) to develop a preliminary geomorphological model for the natural terrain.

1.3 Methodology

This report presents the findings of the detailed study, which comprised the following tasks:

(a) aerial photograph interpretation (API),

(b) limited field mapping including detailed mapping of selected landslides,

(c) development of a series of thematic maps of the Study Area based on the results of the API and field mapping,

(d) detailed regolith mapping of the southeast quadrant of the subject Study Area,

(e) analysis of rainfall data, and

(f) diagnosis of the probable controlling factors that influence the mechanism, spatial distribution and mobility of the landslides.

Further details of the methodology used to carry out these various tasks are discussed under the relevant sections of this report.

The terminology adopted in this report follows that advocated in Special Project Report No. SPR 1/2002, Guidelines for Natural Terrain Hazard Studies (Ng et al, 2002).

2. THE STUDY AREA

2.1 Study Area Description

The Study Area is located in the northeast New Territories about 1 km north of Tai Po (Figure 1). Pat Sin Leng Country Park extends over the northwest part of the Study Area. Vehicular access to the summit of Cloudy Hill is via a single lane road entering from the west. In the south of the Study Area the Wilson Trail follows a north-south trending ridgeline to the summit of the hill. In the north of the Study Area the trail follows the single lane access road.

Based on the natural pyramidal form of Cloudy Hill, the Study Area was divided into quadrants, viz. southeast Quadrant (SEQ), southwest Quadrant (SWQ), northwest Quadrant (NWQ) and northeast Quadrant (NEQ), as shown on Figure 1. The rationale behind dividing the Study Area into quadrants was:

(a) to separate the relatively large Study Area into smaller and more manageable parts, for the purposes of presentation of the study,

(b) to focus the study in the SEQ where the majority of the more significant failures occurred and where access was easier, and

(c) to allow a comparison of the spatial and temporal distribution of landsliding between the quadrants.

The elevation of the Study Area ranges from about 40 mPD to 440 mPD, with an area of 3.9 km^2. The summit of the hill and much of the higher side slopes (above 200 mPD) are generally grass covered. With the exception of the SEQ, the lower slopes are generally covered by a mixture of low shrub and woodland, becoming dense woodland along the major drainage lines. In the SEQ, the woodland is generally only found along the drainage lines with the lower side slopes generally covered in low shrub and grass. Close to the head of some of the major drainage lines, within shallow depressions that allow the accumulation of surface water, dense reed beds have formed. With the general exception of the areas of woodland and along drainage lines, large areas of the hillside have been affected by hillfires over the past 50 years.

Due to the dense vegetation and steepness of much of the terrain, access to much of the Study Area is extremely difficult, with the exception of the ridgelines.

2.2 History of Development

The earliest available aerial photographs of the Study Area were taken in 1945 and 1949, which cover only the north-western portion of the Study Area. At that time there had been no significant development in the Study Area with the exception of many footpaths and graves, which are generally located on the lower slopes, and areas of cultivation in the upland valleys.

By 1963, the Cloudy Hill access road and associated slopes had been constructed. Various areas of anthropogenic disturbance, most probably as a result of military construction, consisting of shallow excavations, trenches and occasional structures are visible, generally located along the ridgelines and around the summit of the hill. A series of parallel dark-toned bands that follow the contours around the summit and many of the surrounding ridgelines are observed on the aerial photographs. Whilst the origin of these features is not known, possible origins include tree plantations planted during reforestation work carried out by the Hong Kong Government in the 1950's or the location of concentric barbed wire fences that were often placed around military redoubts in the 1950's and 1960's. The presence of rusted steel posts at the location of the bands observed during the field mapping supports the second possibility.

Sometime between 1964 and 1975, a series of communication structures were constructed along the ridge forming the summit of the hill, and a small (about 13 m by 7 m) service reservoir was constructed in the south of the SEQ. In late 1986, major excavation works commenced in an area of hillside measuring about 400 m by 200 m, which was located at the southern end of the SEQ. The purpose of the earthworks was to source fill material for the nearby reclamations works in Tolo Harbour.

3. EXISTING DATA

3.1 Topography

The 1:5,000 topographical survey maps of the Study Area supplied by the Lands Department (LD) were used as the base maps for this study. A Digital Elevation Model

(DEM) was derived, based on 10 m grid data extracted from the contours of the 1:5,000 map. The DEM was used to prepare various digital terrain models (e.g. slope angle, aspect, plan curvature) for subsequent analysis.

3.2 Geology

Sheet 3 of the Hong Kong Geological Survey 1:20,000 scale map series HGM20 (GCO, 1991) indicates that the solid geology of the Study Area comprises volcanic rocks of the Tsuen Wan Volcanic Group (Figure 4). The geology of the Study Area is described in detail in both Hong Kong Geological Survey Memoir No. 5 (Lai et al, 1996) and the Pre-Quaternary Geology of Hong Kong (Sewell et al, 2000). The dominant rock type is undivided coarse ash crystal tuff of the Tai Mo Shan Formation. The formation is described as a massive, largely featureless, pale grey to dark grey lapilli-ash or coarse ash crystal tuff. Impersistent metamorphosed bands and interbeds of tuffaceous sandstone occur within the formation. The formation covers the whole of the Study Area apart from the southern part of the SEQ, which consists of the Shing Mun Formation. The Shing Mun Formation is complex and lithologically variable, and may consist of units of block-bearing fine ash, coarse ash and lapilli-ash crystal tuffs, eutaxite, tuff breccia, pyroclastic breccia, tuffite and of occasional conglomerates, breccia, sandstones, siltstones and mudstones.

Two significant faults are inferred on the geological map within the Study Area; a northwest to southeast trending fault that runs along the major drainage line within the SEQ, and a northeast to southwest trending fault that runs along the western end of the NWQ and appears to be associated with an extensive zone of metamorphism. The geological map shows a foliation fabric with a dip of 40º to 42º to the northnorthwest, the foliation appears only to be developed in areas affected by metamorphism.

3.3 Recorded Landslide Incidents

Three minor landslides (GEO Incident Nos. ME93/9/57, ME93/9/58 and ME2001/06/47) are reported to have occurred within the Study Area (Figure 5) according to GEO's landslide database. All three failures occurred upslope from the Cloudy Hill access road and resulted in debris blocking or partially blocking the road. Incidents Nos. ME93/9/58 and ME2001/06/47 involved failure of soil cut slopes Nos. 3SW-D/C124 and 3SW-D/C122 respectively and had estimated volumes of about 5 m^3 and 20 m^3 respectively. Incident No. ME93/9/57 was a natural terrain failure with an estimated volume of about 6 m^3 and occurred about 7 m above the level of the Cloudy Hill access road.

3.4 Natural Terrain Landslide Inventory (NTLI) and Boulder Inventory

The NTLI is a territory-wide catalogue of features considered to be natural terrain landslides as identified from high level (flying height >10,000 feet) aerial photographs. Two phases of NTLI have been carried out. The first phase covered the period from 1945 to 1994 (Evans et al, 1997). The second phase covered the periods 1994 to 1997 (Scott Wilson, 1999). During the second phase, low level aerial photographs (flying height approximately 4000 feet) from 1963 and 1964 were also examined to check for the presence of large landslides, and

Table of Contents
Table of Contents
Table of Contents
Table of Contents

large landslides reported in the earlier phase of the NTLI were cross-checked with large landslides recorded in the GASP reports and shown on the published 1:20,000 scale geological maps.

The locations of NTLI features are shown on Figures ASE6, ASW6, ANW6 and ANE6, and the location of features identified in the large landslide study (Scott Wilson 1999) are shown on Figures ASE7, ASW7, ANW7 and ANE7 (Appendix A of Volume 2). It is noted that a notable number of landslide records in the NTLI have a locational discrepancy when compared with location of landslide based on low level API and limited field mapping which was also carried out with the assistance of orthorectified aerial photographs (see Section 5).

The boulder inventory is a territory-wide catalogue of boulder fields on natural terrain in Hong Kong based on an interpretation of the 1963 and 1964 aerial photographs (Maunsell Geotechnical Services Ltd & ERM Hong Kong Ltd, 1999). The locations of boulder fields interpreted as part of this study broadly agree with that shown on the Boulder Field Inventory.

3.5 GASP

Geotechnical data on the Study Area compiled as part of the Geotechnical Control Office's (GCO, renamed as GEO in 1991) Geotechnical Area Studies Programme (GASP) Report V, North New Territories (GCO, 1988) were produced at a scale of 1:20,000 for regional appraisal and outline and strategic planning purposes. The Geotechnical Land Use Map (GLUM) designated the terrain in the Study Area as generally GLUM Class III to IV (high to extreme geotechnical limitation) along the drainage lines and for many of the steep (>30º) sideslopes, and generally as moderate (GLUM Class II) along the ridgelines. The Physical Constraint Map generally classifies the terrain surrounding the drainage lines as either "zones of colluvium which are subject to overland flow and periodic inundation" or "zones of general instability associated with predominantly colluvial terrain". The sideslopes are generally classified as "zones of general instability associated with predominantly insitu terrain" or "slopes of insitu terrain" which are generally greater than 30º.

3.6 Ground Investigation

A plan showing the locations of previous ground investigation works within the Study Area is presented in Figure 5.

In December 1962, Soil Mechanics Ltd. drilled one borehole (No. 200) within the SEQ under the supervision of Binnie, Deacon and Gourley, for the Plover Cove and Hebe Haven Water Scheme (Binnie, 1962). The geological descriptions used in the log do not follow current standards or guidelines. The borehole log indicates about 3 m of volcanic boulders, underlain by about 6 m of completely to highly weathered volcanic rock (described as felsite), underlain by a 45 m thick sequence of generally moderately to highly decomposed volcanics (described both as felsite and rhyolite) with occasional thin (about 0.3 m to 1.5 m) completely decomposed shear zones. The log contains no record of groundwater levels.

Between January and March 1984, Lam Geotechnics Limited drilled eight boreholes (Boreholes Nos. HE 1, 2, 4, 5, 6, 11, 14, 17) in the south of the SEQ for the New Territories Development Department under Contract No. 18/ST/82 under the supervision of Maunsell Consultants Asia Ltd. (Maunsell, 1986). The project was entitled "S.I.: Tai Po Borrow Area H Extension". All boreholes indicate broadly similar ground conditions consisting of a complex series of completely decomposed interbedded sandstones, siltstones, volcanic tuff and granodiorite ranging from about 2 m to 26.5 m thick, underlain by a similar sequence of highly to moderately decomposed rock with occasional zones ranging in thickness from about 1 m to 6 m of completely decomposed rock. Only one borehole (HE11) recorded colluvium indicating about 1 m of "colluvial soil". The boreholes were terminated at a depth of between about 30 m and 45 m. No piezometers were installed, although water levels monitored in the boreholes at the start of the day prior to commencement of drilling ranged from about 11 m to 26 m below ground level.

3.7 Orthophotographs

Based on a series of 1963 aerial photographs (Y09722 to Y09724), an orthorectified image of the SEQ was prepared by HCL. In addition, Lands Department supplied orthorectified images of the whole Study Area based on 1982 and 1999/2000 aerial photographs.

3.8 Fire Services Department

The Fire Services Department (FSD) have been contacted regarding any relevant records of hillfires within the Study Area. At the time of preparation of this report, no reply has been received.

4. THEMATIC MAPS

4.1 General

In order to investigate landslide susceptibility with respect to potential controlling factors, thematic maps were prepared for each of the quadrants, onto which the locations of all identified landslides were plotted (Appendix A). The sources of the data for the various thematic maps included detailed API, field mapping and terrain parameters, viz. slope aspect and angle and plan curvature, derived from the DEM of the Study Area.

4.2 Landslide Location and Simplified Geological Map

A detailed API was carried out for each of the quadrants to identify evidence of all past landslide activity, both recent and relict. A table of all aerial photographs reviewed is presented in Table B2 (Appendix B, Volume 2). Recent landslides were defined as those with a light tone on aerial photographs that are generally bare of vegetation. The extent of the main scarp of each landslide scar identified was recorded on the map and basic parameters

were estimated and transferred on to the API Landslide Record Sheets (Table B1, Appendix B, Volume 2). The parameters recorded for the landslides comprised:

(a) the year first observed,

(b) estimated coordinates of the centre of the main scarp,

(c) whether the landslide was recent or relict,

(d) estimated dimensions of the scar,

(e) details of the location of the landslide (e.g. below ridgelines, within drainage lines),

(f) slope angle and aspect at the source, and

(g) for recent landslides, the type of landslide (e. g. debris avalanche, debris flow) was identified, where possible, together with an estimation of travel angle and travel distance of the landslide debris.

In addition to the landslide scars, the extent of a number of basic regolith units were mapped based on API. These comprised:

(a) Recent landslide debris – generally light-toned deposits that are bare of vegetation and located below a well defined source.

(b) Relict landslide debris – generally characterized by vegetated lobate or fan-like deposits forming a concave break in slope; always located below a landslide source area.

(c) Colluvium (including valley colluvium) – generally located along drainage lines and other morphologically defined areas of hummocky ground not obviously related to a specific landslide event.

(d) Alluvial fans and terraces – generally level areas where sediments have been deposited, typically at the lower reaches of a drainage system.

(e) Boulder fields – characterized by accumulation of surface boulders. No distinction is made between insitu or transported boulders.

4.3 Isopleth Map

Based on the landslide locations identified on the Landslide Locations and Simplified Geology Map, an isopleth map was prepared showing landslide density (Degraff & Canuti, 1988). The landslide densities were determined based on the number of landslides occurring within a moving count circle, which is stored as a set grid. The values determined for all points on the grid are contoured to show isopleths of landslide density. As the area of the moving count circle was approximately 10,000 m^2 (1 hectare), the map effectively shows the number of landslides per hectare.

4.4 Catchment Morphology

The maps show prominent morphological features consisting of ridgelines (forming drainage divides), drainage lines and breaks in slope. The maps were prepared using both the API and the 1:5,000 topographical maps.

4.5 Anthropogenic Features

Based on a review of all available aerial photographs and field observations, the locations and extent of all visible anthropogenic features were mapped. The observed features were classified into the following groups:

(a) excavated/disturbed ground, generally related to military activity,

(b) cultivated land,

(c) cut and fill slopes, generally related to the formation of the Cloudy Hill access road,

(d) paths and tracks, generally minor tracks across the hillside less than one metre wide, and

(e) graves.

4.6 Hillfires

Based on a review of all available aerial photographs, the extent of identifiable past hillfires that have affected the Study Area were mapped. The hillfires were classified and colour coded as to the date first observed on the aerial photographs, viz. prior to 1969, 1970 to 1979, 1980 to 1989 and 1990 to 2000. The active landslides identified on the aerial photographs were also plotted on the hillfire map, using the same colour code classification as for the hillfires.

4.7 NTLI

The respective maps show the natural terrain landslides identified during Phase I and Phase II of the NTLI as indicated on map Sheet 3SW-D.

4.8 Solid Geology and Structure

As a result of the very limited exposure, often inaccessible terrain and the dense vegetation cover, detailed field mapping proved to be difficult. Where mapping was possible (in general along ridgelines and within landslide scars), the observed geology was generally consistent with that shown on the published 1:20,000 scale geological map (GCO, 1991).

4.9 Slope Angle and Aspect

The slope angle and aspect map was prepared using the terrain slope function in Surfer Version 8. A 10 m by 10 m grid extracted from the 1:5,000 topographical map was used to prepare the DEM from which slope angles and aspects were calculated. Such a grid density was considered appropriate for the relatively large size of the Study Area.

4.10 Plan Curvature

Plan curvature is defined as the curvature of the ground surface in a horizontal plane and is measured as 1/r, where r is radius of curvature in metres. Negative values indicate divergent water flow over the surface, and positive values indicate convergent water flow. Details of the equations used to derive plan curvature are included in Appendix C.

The form of a plan curvature map is highly dependent on the grid spacing of the data points used to generate it and the scale of the topographical map used to extract the data. For the purpose of this study, a 10 m by 10 m grid extracted from the 1:5,000 topographical map was used. It was found that when plan curvature maps were prepared based on a closer grid, the resulting map was highly complex, thereby masking potential correlations. In addition, it was thought likely that much of this complexity was a result of artifacts generated by the contours rather than representing a true model of the actual ground surface.

4.11 Regolith Map

Based on the methodology outlined in Ng et al, (2002) and Maunsell Geotechnical Services Ltd. and Fugro (Hong Kong) Ltd. (2002), detailed regolith mapping was carried out in the SEQ. The mapping was substantially based on the 1963 orthophotographs which show low levels of vegetation cover and high clarity of image relative to the more recent photographs. A review of all available aerial photographs was also carried out to define the extent of recent landslide debris. An iterative process was adopted whereby specific regolith units were interpreted from API followed by ground truthing to check the interpretation followed by revision to the regolith map as appropriate. As noted earlier, the classes finally

adopted and their descriptions were refined from those used for the initial mapping based on API alone with the regolith map revised accordingly.

A summary of the various diagnostic properties of the regolith classes used including general descriptions and typical oblique photographs of their field occurrence are included in Appendix F.

4.12 Landslide Susceptibility and Frequency Distribution

Based on the methodology outlined by Parry (2001), a site-specific landslide susceptibility analysis was carried out for each of the quadrants. Tables 1 to 4 show the slope area for each slope angle class and the resulting landslide density for each slope angle class for the quadrants. Table 5 shows the combined results for all quadrants.

The distribution of landslides in terms of susceptibility and frequency has been characterized for the SEQ by considering a 10 m by 10 m grid over the SEQ. The 10 m by 10 m grid size was considered appropriate in terms of the accuracy of the size of areas with consistent slope angle and aspect and the dimensions of landslides being considered. At each grid point the landslide susceptibility has been assessed with regard to the following factors:

(a) Slope angle,

(b) Slope aspect,

(c) Regolith type,

(d) Proximity to zero plan curvature,

(e) Proximity to a ridgeline,

(f) Proximity to the head of a drainage line, and

(g) Proximity to landform boundary.

The landslide susceptibility at each grid point has then been determined by using the following equation.

$$\text{Susceptibility } N_s = (\text{Slope Angle Factor} + \text{Slope Aspect Factor} + \text{Plan Curvature Factor} + \text{Ridgeline Factor} + \text{Drainage Line Factor} + \text{Landform Factor}) \times \text{Regolith Factor}$$

The derivation of the factors is shown on Figures ASE15 to ASE21. The Slope Angle Factor is derived by dividing the total landslide source area in a specified slope angle range by the total area in that slope angle range within the SEQ. The Slope Aspect Factor is derived by dividing the total landslide source area in a specified slope aspect range by the total area in that slope aspect range within the SEQ. The Plan Curvature Factor is derived by dividing the total landslide source area in or outside a buffer zone, which extends 10 m from the zero plan curvature line toward the region of convergent flow, by the total area in or outside that plan

Table of Contents
Table of Contents
Table of Contents
Table of Contents

curvature buffer zone within the SEQ. The Ridgeline Factor is derived by dividing the total landslide source area in or outside a buffer zone, which extends 15 m either side of the ridgeline, by the total area in or outside that ridgeline buffer zone within the SEQ. The Drainage Line Factor is derived by dividing the total landslide source area in two buffer zones, which extend 10 m and 20 m from the head of the drainage line, by the total area in the two drainage line buffer zones within the SEQ. The Landform Factor is derived by dividing the total landslide source area in or outside a buffer zone, which extends 20 m down slope from the landform boundary line, by the total area in or outside that landform boundary buffer zone within the SEQ. The Regolith Factor is derived by dividing the total landslide source area within a specified regolith type by the total area underlain by that regolith type within the SEQ.

The resulting landslide susceptibility at each grid point, N_s, has then been divided by the sum of the susceptibility of all grid points. This ratio provides a relative susceptibility value that has then been multiplied by the annual landslide frequency for the SEQ to obtain the spatially distributed relative annual landslide frequency at each grid point.

$$\text{Frequency } N_f = (N_s / \Sigma N_s) \text{ x landslide frequency in SEQ}$$

The landslide frequency in the SEQ is taken as the annual frequency of landslides with volume greater than 10 m³ and is determined to have a value of 7. This annual frequency of landslides with volume greater than 10 m³ has been estimated by dividing the total number of recent and relict landslides in the Study Area (i.e. 330) by an observation period of 49 years (i.e. 1953 to 2002). Year 1953 has been used as this extends the period of observation to 10 years prior to the earliest photographs considered in the assessment (i.e. 1963).

The resulting landslide frequency distribution for the SEQ is shown in Figures ASE22 and ASE23. The distribution of landslide frequency shown is for landslides of all volumes.

5. CHARACTERISTICS OF THE NATURAL TERRAIN LANDSLIDES

5.1 General

An initial visit to the Study Area was undertaken by HCL on 10 May 2001 to carry out a preliminary inspection of three landslides in the southeast catchment that were first reported to the GEO in April 2000. Subsequently more than forty landslides occurred on Cloudy Hill in early June 2001, including a cut slope failure, the debris from which blocked the access road to the summit of Cloudy Hill (GEO Incident Report No. ME 2001/06/047).

The locations of about forty visible recent landslides were identified using oblique aerial photographs of the Study Area that were taken during a helicopter reconnaissance flight on 9 July 2001 (Plates 1 and 2). Approximate locations of the landslide sources were marked on a 1: 5,000 scale map of the Study Area, and subsequently a field reconnaissance survey was carried out. The numbering system used to identify the landslides (e.g. 01K) comprises two digits to represent the year first observed (e.g. 01 = 2001) and a unique alphabetical letter(s).

The field reconnaissance survey of the Study Area comprised a walkover survey and preliminary inspection of 34 landslides. For each of the landslides an accurate location was determined using a Global Positioning System (GPS) and preliminary measurements and general observations were made and recorded on landslide reconnaissance fieldsheets. A location plan of the inspected landslides as well as the sections of drainage lines is presented in Figure 3 and the completed landslide reconnaissance fieldsheets for the 34 landslides are presented in Appendix D (Volume 3).

From a review of the fieldsheets prepared for the 34 landslides inspected, eight landslides were selected for more detailed study and documentation using fieldsheet pro-formas developed for the Tsing Shan Foothills Natural Terrain Hazard Study. The criteria for selection of the eight landslides included large failure volume, evidence of reactivation, possible structural control, tension cracks or other evidence of pre-detachment deformation over a period of time such as folded quartz veins or clay infilled joints. The completed detailed fieldsheets for the eight landslides are presented in Appendix E (Volume 3). It should be noted that some of the debris trails could not be inspected completely as safe access was precluded by steep terrain and dense vegetation.

5.2 Characteristics of the Landslides

5.2.1 Description of the Landslide Sources

In general the majority of the 2000 and 2001 landslides on Cloudy Hill were relatively shallow (about 1 m deep) failures that were typically situated at the heads of drainage lines or on the flanks of drainage lines and below ridgelines. Debris from several of the landslides ran into drainage lines which resulted in relatively long (up to 200 m) runout distances. The 2000 and 2001 landslides were also observed to have occurred generally on terrain with a southerly aspect**.**

The characteristics of the landslides based on information from field inspections at the Cloudy Hill Study Area are summarised in Table 7. The slope angle and aspect recorded were based on field measurement at the source of the landslide. When compared with the slopes angles and aspects derived from the DTM in general the recorded slope angle were about 5º less than those derived from the DTM, while the slope aspect were generally within +/-20º of those generated by the DTM, although occasional significant variation of about 40º were found.

About 70% of the landslides inspected occurred in colluvial deposits that typically comprised a matrix-supported, loose to medium dense, light reddish brown silty sand (or firm sandy silt) with some gravel and some to many angular cobbles of moderately decomposed tuff **(**Plate 3**)**. In some landslide scars, cobbly or bouldery clast-supported colluvium was observed **(**Plate 4**)**. The cobbly or bouldery colluvium was usually very localised and only observed in the flanks of the main scarp, although much of the material mobilised from the source of Landslide 01N appeared to be cobbly and bouldery colluvium (Plate 4).

The recent landslides at Cloudy Hill had estimated failure volumes ranging from 12 m^3 to 630 m^3. The average estimated landslide volume was about 100 m^3.

The surface of rupture at most of the landslides was along the colluvium/saprolite interface (e.g. Landslide 01H, Plate 5), although the surface of rupture at some of the landslides (e.g. Landslide 01B, Plate 6) occurred through the saprolite soil. The saprolite, which was exposed at the central portion of the source floor of most landslides, typically comprises completely decomposed tuff (light pinkish to reddish brown silty/clayey sand with occasional fine gravel of quartz).

The main scarps at most of the landslides inspected were either planar or slightly concave in shape. Generally, where the surface of rupture was along the colluvium / saprolite interface, the surface of rupture was concave or slightly irregular (e.g. Landslide 00C shown in Plate 7). At landslides where the surface of rupture has cut through the saprolite, the main scarp was typically planar to slightly convex in shape (e.g. Landslide 01B and 01K shown in Plates 6 and 8 respectively).

Erosion pipes were observed in the main scarps at several of the landslides, notably Landslides 00C, 01N, 01W and 01EE. The erosion pipes were typically located near the base of the colluvium and the erosion pipe at Landslide 01W appeared to have a partially graded infill (Plate 9). Commonly observed at the landslide sources were quartz veins that were usually deformed or folded consistent with downhill deformation, possibly indicating intermittent movement and progressive deterioration of the insitu saprolite or near surface 'creep' processes. As the deformed quartz veins were only exposed in the floor of the landslides inspected, it was not possible to determine whether the deformation of the near surface saprolite occurs only at the source of the landslides or is a common process relating to 'creep' and present over much of the hillside. The quartz veins typically strike north-south and in general dip towards the west. Examples of the quartz veins encountered are shown in Plates 10 and 11 from Landslides 00C and 01H1 respectively. Notably, at Landslide 01N, a fractured quartz vein, up to 60 mm wide with soft brown clay between fractures (Plate 12), was observed to be sub-parallel to the source floor indicating a possible partial structural control to the landslide.

Possible partial structural control was also observed at Landslide 01EE. In the north western flank of the landslide source, moderately decomposed tuff forms a planar surface from which the overlying saprolite and colluvium have been displaced. The surface appears to be a single continuous discontinuity (Plate 13) dipping 45°/100°. Slickensides, with an east-west trend, were observed on the discontinuity surface (i.e. parallel to the direction in which the displaced material was mobilised). Clay-infilled joints and the fractured nature of the rock indicate that deterioration of the condition of the insitu weathered rock had occurred prior to detachment (Plate 14).

Tension cracks were observed at a number of the landslides, with the tension cracks typically located to one side of the landslide crown (Plate 15) and usually discontinuous and less than 1 m long. Significantly, at Landslide 01N, much of the landslide crown is delineated by a continuous tension crack, about 42 m long and 1.5 m high. Only colluvial material below a 12 m wide section near the central part of the tension crack was fully detached during the landslide (Plates 16 and 17).

5.2.2 Description of the Landslide Debris Trails

Inspections of the debris trails indicated that only minor entrainment of material from the drainage lines had occurred as a result of the recent landslides. The reason for little observed evidence of entrainment is not certain, but is likely to be due to a combination of factors including the relatively small magnitude of recent failures, the general coarse nature of the valley colluvium present within the drainage lines which may require a relatively significant event exceeding a certain threshold momentum to be mobilised and the general linear nature of many of the drainage lines which will minimise potential erosion during the passage of stream and debris flows.

The drainage line below Landslide 01EE has a gradient of about 18° with the substrate being a firm dark grey silt. Below the uppermost 200 mm thick soil layer a colluvial layer, which was typically a slightly sandy, silt/clay with occasional angular cobbles up to 200 mm in size, was exposed at a few locations along the drainage line. In section the drainage line has an open 'U' shape with a relatively flat base and longitudinally has a smooth gently undulating form, which probably significantly influenced the debris run-out distance. Field observations suggest that the landslide debris travelled along the drainage line primarily stripping off only the vegetation with most of the top soil left intact. The drainage line below Landslide 01N is poorly developed and in section has a slight 'U' shape. The gradient of the drainage line decreases from about 24° immediately below the landslide source to about 10° some 80 m from the source. The shallow gradient and much vegetation within the drainage line appear to have impeded the flow of the debris from the source resulting in a relatively short travel distance. Diagrammatic sections through the drainage lines are presented in Appendix E as Figure 4 of the respective detailed field inspection sheets for both landslides.

5.2.3 Inspection of Drainage Lines

Inspection of a 300 m section of drainage line within the upper part of the southeast catchment revealed that the drainage line has an almost 'V' shaped section with much colluvium deposited at its base. The colluvium comprises some to many angular cobbles and boulders with a sandy clay/silt matrix (Plate 18). Running water was observed near the upper part of the drainage line (elevation about 320 mPD), and dense vegetation comprising reeds and tall thick barbed grasses suggest that water is present for much of the year.

Inspection of the drainage line beyond about 300 m from the summit ridge-line was prevented by the presence of a series of sub-vertical rock steps, over 10 m in height, crossing the drainage line. Further inspection of the drainage line was therefore carried out upstream from the mouth. Surrounding the mouth of the drainage line, up to 3 m thick alluvial deposits are exposed in the sides of the streamcourse. The alluvium typically comprises rounded boulders (maximum size 0.5 m^3), with many rounded cobbles in a matrix of medium to coarse sand (Plate 19). There was no apparent evidence that the alluvium had been deposited in lobes, although cultivation in the flood plain would probably have destroyed such evidence.

Within the drainage line, colluvium up to 3 m in thickness is exposed at some locations along the sides of the streamcourse. The colluvium typically comprises sub-rounded to sub-angular cobbles and boulders of tuff (maximum size 0.25 m^3) in a matrix of silty sand. The colluvium does not appear to have been deposited in layers although at some locations a

possible layering of fine sandy colluvium over cobbles and boulders was observed (Plate 20). This indicates that the valley colluvium deposits were reworked by alluvial processes. Rock is exposed at several locations within the lower section of the drainage line. The rock is typically a fine ash tuff.

There was no evidence that the debris from the recent landslides had travelled a significant distance along the drainage line, although it is likely that much of the debris that travelled into the drainage line was subsequently washed out by the water flowing along the streamcourse. During field inspections along the drainage lines, no evidence was observed of landsliding or entrainment within the valley colluvium deposits. The section of drainage lines that were inspected are indicated in Figure 3.

5.3 Landslide Classification

5.3.1 Debris Avalanches and Flows

Observations at the recent landslides on Cloudy Hill indicate that the majority are of the shallow debris avalanche type (Ng et al, 2002), where the displaced material has broken up and become remoulded. There is much evidence from the planar main scarps and intact displaced masses found at most landslide sources, that several of the landslides were initially debris slides (Ng et al, 2002) that translated into debris avalanches. Debris from several of the landslides ran into drainage lines and became channelized. However there is insufficient evidence to suggest that the landslides developed into debris flows (Ng et al, 2002) where the debris became sufficiently mixed with water for a slurry flow to occur. The debris from Landslide 00C (Plate 21), which could not be inspected fully due to the steep terrain, may possibly have developed into a debris flow and this may have also occurred in the case of the Landslide 93C. The relatively high mobility of the debris from Landslides 00C and 93C is indicated by travel distances of about 250 m and 320 m respectively. This is partially explained in that the debris from both landslides were funnelled into narrow drainage channels becoming channelised. The debris travel distances would also reflect the influence of the steep terrain (>40°) below the sources of the landslides.

5.3.2 Deep-seated Landslides

Landslide 01M is an example of a deep-seated retrogressive landslide located on open hillside with toe of the source area feeding into the head of a narrow drainage line (Plate 22). The failure appears to be controlled by adversely orientated relict joints within the completely decomposed tuff and along preferential weathered joints within the moderately decomposed tuff, which daylight from the almost vertical 6 m to 8 m high main scarp.

Debris from the recent failures (widening of the main scarp) has not travelled beyond the large relict landslide source area, resulting in an accumulation of loose debris near the toe of the landslide. Dense and mature vegetation has become established on lobes of debris from previous failures suggesting that a large-scale landslide has not been mobilised from the source area for a considerable period.

The narrow (about 1.5 m to 2 m wide) head of the drainage line below the toe of the source (Plate 23), relative to the large size (about 60 m by 80 m) of the relict scar, indicates that the large scar has formed through multiple failures progressively widening the source area rather than a previous single large-scale event.

6. RAINFALL

A detailed rainfall analysis relative to landslide occurrence has not been possible since the exact dates and times when the recent landslides occurred are not known. However, the 2000 landslides were first reported to the GEO in April 2000, and it is likely that the landslides occurred during the only significant rainstorm in April 2000, around the 14 April 2000, that brought more than 350 mm of rainfall to parts of Hong Kong. The 2001 landslides were first observed in June 2001 and, based on GEO Incident Report No. ME 2001/06/047 for a landslide that affected the access road to the summit of Cloudy Hill and rainfall records, the landslide probably occurred before the 10 June 2001. For the purposes of the rainfall analysis, the landslides are assumed to have occurred at the end of the rainstorm of the 9 June 2001 at 2:00 p.m.

The nearest GEO automatic raingauges, Nos. N05, N35 and N45, are located about 3.5 km northwest, 2.6 km southwest and 4 km southeast of the Cloudy Hill summit, respectively. Raingauge No. N05 was first installed on 22 March 1983 and relocated on 6 June 1990. Both raingauges Nos. N35 and N45 were installed on 1 November 1999. The raingauges record and transmit rainfall data at 5-minute intervals via telephone lines to the GEO. The rainfall data are considered to be indicative of the probable rainfall pattern and intensity at Cloudy Hill. Daily records of rainfall at the three raingauges for the period between 1 January 2000 and 30 September 2001 are shown in Figure 6, which illustrate the significant regional differences in the rainfall recorded around Cloudy Hill.

Table 8 presents the estimated return periods for the maximum rolling rainfall as recorded by raingauge No. N05 for various durations based on historical rainfall data at the Hong Kong Observatory (Lam & Leung, 1994). The 4-hour rolling rainfall (225.5 mm) for the period ending 11:00 a.m. on 9 June 2001 was the most severe with a return period of about 22 years. This simplified method of rainfall analysis does not necessarily give the true return period for a particular site, as several contributory factors are not taken into account (Wong & Ho, 1996b). Nonetheless, it provides an indication of the relative severity of the various rainstorms assessed.

Isohyets of rainfall recorded for April 2000 and June 2001 for the whole of Hong Kong (Figures 7 and 8) show that there was a cumulative rainfall of between about 1200 mm and 1700 mm at the Cloudy Hill area in June 2001 as compared with a cumulative rainfall of between 500 mm and 600 mm in April 2000.

A comparison of the pattern of the rainfall preceding the June 2001 landslides with that of selected previous major rainstorms affecting the area, as recorded by raingauge No. N05, which is located at Cheung Chi House, Cheung Wah Estate, Fanling, since its installation in 1983, is shown in Figure 9. The rainfall comparison shown in Figure 9 indicates that the 9 June 2001 rainstorm was more severe than the previous rainstorms recorded by raingauge No. N05 over the 11 hour period preceding the assumed date of the landslides. This

Table of Contents
Table of Contents
Table of Contents
Table of Contents

comparison is indicative only because other factors (especially possible orographic influences and micro-climate) have not been taken into account.

A review of wind direction data from the weather stations at Tai Mo Shan and Tai Mei Tuk, was made for 14 April 2000 and 9 and 10 June 2001 when the recent landslides are assumed to have occurred. The dominant wind direction on each of the above dates was from the south and occasionally from the southwest.

7. GEOLOGICAL AND GEOMORPHOLOGICAL MODEL

7.1 Solid Geology and Structure

The solid geology of the Study Area is dominated by undivided coarse ash crystal tuff and block-bearing tuff and tuffite occasionally interbedded with sandstones and siltstones (Section 3.2). The interbedded units are recorded on the geological map to be dipping relatively steeply (25º to 48º) towards the north-northwest. The tuffs are poorly exposed and where exposure does occur there is little evidence of bedding. The lithological orientation of the tuff is evidenced by a discontinuous band of exposed rock, probably representing a more resistant lithology, that transverses the north of the SEQ and is clearly visible on the regolith map (Figures ASE13 and ASE17, Appendix A of Volume 2). Furthermore, the orientation of some of the ridges and drainage lines along the western flank of the SEQ also follows this trend. The only significant areas of exposed rock were found within the northern part of the SEQ and the eastern flank of the SWQ. The areas of exposed rock are generally highly to moderately decomposed, occasionally slightly decomposed. Where insitu rock was found exposed on the surface of rupture of landslides, it was typically completely to highly decomposed tuff, occasionally moderately decomposed. The extent of weathering of the bedrock is very variable and is discussed in more detail in Section 7.2.

The orientations of joints were recorded where insitu rock was exposed on the surface of rupture of the landslides inspected. The readings indicated two distinct primary joint sets, viz. 34º/209º and 53º/354º, both generally closely spaced. A less well developed set orthogonal to the primary sets with a typical orientation of 67º/263º (generally widely spaced) was also recorded. In general, no evidence of stress release (sheeting) type joints were observed within the areas of exposed rock of the landslide scars.

In addition to the faults inferred on Sheet 3 of the Hong Kong Geological Survey 1:20,000 scale map series HGM20 (GCO, 1991), a prominent northeast to southwest trending photogeological lineament was identified in the SWQ (Figure ASW1, Volume 2).

Minor quartz veins occur throughout the Study Area and were found in many of the landslide scars (typically 10 mm to 50 mm wide). The veins typically strike north-south dipping towards the west.

The foliation recorded on the geological map was generally not observed within areas of exposed rock in the source areas of the landslides. The foliation appears to be developed only in areas affected by metamorphism.

7.2 Regolith Mapping

It should be noted that the nature and extent of the mapped regolith units are generally inferred based on tonal variations on the aerial photographs, topographical and morphological setting, and where possible, ground truthing. Consequently, in areas of dense vegetation, such as that surrounding many of the drainage lines within the Study Area (even in the 1963 photographs) and areas lacking distinctive morphological or textural features, such as the lower flanks of the hillsides, the regolith unit is inferred based on very limited data. In such areas, the accuracy of the interpretation could be less reliable or consistent because of the above constraints.

Typically the regolith within the SEQ consists of volcanic saprolite (Sv). Along the major catchment boundaries, the saprolite in places was interpreted as being deeply weathered [Sv(dw)]. The deeply weathered saprolite is generally related to the older and typically, more weathered upper geomorphological landform as described in Section 7.4. In general a continuous thin layer (typically between 0.5 m to 1 m thick) of colluvium covers these areas of deeper weathering.

Occasional areas of rock (Rv) occur along the ridgelines, generally in the form of intermittent linear exposures located directly along the crest of the ridge or as isolated tors. In the north of the SEQ, cliffs of exposed rock are developed forming a discontinuous band of exposed rock across the area. In addition, local areas of exposed rock were mapped within the relict landslide scars. Whilst not common within the SEQ, within the SWQ and NWQ multiple failures have coalesced stripping of the soil to expose areas of rock up to about 80 m wide. Below these areas of exposed rock, rock-fall debris (Crf) was sometimes identified, although in general, within the SEQ the hillside gradient directly below the areas of exposed rock was too steep to allow accumulation of such talus deposits.

Below the ridgelines a discontinuous veneer of colluvium is generally developed over the saprolite (Sv+) whilst, in places, concentrations of boulders have developed (Sv+B). No attempt has been made to distinguish insitu boulders from colluvial boulders. Towards the lower flanks of the hillside, residual colluvium (Cr) has been interpreted as forming a nearly continuous blanket over the area.

Valley colluvium (Cv) was inferred to be present along most of the drainage lines, although within the steeper terrain (generally >30º), exposed rock was generally present and there was no significant accumulation of superficial deposits.

Depression colluvium (Cd) was interpreted in two separate settings:

(a) within relatively small (generally <20 m wide), often lens shaped, hollows that are developed both in areas of exposed rock and within areas of saprolite, and

(b) within broad down-slope orientated concave depressions without a distinct drainage line.

Alluvium (Al) was interpreted in generally level areas surrounding the main drainage lines towards the outlet of the catchment.

Relict landslide debris (Clb) was interpreted below the location of relict landslides scars where a clearly definable debris lobe was visible. Recent landslide debris (Cla) was interpreted at the location of recent landslides, based on a review of all available aerial photographs and where a fresh, generally unvegetated debris lobe was visible.

7.3 Geomorphology

Many engineering geomorphological features are included in the various thematic maps prepared from this study (Appendix A, Volume 2), rather than presented separately within a specific engineering geomorphology map. In particular, the regolith mapping described in Section 7.2 above relates the form of the ground surface to the nature of the material of which the surface is composed.

The terrain forming the Study Area is generally angular and is characterized by moderately to steep slopes (typical 20º to 40º), gently concave sideslopes rising to either sharp concave ridgelines or rounded convex ridgelines generally with a prominent convex break in slope below. Such terrain is typical of areas of volcanic rock. Based on site observations, the rounded ridgelines are generally draped with a continuous, thin (generally <1 m) veneer of colluvium underlain by deeply weathered saprolite. The sharper ridgelines are characterized by a shallow layer of saprolite with occasional minor areas of exposed rock and with generally little of no colluvium cover. Below the ridgelines, a thin layer (generally between 0.2 m and 2 m) of typically cobbly colluvium mantles the hillside. With the exception of local areas of erosion adjacent to the Cloudy Hill access road (Section 8.1.1), no significant areas of surface or gully erosion were observed within the Study Area.

The SEQ, SWQ, NWQ and NEQ comprise one, three, four and three separate catchments respectively. Typically the drainage pattern follows a primary northwest to southeast trend with a secondary west to east or northwest to southeast trend, forming a broadly rectilinear pattern typical of Hong Kong (Sewell et al, 2000). The most significant exception to this is a pronounced northeast to southwest trending drainage line in the SWQ that follows a pronounced photolinement (see Section 7.1). Outside the Study Area, the drainage line from the NEQ shows evidence of river capture. Catchments are generally of second or third order. The drainage lines on the hillside are generally moderately closely spaced (typically separated by between 20 m and 80 m) and tend to be linear, particularly towards the heads of the drainage lines. Often pronounced hollows have developed at the heads of the drainage lines.

With reference to the geomorphological model proposed by Hansen (1984), two distinct landform assemblages can be recognized within the Study Area, each consisting of convex-concave elements. The upper landform generally occurs adjacent to rounded ridgelines and is characterized by slightly convex, almost planar surfaces with few drainage lines and a generally smooth surface texture. Typically the upper landform represents an area of deep weathering and is often covered with a mantle of ‘old’ weathered colluvium, probably deposited as a result of long continued ‘creep’ and wash processes. Locally areas of exposed rock and boulder fields derived from the weathering out of corestones are found. The upper landform is particularly well developed in the southwest of the SEQ and can be seen clearly on the 1987 aerial photographs (Plate 24). It was observed that the boundary is more visible in the aerial photograph taken during periods of less dense vegetation and after hillfires. A

generally distinct convex break in slope marks the boundary between the upper and lower landform. The boundary with the lower landform is characterized by a zone of instability (representing a zone of 'hillside retreat'), which can either be active or relict, that has progressively consumed the older upper landform as it has propagated upslope. A series of landslides is often visible on the oversteepened slopes forming the boundary between the upper and lower landforms (Plate 25). In places, the process of 'hillside retreat' has reached the ridgeline resulting in knife-edge ridges (Plate 24). Evidence of the upper and lower landform is found in all the quadrants apart from the NEQ. Figure ASE21 shows the interpreted boundary between the upper and lower landforms in the southeast quadrant. It is appreciated that the geomorphological model described is a simplification of the actual geomorphology of the Study Area and a more accurate model would involve a complex series of 'erosion fronts'.

7.4 Landslide Models

7.4.1 General

Based on the field observations, landslide characteristics and morphological setting, the recent landslides at Cloudy Hill have been grouped into two broad types, viz. Types I and II, for the purpose of this study. The general geomorphological settings of Type I and Type II landslides are presented in Appendix G and their typical characteristics are discussed below. One landslide that was inspected did not fall into either of the two above types, but lacked sufficient characteristics to allow a third landslide type to be postulated.

Based on the inspection of the recent landslides, the distribution of the two landslides types are shown in Figure 3.

7.4.2 Type I

The Type I landslide is illustrated in Figure 10. The typical setting for a Type I landslide is above the head of a drainage line or below a ridge line and typically at a prominent convex break in slope. In the field, the landslides usually have a planar main scarp with a slightly convex surface of rupture. The failure generally occurs through the uppermost portion of the deeply weathered saprolite and may include the failure of an overlying thin (typically less than 1 m thick) layer of older weathered colluvium (Plate 26). Landslide 01B and 01K are examples of Type I landslides (see Plates 27 and 28).

Type I landslides are generally located at, and essentially define, a zone of instability, representing a zone of 'hillside retreat', that progressively advances up through the older upper landforms. Commonly a number of the Type I landslides will fail along the zone of instability to form a single large curved depression which may be misinterpreted as a previous large-scale failure (Plate 25). There is evidence from field inspection (Landslides 01K and 01L) and aerial photograph interpretation that Type I landslides often tend to occur simultaneously as clusters, i.e. usually under the same rainstorm.

7.4.3 Type II

The Type II landslide is illustrated in Figure 11 and Plate 29. Type II landslides occur from concave depressions or hollows that are typically situated at the head of a drainage line and below ridgelines (Plate 30). Type II landslides probably occur once sufficient debris has accumulated in a hollow or when the debris attains a critical thickness. The debris filling the hollow derives from collapse of a previously exposed back scarp, multiple Type I failures depositing debris into the hollow together with slope wash processes. The Type II landslide then occurs, typically when a perched water table develops within the colluvium that has accumulated above the colluvium/saprolite boundary.

Type II landslides usually have an inverted "tear drop" shape when viewed in plan and are identified in the field as landslides with a typically concave source floor, which may sometimes be irregular, and a surface of rupture along the colluvium/saprolite boundary. The exposed surface of rupture may also exhibit signs of previous exposure through the presence of a patina of relic algal growth as was observed at Landslide 00C (Plate 7). Similar evidence of previous exposure was also observed on the exposed surface of rupture of Landslide 00C, where the upper 50 mm of exposed saprolite was paler than that below.

In general, erosion pipes are more commonly observed in the colluvium in the main scarps of Type II landslides than in Type I landslides and other evidence of possible deterioration of the insitu saprolite, such as deformed quartz veins and sediment infilled joints, are also more common in Type II landslides.

7.4.4 Other Landslides

Other landslides are those that do not satisfy the general definitions of either the Type I or II landslides, but lack sufficient common characteristics to allow a third type to be defined. They tend to be open hillside failures that have no apparent relationship to the topographical setting or the geological setting.

An example of a other landslides that are not of Type I or II is Landslide 01N, located about 100 m north of the summit of Cloudy Hill (Figure 1 and Plates 1 and 16). The landslide is situated on open hillside, with the terrain gradient in the vicinity of the landslide of between 24° and 29°. The landslide involved shallow translational failure of a layer of bouldery colluvium (Plates 4 and 12), with a maximum thickness of about 1 m and with the surface of rupture along the colluvium/saprolite interface. The landslide source is about 42 m wide by 20 m long, and the estimated failure volume is about 630 m^3, although only approximately 250 m^3 of material was detached from the source. Much of the landslide crown is delineated by a tension crack, that is about 42 m long and generally between 1 m and 1.5 m deep, with only the colluvial material below a 12 m wide section near the central part of the tension crack having fully detached during the landslide.

Other landslides that are not of Type I or II include those that occur within drainage lines, usually only a very short distance from the axis of the drainage line. These landslides are interpreted as been essentially related to minor erosional events and are usually small in size.

8. DIAGNOSIS OF THE NATURAL TERRAIN LANDSLIDES

8.1 Correlation between Landslide Susceptibility and Terrain Attributes

The following sections review the landslide susceptibility of the Study Area with reference to the thematic maps (Appendix A, Volume 2).

8.1.1 Anthropogenic Influence

Plans of anthropogenic features for the individual quadrants are presented as Figures ASE4, ASW4, ANW4 and ANE4 (see Volume 2). With the exception of the landslides associated with cut and fill slopes constructed for the Cloudy Hill access road, no obvious correlation was identified between either the relict or recent landslides and anthropogenic features.

The trenches on the ridgelines and hilltops, probably of military origin, provide a potential for concentrating infiltration of surface water. However, no relationship was found between the trenches and landslide susceptibility. It was however observed during site inspection that, during intense rainfall, the Cloudy Hill access road tended to concentrate surface water flow. During a rainstorm on 9 September 2001, a surface water depth of over 200 mm was recorded on the road surface. These areas of concentrated surface water tended to discharge downslope at bends on the road, resulting in areas of significant surface erosion.

8.1.2 Hillfires

Plans of the extent of historic hillfires for the individual quadrants are presented as Figures ASE5, ASW5, ANW5 and ANE5 (see Volume 2). Based on the available information, no significant correlation between the location of landslides and the areas of the hillside affected by historic hillfires was found for the Cloudy Hill area. There are however severe limitations in these maps and any attempted correlation with locations of landslides as discussed below:

(a) The hillfire thematic map is based on interpretation from an incomplete aerial photograph record with only one set of low quality photographs prior to 1963 and significant gaps of over 10 years with no coverage, post 1963 (Table B2). While the photographic record since 1975 is good, not all flights cover the whole Study Area and the past 27 years of good coverage may not be sufficient to identify any reliable trends.

(b) Where the hillfires occurred some years prior to the date when an aerial photograph was taken, it often proved difficult to define the extent of the hillfire accurately. In some circumstances, evidence of hillfires was no longer visible after only two or three summers of vegetation re-growth.

(c) As a result of the limited temporal aerial photographic coverage, it was often not possible to estimate accurately the timing of either the hillfire or the landslides.

It was noted that some of the hillfires, which were often separated by many years, apparently have almost identical boundaries resulting in the same portions of the hillside being burnt repeatedly over the last 30 years. The reason for the propensity of certain sections of hillside to hillfires is not known but is probably a combination of factors including:

(a) proximity to ignitions points (i.e. the locations of graves or footpaths),

(b) the nature of the vegetation coverage i.e. dense mature woodlands surrounding drainage lines tend to act as firebreaks while grasslands tend to be extensively burnt, and

(c) surface and subsurface drainage effects.

A further observation on the affect of hillfires was that subtle variations in hillside morphology, such as breaks in slopes and shallow hollows, often mark the boundaries of the burnt area and thereby accentuate the presence of such features in photographs. Such highlighted boundaries proved useful when preparing some of the other thematic maps, especially the regolith map and the landslide location map.

8.1.3 Slope Angle and Aspect

Plans of slope angle for each quadrant are presented as Figures ASE9, ASW9, ANW9 and ANE9 (Volume 2). Plans of slope aspect are similarity presented as Figures ASE10, ASW10, ANW10 and ANE10 (Volume 2). A slope angle susceptibility analysis based of landslide point locations (Tables 1 to 4) shows that there is a generally consistent pattern of landslide susceptibility distribution with slope angle. Table 5 is a summary of the landslide density for the four quadrants combined. In general, susceptibility increases with slope angle until gradients of between 30º and 40º, with a subsequent decline as slope angle increases further. The observed trend is consistent with data recorded in other similar studies in Hong Kong (e.g. Evans & King, 1998).

The trend in the SEQ is somewhat different, the susceptibility increases until a slope gradient of 45º to 50º. This is explained by the inclusion in the data set of a series of landslides just below the western ridgeline of the quadrant on steeply inclined terrain. Due to the distribution of slope angle classes, a relatively small number of landslides within the classes can skew the data significantly. In particular it will also be a function of the nature of the material in the steeply sloping terrain (e.g. whether it is rock or soil).

Figures ASE11, ASW11, ANW11 and ANE11 (Volume 2) show the distribution of landslide density with respect to slope aspect for each of the quadrants. Based on a review of all historic and recent landslide together, in general there is no significant correlation between landslide location and slope aspect within any individual catchment or within the whole Study Area. It was noted in the SWQ that a high proportion of the landslides did occur on slopes

with a north-easterly aspect, although this is probably due to a single cluster of landslides on northeast facing slopes and is not considered significant. It is therefore concluded that slope aspect is not a significant controlling factor for landslide susceptibility at Cloudy Hill.

Whilst no significant correlation with landslide susceptibility was identified when looking at the whole landslide record, it was noted that of the recent landslides inspected as part of this study over 56% of them occurred on slopes with a south or southwest aspect (Table 7), suggesting that slope aspect may be a notable controlling factor for landslide susceptibility for the recent landslides. As discussed in Section 6, the majority of these recent landslides are thought to have resulted from just two rainstorms that occurred in April 2000 and June 2001, for which the wind direction was from the south and southwest. Considering such a relationship was not observed for the landslide record as a whole, this would suggest that the apparent relationship between the slope aspect and the recent landslides could be a result of orographic effects. Slope aspect may be a controlling factor for landslide occurrence during a particular storm but cannot be used in determining susceptibility over a period of time.

Within the SEQ a comparison of slope angle susceptibility using point location (Figure ASE11) and source area (Figure ASE15) shows in general both methods give a broadly similar result. A similar comparison of slope aspect susceptibility using point location (Figure ASE11) and source area (Figure ASE16) indicates that the susceptibility of the various aspects to be broadly similar when the analysis is based on point location, but based on source area a significant susceptibility for northeast and east facing slopes was found.

It was noted that slope angle recorded in the field were generally 2º to 5º less than those taken from the DTM, furthermore slope aspects were generally found to be with +/-20º of those taken from the DTM, although occasional significant variation of about 40º were found. The reason for this variation is thought to the relatively coarse spacing of the grid used to derive the DTM.

8.1.4 Plan Curvature

Plan curvature maps of the quadrants are presented as Figures ASE12, ASW12, ANW12 and ANE12 (see Volume 2). A review of the maps indicates that 78%, 74%, 86% and 89% of the landslides occurred in areas of convergent flow for the SEQ, SWQ, NEQ and NWQ, respectively. Furthermore, many (estimated at about 75%) of the landslides occurred close (within about 20 m) to the boundary line between divergent and convergent flow (the zero line).

The reason for this apparent relationship is believed to relate to the geomorphological setting of the majority of the landslides that have occurred on Cloudy Hill (Section 7.4). The Type I landslides generally occur along distinct convex breaks in slope located below ridgelines, while the Type II landslides generally occur within hollows located at the heads of drainage line, also generally located below ridgelines. Both locations would generally tend to fall on or close to the boundary between divergent and convergent flow.

8.1.5 Solid Geology

Only limited information on the solid geology was available, and consequently no definitive relationship between solid geology and susceptibility can be made. A visual review of the geology plans (Figures ASE8, ASW8, ANW8 and ANE8 in Appendix A, Volume 2) does not indicate a clear relationship between landslide susceptibility and either the solid geology or geological structure. It was noted that in general very few landslides occurred in the debris flow deposits interpreted along the drainage lines.

It is possible that, to some extent, the relatively few landslides identified during the API in such areas may be a result of the often dense vegetation cover present along the drainage lines, even in the 1963 aerial photographs, as that would obscure the failure scars. The apparent low landslide susceptibility of the valley colluvium was verified during the field inspection of some of the drainage lines, where little or no evidence of either landslides or significant entrainment was observed (Section 5.2.3). In general, the interpreted solid geology within the Study Area is comparatively homogeneous, and only two significant faults have been interpreted. Consequently, it is to be expected that no significant relationship between landslide susceptibility and solid and structural geology could be identified.

8.1.6 Geomorphology and Regolith Mapping

The regolith map of the SEQ is shown as Figures ASE13 and ASE17 (Appendix A of Volume 2). Table 6 shows the slope area for each regolith class, the number of landslides that have occurred within the class and the resulting landslide density. In contrast to the landslide reference point located at the centre of the main scarp used in the analysis of the thematic maps, a reference point located at the crown of the landslide was used for this susceptibility analysis. The following susceptibility classes were assigned specifically for this study:

(a) very low (<10 landslides/year/km^2),

(b) low (10-50 landslides/year/km^2),

(c) moderate (50-200 landslides/year/km^2),

(d) high (200-600 landslides/year/km^2), and

(e) very high (>600 landslides/year/km^2).

The apparent susceptibility of the various regolith classes are discussed below.

As would be expected, no landslides were identified within the alluvium deposits (Al).

A very high susceptibility was indicated for areas interpreted with regolith class ‘Rv’ (intermittent exposed volcanic rock). This is likely to relate to the fact that exposed rock is often exposed on the relict surface of rupture of landslides scars, especially where multiple failures have coalesced to result in a near continuous band of exposed rock, such as in the north of the SEQ (Plate 30). In general, the regolith class ‘Rv’ was used in preference to ‘Bv’

(exposed volcanic rock), which was only used where single isolated rock exposure was observed.

A very high susceptibility was indicated for areas interpreted with regolith class 'Cd' (depression colluvium). This is attributable to the high proportion of Type II landslides within the SEQ, occurring within hollows located generally at the heads of drainage lines (Plates 21 and 29).

A moderate susceptibility was indicated for areas interpreted with regolith class 'Cr' (residual colluvium). Since this regolith class was generally interpreted as occurring on the less steeply inclined lower sideslopes and within material which has previously been mobilised and subsequently deposited on less steep terrain, such a moderately susceptibility is not unexpected.

A high susceptibility was indicated for areas interpreted with regolith class 'Crf' (rockfall debris). However, this result is not generally reliable because the regolith class occurred over only a very small portion of the Study Area and the high susceptibility was actually the result of a single landslide. This highlights the importance of examining the raw data in conjunction with the simple susceptibility analyses to avoid the use of potentially misleading results.

A low susceptibility was indicated for areas interpreted with regolith class 'Cv' (valley colluvium) based on the available data. This is consistent with site observations and the interpretation of the thematic maps.

The initial analysis indicated very high susceptibility for areas interpreted with regolith classes 'Cla' (recent landslide debris) and 'Clb' (relict landslide debris). However, inspections in the field generally do not concur with this finding and relatively few failures were observed to have occurred within either relict or recent landslide debris. This apparent high susceptibility is likely to be an anomaly resulting from the close proximity of many of the landslides, minor errors in the locations of landslides scars and debris trails on the thematic maps, temporal inconsistencies (i.e. a relict landslide shown as occurring on recent landslide debris where the recent landslide has occurred upslope, and clearly later than, the relict failure) and a statistical anomaly as a result of the relatively small proportion of the area classified as of these regolith classes. Hence a relatively small number of landslides occurring within these regolith classes would significantly skew the analysis. The analysis was manually edited in order to remove these inconsistencies. The revised analysis indicates a moderately low susceptibility for both regolith types. Again, this emphasizes the importance of close scrutiny of the raw data and cross checking against the field inspections.

A moderate susceptibility was indicated for areas interpreted with regolith class 'Sv(dw)' (deeply weathered volcanic saprolite). This is generally consistent with the site observations. The regolith class generally represents the upper landform unit (as described in Section 7.3) which usually comprises slightly convex planar slopes with relatively few landslides. Whilst the boundary between the upper and lower landforms is an active zone of instability, in general landslides that occur in the zone have fallen into one of the 'Sv' regolith classes (Plates 22 and 26).

A high susceptibility was indicated for areas interpreted with regolith classes 'Sv' (Volcanic Saprolite), 'Sv+B' (volcanic saprolite with a veneer of colluvium and boulders) and 'Sv+' (volcanic saprolite with a veneer of colluvium). This is generally consistent with site observations. Many of the Type I landslides occur within these regolith classes.

8.2 Mechanisms and Causes of Failure

8.2.1 General

The close correlation between rainstorms and the first observations of the recent landslides at Cloudy Hill confirms that the landslides are triggered by rainfall. Based on field observations and API, contributory factors include morphological setting, ripening of the terrain and erosion. It is noteworthy that the size of the catchments above most of the landslides tends to be very small, and for landslides below the ridgelines there are practically no catchments.

8.2.2 Type I Landslides

Type I landslides typically occur at prominent breaks in slope that delineate the limit of a zone of instability (''hillside retreat''). The process involved retrogressive failure of oversteepened slopes. The progressive deterioration of saprolite at the location of the Type I landslides, together with local adverse geological and/or groundwater conditions, can lead to landslides occurring at the same location over several tens of years, as evidenced by Landslide 01M (Section 5.3.2).

Based on the limited solid geology information available, the Type I landslides observed at Cloudy Hill do not appear to be significantly influenced by the underlying geology (rock type). The Type I landslides may however be influenced by the geological structure, and although a structural influence of the landslides at Cloudy Hill was not a key site observation, the presence of joints within the saprolite with orientations sub-parallel to the direction along which some of the landslides were mobilised may demonstrate a partial structural influence.

8.2.3 Type II Landslides

The failure mechanism of the Type II landslide is related to the morphological setting. It is likely that such landslides result from the development of perched water, within the depression colluvium, at the convergence of both surface and subsurface water flow. The relative permeability of the colluvium deposits compared with the underlying saprolite is conducive to the development of transient perched water tables above the interface during or following periods of intense rainfall. This results in a build-up of positive water pressure within the depression colluvium subsequently resulting in a sliding failure along the colluvium/saprolite interface. Erosion pipes are also likely to be more numerous at the location of hollows, and are considered to be a contributory cause of failure.

Type II landslides are interpreted as being related to a 'ripening' of the depression, with the gradual accumulation of depression colluvium until it reaches a critical level that is susceptible to failure. Since ripening is generally a slow and progressive process that takes place over a very long time, Type II landslides are unlikely to occur from the same location for a considerable period of time. The occurrence of 'ripening' is evidenced both by the observation of repeated failures from the same hollows based on the API, and the field inspection of the source areas of recent landslides, that were observed to have occurred within distinct hollows containing significantly thicker colluvial deposits than those on the surrounding hillside (Plate 29). Since Type II landslides are typically located at the heads of drainage lines, they have the greatest potential to develop into debris flows.

8.2.4 Other Landslides

Other open hillside type landslides observed at Cloudy Hill that are not of Types I or II, which are relatively rare, occur on planar side slopes, and do not appear to be related directly to topography. Observations at landslide 01N (Section 5.2), the only landslide of this type inspected, found a single colluvial layer, which is cobbly and bouldery in nature, and the development of tension cracks. Observations suggest that there may be a partial structural influence, although the underlying solid geology does not appear to be an influencing factor, since the failure has primarily occurred along the colluvium/saprolite boundary. The most probable mechanism of failure is the development of a perched water table over the colluvium/saprolite interface. From just one landslide of this type inspected in detail as part of the study, there was insufficient evidence to allow for the definition of a third landslide model.

The small landslides that occur adjacent to stream courses and near to the axes of the drainage lines are most probably caused by the undercutting action of the stream. These landslides are more commonly located on the outside bends in the stream course where erosion is greatest.

9. DISCUSSION

9.1 Geomorphological Regolith Mapping

Most of the landslides at Cloudy Hill are shallow and occur within superficial horizons (mostly colluvium). Field inspections of individual landslides show that the solid geology generally has no direct influence. It is found instead that factors controlling landslide susceptibility at Cloudy Hill relate primarily to the nature of the regolith and morphology of the terrain and regolith mapping has therefore proved very useful.

Regolith mapping requires interpretation of indicative terrain attributes rather than primary observation of sub-surface information. This is straight forward for certain units such as areas of exposed rock but much greater judgment is required to decide whether, for example, a featureless hillside is underlain by deeply weathered saprolite or by relict colluvium ('residual colluvium'). This judgment will limit the repeatability. Furthermore, the methodology adopted here for mapping may not be directly transferable to other areas where

terrain and geological settings are different. Refinements may be required to optimize the mapping techniques.

9.2 Landslide Mobility

The travel angle of the debris, as defined by Cruden & Varnes (1996), is measured from the crest of the scarp to the distal end of the debris and this concept is simple and appropriate in risk assessments in that it reflects directly the debris influence zone. It also resembles closely the rate of energy loss during debris movement and incorporates the effect of downslope gradient.

In the case of man-made slopes where the downslope gradient is usually fairly flat and the length of the downslope path is not significant, the travel angle concept generally provides a reasonable resolution in predicting the debris travel distance and thus can be adopted in consequence assessments. Natural terrain landslides, however, are somewhat different in that they usually involve a comparative steep downslope profile and the use of the travel angle alone in consequence assessment may not be sufficient. This is due to the comparatively poor resolution in predicting debris travel distance because of the relatively small difference between the downslope angle and the travel angle.

The travel distance of the debris from the recent landslides ranged from 10 m to 250 m measured from the landslide crown to the distal end of the debris lobe. Travel angles ranged between 12° and 42°. The average travel distance is about 80 m with a corresponding average travel angle of about 30°. The terrain in the vicinity of the source location of the recent landslides varied in inclination between 24° and 42°, although the majority (over 75%) of the landslides occurred on terrain inclined at angles greater than 34°. It is apparent that landslide 01EE (source volume of about 90 m^3), with a travel distance of 125 m and a travel angle of 12°, was a particularly mobile landslide. There was very little evidence of entrainment (<2 m^3) and the run-out distance was clearly influenced by the landslide debris running directly into a drainage line which, although not steep, did possess a regular base and a near linear alignment.

Debris from most of the 34 inspected landslides ran into drainage lines, either immediately below the source or a short distance (20 m to 30 m) below the source. In the case of landslide 00C, the debris was channelised for a distance of over 200 m. Notably there was only minor (<3 m^3) entrainment. Based on the estimated overall travel distance of 250 m for landslide 00C, the estimated travel angle is about 42°, which according to Wong & Ho (1996a) is indicative of a landslide with low mobility for man-made slope failures. However, for natural terrain failures, the travel angle will be influenced by the steep gradient of the stream channel immediately below the landslide source and it may therefore not be sufficient to rely on the travel angle alone as an indicator of landslide mobility without refining it with reference to the morphology of the debris path. This applies particularly to channelised debris flows where other factors such as surface water flow and temporary debris damming of the stream course could be important influencing factors.

The travel angles of the recent landslides were plotted against landslide volume (Figure 12) and differentiated by landslide type, in order to assess the mobility of landslide types with respect to volume. The resultant plot closely correlates with that of Parry (2001).

The plot indicates that the travel angles of Type I landslides vary within a narrow rage of between 25° and 37°, while the travel angles of the Type II landslides are significantly more variable at between 12° (landslide 01EE) and 42° (landslide 00C). However, significantly fewer Type I landslides were identified from the recent landslides at Cloudy Hill, which may partially explain the lack of scatter. Only one sizeable open hillside failure was identified (landslide 01N), the debris from which was also partially channelized. No attempt has been made therefore to differentiate between open hillside and channelized failures.

The travel angles of landslides identified from the aerial photograph interpretation (Figure 13) fall within the ranges identified for landslides from field inspections. However, differentiation of landslide by type was not feasible from the aerial photographs and because the distal end of the debris lobe is often obscured by dense vegetation along drainage lines, the estimated travel distances are prone to greater errors than for the recent landslides. It would appear that the run-out distances of the debris from the landslides at Cloudy Hill have been influenced by the morphological setting of the landslides and the inclination of the terrain below the sources. Very little (<5 m³) entrainment occurred as a result of the recent landslides. It is also apparent that for the smaller landslides the dense vegetation present within the drainage lines at Cloudy Hill has limited the travel distance of the debris.

9.3 Landslide Volume

The recent landslides at Cloudy Hill had estimated source volumes ranging from 12 m^3 to 630 m^3. The average estimated landslide volume was about 100 m^3 but less than a third (10 out of 34) of the landslides inspected had an estimated volume greater than 100 m^3.

The volume of a Type II landslide is influenced by the physical dimensions of the hollow within which the source is located, and in general the Type II landslides observed at Cloudy Hill had estimated volumes of less than 250 m^3 (Figure 12). There are less physical constraints for Type I landslides, which, although typically observed to be minor failures of less than 50 m^3, can be significantly larger in volume as demonstrated by Landslides 00B and 01B with volumes of 550 m^3 and 360 m³ respectively (Table 7 and Figure 12).

The landslides greater than 500 m^3 in volume were landslides 00B and 01N. Landslide 00B (volume = 550 m³), a Type I landslide, involved the mobilisation primarily of a thin veneer of colluvium and a small proportion of the underlying saprolite. The landslide debris travelled into a drainage line below the source toe and is estimated to have travelled a total distance of about 150 m with minor (<5 m³) entrainment. Landslide 01N (volume = 630 m³) was the only open hillside failure and was characterised by a tension crack of about 42 m in length. Much of the debris (about 400 m^3), a bouldery colluvium, remained within the source area as intact rafts. The debris (about 250 m^3) travelled into a poorly defined drainage line below the source and travelled a distance of about 85 m.

9.4 Rainfall Characteristics

A detailed evaluation of the rainfall relating to the landslide events has not been possible due mainly to the uncertain timing of the occurrence of the landslides and partly the large distance of the nearest raingauges from the Cloudy Hill area. Furthermore, the available

Table of Contents
Table of Contents
Table of Contents
Table of Contents

rainfall data are from raingauges located at low altitude within the valleys surrounding Cloudy Hill and these data may not adequately account for the orographic influences. Nevertheless, the available rainfall data provide an useful indication of the characteristics of the rainstorms that probably resulted in recent landslides.

An indication of the severity and intensity of the June 2001 rainstorm is given by the 4-hour rolling rainfall of 225.5 mm, for the period ending at 11:00 hrs on 9 June 2001, recorded by GEO raingauge No. N05. This is the most severe 4-hour rainfall ever recorded by raingauge No. N05, with an estimated return period of about 22 years. Rainfall over the 11-hour period ending at 14:00 hrs on the 9 June 2001 preceding the landslides (Figure 9) was the most severe when compared with previous rainstorms recorded by raingauge No. N05.

The temporal distribution of landslides in each of the quadrants is shown in Figure 14, which also presents the years for which aerial photographs are available. Figure 14 shows that a significant number of landslides occurred at Cloudy Hill in 1982, to a lesser extent in 1993, and again in 2000 and 2001. Notably few landslides are identified at the Cloudy Hill area in 1997, which is the wettest year to date for Hong Kong generally. However, no significantly severe storms were recorded at raingauge No. N05 in 1997 (Figure 9). Franks (1998) infers that as well as a high antecedent rainfall, a sustained level of heavy rainfall over a period of in excess of 1 hour is required to cause widespread landsliding in natural terrain. The maximum rolling rainfall thresholds suggested by Franks (1998) for 1-hour and 4-hour periods of 90 mm and 200 mm respectively compare closely with those recorded at raingauge No. N05 for the 9 June 2001 rainstorm (Table 8). The 24-hour rolling rainfall (i.e. 315 mm) is also above "Threshold II" suggested by Evans (1997), for the "start of landsliding at medium densities (1-10/sq km)" for areas where the mean annual rainfall is greater than 2400 mm.

The 6 August 1994 and 24-25 June 1996 rainstorms had 24-hour rolling rainfall greater than the 9 June 2001 rainstorm (Figure 9), but apparently fewer landslides occurred at Cloudy Hill. Since the 1-hour and 4-hour rolling rainfalls were significantly less for both the 6 August 1994 and 24-25 June 1996 rainstorms than for the 9 June 2001 rainstorm, it would therefore appear that the 1-hour and 4-hour rolling rainfall thresholds are significant for triggering natural terrain landslides. Following the June 2001 rainstorm both Type I and Type II landslides were observed to have occurred at Cloudy Hill. There appears to be no direct correlation between specific rainstorm characteristics and the type of landslide induced.

The 2000 and 2001 landslides at Cloudy Hill were observed to have occurred on slopes with a generally southerly aspect, which does not conform with the general observation of Evans et al (1997), from the Natural Terrain Landslide Inventory (NTLI) data, that landsliding on south-facing slopes is less common. This is possibly explained by the fact the predominant wind direction for the rainstorm on the 9 June 2001 that triggered the landslides was from the south over the longer term and there appear to be no general landslide susceptibility-slope aspect relationship

9.5 Variations in Landslide Characteristics between Quadrants

A review of the thematic maps in Volume 2 generally indicates that many of the characteristics of the quadrants are similar.

Table of Contents
Table of Contents
Table of Contents
Table of Contents

A review of the landslide density maps indicates apparently significantly fewer landslides in the SWQ and significantly higher density of landslides in the SEQ. The higher apparent landslide density in the SEQ is however due in the main part to the recording of additional, generally minor relict landslides, during the detailed regolith mapping based on observations from enlarged aerial photographs and orthophotographs based on the 1963 aerial photographs. This process was not done for the SWQ. Nevertheless, disregarding this fact there is still an anomalously low density of landslides in the SWQ. As shown in Figure ACH1, prior to the identification of these additional relict landslides during field mapping, the landslide density within the SEQ, NWQ and NEQ was similar. The lower landslide density observed in the SWQ quadrant is probably a result of a number of factors including:

(a) the significantly higher vegetation cover within the quadrant which would have the affect of both stabilising the hillside and obscuring the landslide scars and thereby preventing their identification during the API, and

(b) almost all the landslides observed in the SWQ appear to be of Type II. In this quadrant, there are no areas of ‘‘hillside retreat’’ (where Type I landslides would occur).

From detailed field inspections of the landslides, it was found that the geomorphological setting, characteristics, causes and mechanisms of the recent landslides were similar between the quadrants, except for the SWQ.

9.6 Factors Affecting Landslide Susceptibility

A review of the thematic maps and regolith mapping at Cloudy Hill indicates that a complex combination of interconnected factors control landslide susceptibility, of which the most critical factors are slope angle, regolith type, morphological setting and geomorphological development (terrain maturation). The relative influence of these factors has been assessed here using multi-variant statistical analysis.

The distribution of landslides with respect to different terrain attributes (slope, aspect, proximity to landform boundary etc.) can be investigated by making an assessment of the proportion of landslides that are inside and outside the areas occupied by these attributes. The proportion of landslides can be determined by:

(a) Treating the landslides as point sources and counting the number of points inside and outside the area occupied by an attribute, or

(b) Treating the landslides as area sources (see for example Figure No. ASE17) and determining the proportion of the surface area of landslides source area inside and outside the area occupied by an attribute.

Both methods are correct and generally give broadly similar results, although it was found the similarity varies depending on which specific factor is being compared and most probably between sites. One perceived benefit of the point source calculation is that it is simple and easy to apply and check. The area source calculation is computationally more time consuming and typically is carried out using GIS methods. Although the calculation is simple it is difficult to check by a third party without access to the data. One benefit of the area source calculation is that landslide area correlates well with volume and therefore leads better into more detailed assessments involving relationships between landslide frequency and volume. A possible future approach could be to use a combination of both point location and source areas for the various factor been examined, depending of which method gives the optimum susceptibility for the specific factor.

9.7 Hazard Assessment

The classification of landslide type based on the geomorphological models developed for this study, allows inferences to be made on the nature of the hazard generated. Figure G5 in Appendix G of Volume 3 shows a preliminary hazard assessment based on the geomorphological models developed. Areas of high hazard include:

(a) The boundary between the upper and lower landforms, which represents the zone where Type I landslides occur. Such landslides can potentially be large and deep-seated. Based on site observations at Cloudy Hill, typically the landslides involve multiple minor failures of an oversteep main scarp and generally have relatively high travel angles. As the multiple failures often result in the formation of what appears to be a single, very large landslide scar, there is a danger that this can be misinterpreted, thereby resulting in significant over-estimate of the design event.

(b) Well defined hollows located at the heads of minor drainage lines just below ridgelines, which represent the zones of Type II landslides. As the landslide sources are located directly above drainage lines, there is a high propensity for such landslides to develop into channelised debris flows. Furthermore, it has been observed that such landslides will often occur as multiple events frequently within the same catchment or even the same flank of a catchment during a single rainstorm event. The resulting coalescence of the debris may result in relatively large debris flows and possibly the formation and breaching of debris dams, resulting in significantly high travel distances.

9.8 Key Observations

Key observations from this study include:

(a) While API is an essential tool for the identification and characterisation of historic landslides within a Study Area, care should be taken when estimating parameters from API alone. Where possible the interpreted parameters should be confirmed by ground truthing. In particular, it has proved very difficult to identify and characterise rock failures from API, especially on steep terrain, and distinguish between single and multiple relict failures.

(b) For Cloudy Hill, a significant correlation was found between landslide susceptibility and morphological setting. This was used to develop two simple geomorphological landslide models, each with distinct field characteristics. This approach allowed individual landslides to be categorised, commonality between the landslides recognised and a simplified geomorphological model of the Study Area to be developed.

(c) Classifying the observed landslides based on the geomorphological setting of their sources was found to be useful when studying the commonality in characteristics and factors affecting the susceptibility of natural terrain landslides.

(d) Use of accurate, high quality orthophotographs based on low level aerial photographs with minimal vegetation cover (i.e. the 1963 aerial photographs) was found to be critical for the study, and in particular the regolith mapping.

(e) There are potentially significant advantages for susceptibility assessments to be based on quantitative factors, such as slope angle and plan curvature that can be generated automatically, and supplemented by qualitative expert interpretation, such as geomorphological mapping.

(f) The use of multi-variant analyses in establishing apparent correlations in a ‘black-box’ manner with inadequate field validation and careful consideration of the reliability of the data could potentially lead to misleading results. The numerical complexity and apparent statistical fit may in fact provide a false sense of accuracy.

9.9 Further Studies and Recommendations

Whilst the thematic maps and regolith maps include considerable geomorphological data, a single comprehensive engineering geomorphological map of the Study Area was not prepared. Based on the lessons learnt during the study, it is considered that such a map would potentially be very useful for identifying specific hazards and in developing hazard maps of the site. Such maps cannot be prepared from API alone and require a significant element of field work in order to facilitate a comprehensive assessment.

Based on site observations and API, it is not possible to make more than a preliminary model of the likely subsurface hydrogeological process which occurs during and after a rainstorm. In order to understand and relate these critical processes to landslide events and setting, valuable information could be obtained by installing a line of piezometers from a ridgeline downslope to a drainage line and using an automatic data logger to monitor the fluctuations in pore pressure within the rock mass, saprolite and overlying superficial deposits. Ideally, a temporary weather station should be installed for better interpretation of the data.

A preliminary attempt to develop a susceptibility map based on plan curvature and slope angle for the SEQ is presented in Figure ASE14 of Appendix A. While the map produced, indicates a reasonable correlation between areas of high and very high susceptibility to landslide sources for the SEQ, it is difficult to come up with a susceptibility model that gives good correlation with the overall landslide data. The relative importance of the various structural, hydrogeological, topographical and geomorphological factors may be different for other sites.

A further attempt to develop a susceptibility map based on several factors is presented in Section 4.1.2 and Figures ASE22 and ASE23 in Appendix A. It is noted that the ratio of predicted annual landslide frequency of 'Very High' susceptibility and 'Very Low' susceptibility is about 20 to 25. For predictive purposes it would be desirable to be able to have a better resolution in respect of the relative degrees of susceptibility.

With respect to the slope angle and aspect analysis, it was noted that not only did the use of different grid sizes result in large variations in slope or aspect distribution, but also the different software packages resulted in significantly different distributions.

9.10 Comparison with Tsing Shan

As the Tsing Shan Area Study Report has yet to be published, it is not possible to make detailed comparison between the two Study Areas. However, based on observations from the Landslide Study Report entitled Detailed Study of Selected Landslides above Leung King Estate of 14 April 2000 (Halcrow China, 2001), the following differences to the Tsing Shan area were observed:

(a) No areas of persistent surface erosion were found at Cloudy Hill.

(b) With the exceptions of areas of exposed rock in the north of the SEQ, little or no exposed rock was found within the Cloudy Hill Study Area.

(c) Where rock is exposed, persistent stress relief jointing was not found.

(d) Inspection of the drainage lines at Leung King identified extensive areas of entrainment and many minor failures of oversteep flanks to the channels, particularly where the direction of the channel altered. No such areas of entrainment or instability were found at Cloudy Hill during the API or field inspections.

(e) The characteristics of the failures were generally very different for the two Study Areas. At Leung King, the failures were generally controlled by adversely orientated joints (generally sheeting joints) and occurred within a rock mass which showed significant signs of deterioration. The Cloudy Hill failures generally occurred either within colluvium or on oversteep breaks in slope within the saprolite. Only occasional evidence was found of structural control or pre-failure disturbance of the rock mass.

(f) While a number of the landslides at Leung King were due to anthropogenic disturbance of the natural terrain (i.e. past mining activities), there was little evidence of landslides caused by such disturbance at Cloudy Hill.

10. CONCLUSIONS

Detailed analysis of a wide range of available information, including data obtained from field inspection, desk study and API has been carried out for this study. However, only focussed field mapping of selective landslides was carried out and not extensive field mapping of the whole Study Area due to time and access constraints. The following key observations from the study should therefore be viewed in perspective, bearing in mind the above stated constraints.

Based on a correlation of over 700 landslides with the thematic maps prepared for this study, the key factors that probably control landslide susceptibility within the Study Area include:

(a) slope angle (with typically about 80% of all landslides having occurred within a terrain gradient of 25º to 40º),

(b) morphological setting (where approximately 97% of the inspected landslides occurred within well defined hollows

located at the heads of minor drainage lines, below ridgelines or at distinct breaks in slope),

(c) plan curvature (where approximately 82% of all landslides occurred within areas of convergent flow, generally close to the boundary between divergent and convergent flow), and

(d) nature of the regolith.

The regolith mapping and subsequent susceptibility analysis provide a useful tool for terrain characterisation and a basis for identifying areas of high landslide susceptibility. As it is a finding of this study that the critical factors probably controlling landslide susceptibility at Cloudy Hill relate primarily to the nature of the regolith and the morphology of the terrain, the technique is considered to be useful and in generally applicable for Cloudy Hill. The process does however require experienced staff with an understanding of local geomorphological and geological conditions and extensive field mapping with particular reference to the likely hillside processes.

Based on the observed geomorphological characteristics, geomorphological models are proposed for the landslides at Cloudy Hill. The models presented have allowed individual landslides to be categorised, commonality between the landslides to be recognised and an overall geomorphological model of the site to be developed. The proposed geomorphological models may potentially allow better prediction as part of a natural terrain hazard assessment. Adoption of such models can add value to an approach in which landslides are classified only on factors such as size, mechanism of failure and mobility of the resulting debris.

Based on the apparent correlation between landslide occurrence and zero plan curvature line (i.e. the boundary between divergent and convergent flow) and with slope angle, a quantitative landslide susceptibility map has been prepared. A visual review of the map indicates a good correlation was achieved, although further work would be required to verify the validity of the proposed methodology and the applicability to other sites in Hong Kong.

The field inspections of the 2000 and 2001 landslides on Cloudy Hill revealed that the majority of the landslides are relatively shallow (<2 m from the ground surface) sliding failures that occurred either along the colluvium/saprolite boundary or just within the saprolite. Landslides are typically situated at the heads of drainage lines or at breaks in slope on the flanks of drainage lines and below ridgelines.

Field inspection along the drainage lines revealed significant deposits of colluvium, but based on the available aerial photographs there was little evidence of entrainment or initiation of landslides within these colluvial deposits.

11. REFERENCES

Binnie, Deacon & Gourley (1962). Full Report on the Plover Cove & Hebe Haven Water Scheme. Volume III.

Cruden, D.M. & Varnes, D.J. (1996). Landslide Types and Processes: A.K. Turner & R.L. Schuster, Landslides: Investigation and Mitigation. Transportation Research Board Special Report No. 247, National Research Council, National Academy Press, Washington, D.C., pp 36-75.

Degraff, J.V. & Canuti, P. (1988). Using Isopleth Mapping to Evaluate Landslide Activity in Relation to Agricultural Practices. Bulletin of the International Association of Engineering Geology, vol. 38, pp 10-19.

Evans, N.C. (1997). The Natural Terrain Landslide Study. Preliminary Assessment of the Influence of Rainfall on Natural Terrain Landslide Initiation. Discussion Note No. DN 1/97. Geotechnical Engineering Office, Hong Kong, 28 p.

Evans, N.C. Huang S.W. & King J.P. (1997). The Natural Terrain Landslide Study. Phases I and II. Special Projects Report No. SPR 5/97. Geotechnical Engineering Office, Hong Kong, 119 p.

Evans, N.C. & King J. P. (1998). The Natural Terrain Landslide Study. Debris Avalanche Susceptibility. Technical Note No. TN 1/98. Geotechnical Engineering Office, Hong Kong, 96 p.

Franks, C.A.M. (1998). Study of Rainfall Induced Landslides on Natural Slopes in the Vicinity of Tung Chung New Town, Lantau Island. Geotechnical Engineering Office, Hong Kong, 102 p. plus 3 drgs. (GEO Report No. 57).

Geotechnical Control Office (1988). Geotechnical Area Studies Programme - North New Territories. Geotechnical Control Office, Hong Kong, GASP Report No. V, 135 p. plus 4 maps.

Geotechnical Control Office (1991). Sheung Shui: Solid and Superficial Geology, Hong Kong Geological Survey, Map Series HGM 20, Sheet 3, 1:20,000 scale. Geotechnical Control Office, Hong Kong.

Hansen, A. (1984). Engineering geomorphology: The application of an evolutionary model of Hong Kong's terrain. Zeitschrift fur Geomorphologie, supplementary vol. 51, pp 39-50.

Halcrow China Ltd (2001). Detailed Study of Selected Landslides above Leung King Estate of 14 April 2000. Landslide Study Report No. LSR 9/2001, Geotechnical Engineering Office, Hong Kong, 140 p.

Lai K. W., Campbell S. D. G. & Shaw R. (1996). Geology of the Northeastern New Territories. Hong Kong Geological Survey Memoir No. 5. Geotechnical Engineering Office, Civil Engineering Department, 144 p.

Lam, C.C. & Leung, Y.K. (1994). Extreme Rainfall Statistics and Design Rainstorm Profiles at Selected Locations in Hong Kong. Royal Observatory, Hong Kong, Technical Note No. 86, 89 p.

Table of Contents
Table of Contents
Table of Contents
Table of Contents

Maunsell Consultants Asia Ltd. (1986). Tai Po Borrow Area H Final Excavation Stability Evaluation.

Maunsell Geotechnical Services Ltd. and ERM-Hong Kong Ltd (1999). Territory Wide Quantitative Risk Assessment of Boulder Fall Hazards, Stage 1. Report to Geotechnical Engineering Office, Hong Kong, 116 p. plus Appendices A-H.

Maunsell Geotechnical Services Ltd. and Fugro (Hong Kong) Ltd. (2002). Pilot Study Regolith Guide, Rock Guide and Field Mapping Proformas. Natural Terrain Hazard Study for Tsing Shan Foothill Area. Agreement No. CE 47/2000.

Ng, K. C., Parry, S., King, J. P., Franks C. A. M. & Shaw, R. (2002). Guidelines For Natural Terrain Hazard Studies. Special Project Report No. SPR 1/2002. Geotechnical Engineering Office, Hong Kong, 136 p.

Parry, S. (2001). Natural Terrain Hazard Study Shek Pik. Advisory Report No. ADR 2/2001, Geotechnical Engineering Office, Hong Kong, 60 p. plus 3 drgs.

Scott Wilson (Hong Kong) Ltd. (1999). Specialist API Services for the Natural Terrain Landslide Study – Task B Factual Report. Report to Geotechnical Engineering Office, Hong Kong, 9 p. plus 4 Appendices.

Sewell, R. J., Campbell, S. D G., Fletcher, C. J. N., Lai, K. W. & Kirk, P. A. (2000). The Pre-Quaternary Geology of Hong Kong. Geotechnical Engineering Office, Hong Kong, 181 p. plus 4 maps.

Wong, H.N. & Ho, K.K.S. (1996a). Travel distance of landslide debris. Proceedings of the Seventh International Symposium on Landslides, Trondheim, Norway, vol. 1, pp 417-422.

Wong, H.N. & Ho, K.K.S. (1996b). Thoughts on the Assessment and Interpretation of Return Periods of Rainfall. Discussion Note DN 2/96, Geotechnical Engineering Office, Hong Kong, 12 p.

LIST OF TABLES

Table 1 –SE Quadrant - Landslide Densities and Slope Angle Areas for Each Slope Angle Class

Slope Angle class	Area (m^2)	Area (km^2)	No. of landslide	Landslide Densities (per km^2)
0° to 15°	109858.00	0.110	2	18.21
15° to 20°	22765.76	0.023	5	219.63
20° to 25°	42309.04	0.042	5	118.18
25° to 30°	112645.39	0.113	17	150.92
30° to 35°	160985.40	0.161	80	496.94
35° to 40°	148491.29	0.148	90	606.10
40° to 45°	96431.10	0.096	85	881.46
45° to 50°	42971.99	0.043	40	930.84
50° to 55°	13681.92	0.014	5	365.45
55° to 60°	3116.42	0.003	0	0.00
>60°	1286.10	0.001	0	0.00

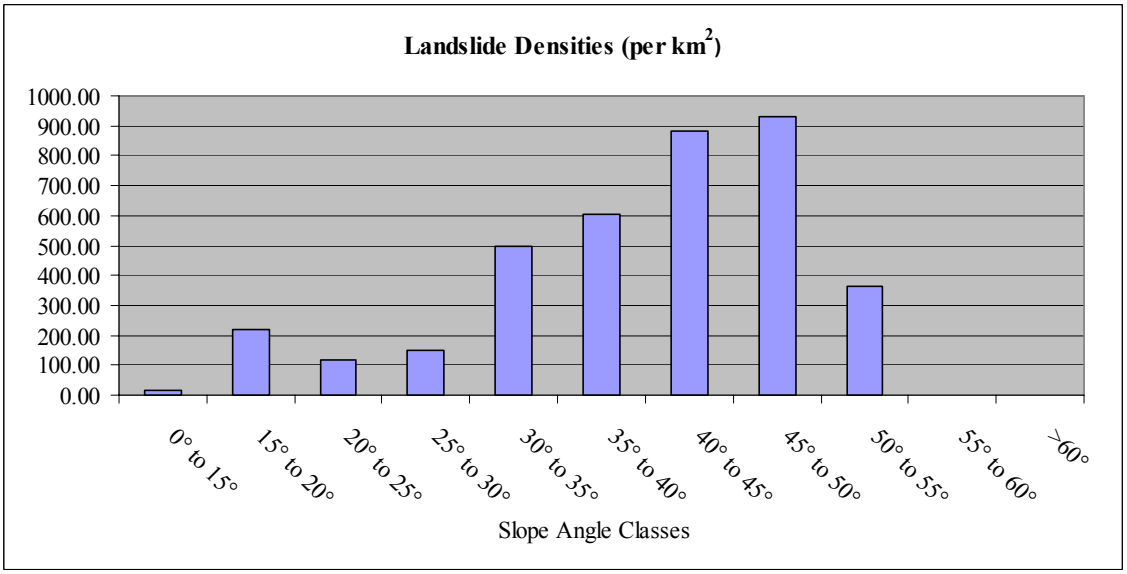

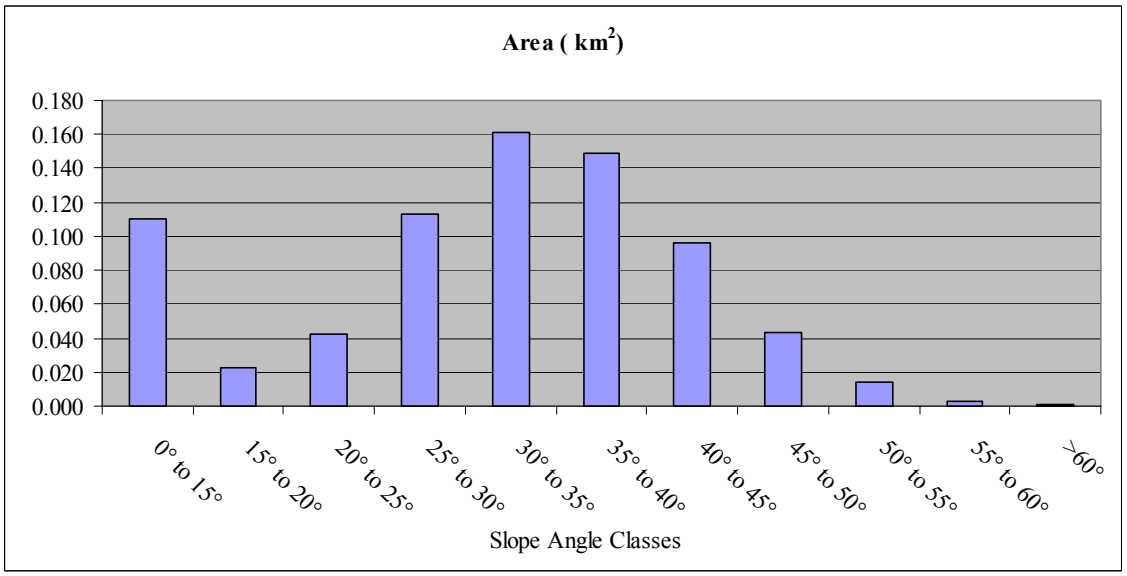

Table of Contents
Table of Contents
Table of Contents
Table of Contents

Table 2 –SW Quadrant - Landslide Densities and Slope Angle Areas for Each Slope Angle Class

Slope Angle class	Area (m^2)	Area (km^2)	No. of landslide	Landslide Densities (per km^2)
0° to 15°	87800.15	0.088	0	0.00
15° to 20°	134147.06	0.134	1	7.45
20° to 25°	214876.89	0.215	13	60.50
25° to 30°	281916.62	0.282	20	70.94
30° to 35°	204193.65	0.204	31	151.82
35° to 40°	110182.10	0.110	19	172.44
40° to 45°	39554.60	0.040	4	101.13
45° to 50°	12249.28	0.012	0	0.00
50° to 55°	1394.15	0.001	0	0.00
55° to 60°	0.00	0.000	0	0.00
>60°	0.00	0.000	0	0.00

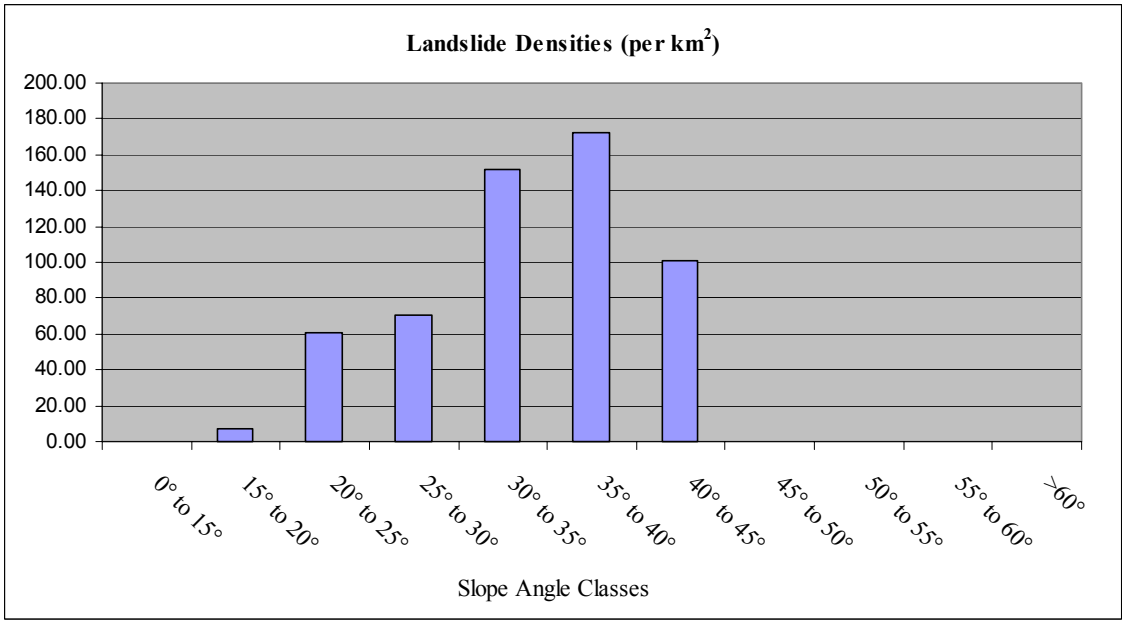

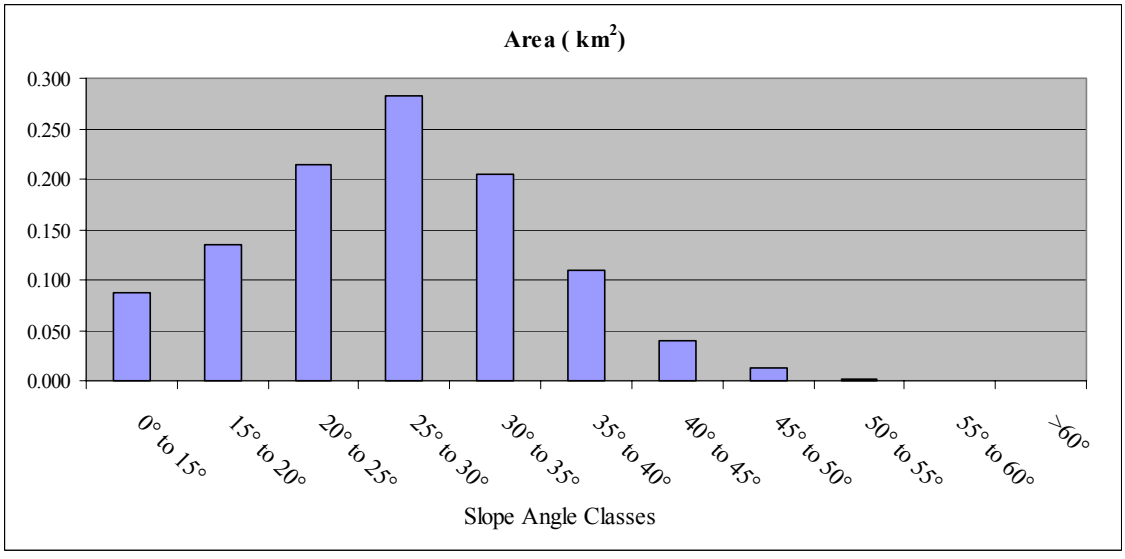

Table of Contents
Table of Contents
Table of Contents
Table of Contents

Table 3 –NW Quadrant - Landslide Densities and Slope Angle Areas for Each Slope Angle Class

Slope angle class	Area (m^2)	Area (km^2)	No. of landslide	Landslide Densities (per km^2)
0° to 15°	94739.75	0.095	0	0.00
15° to 20°	122251.17	0.122	3	24.54
20° to 25°	225549.30	0.226	19	84.24
25° to 30°	369163.01	0.369	58	157.11
30° to 35°	296960.84	0.297	69	232.35
35° to 40°	119103.83	0.119	27	226.69
40° to 45°	26081.31	0.026	4	153.37
45° to 50°	1472.56	0.001	0	0.00
50° to 55°	0.00	0.000	0	0.00
55° to 60°	0.00	0.000	0	0.00
>60°	0.00	0.000	0	0.00

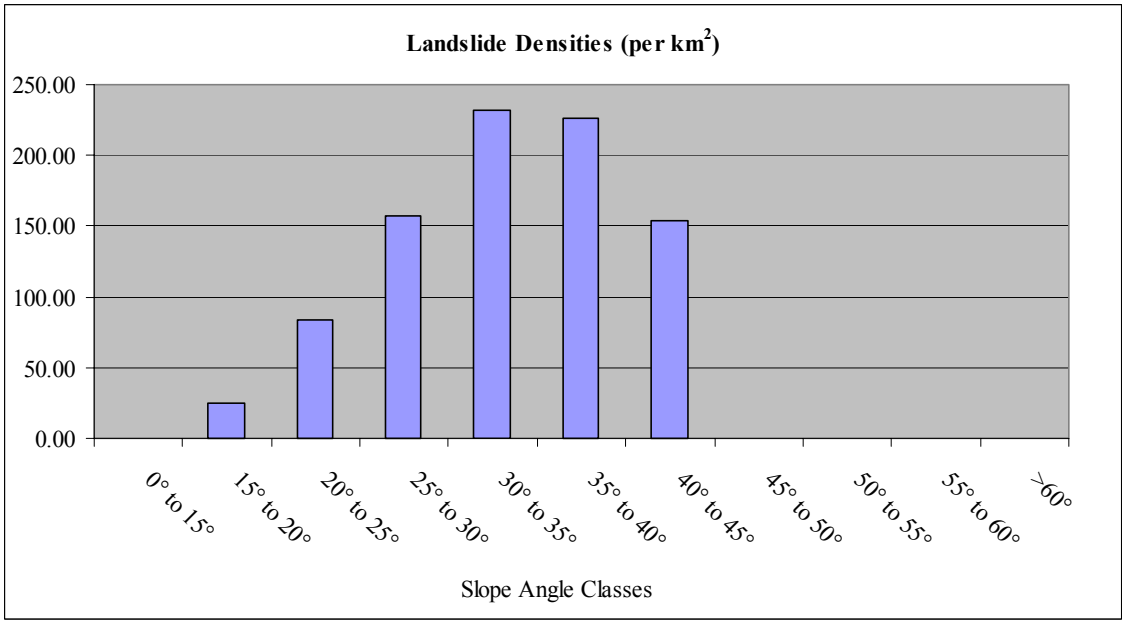

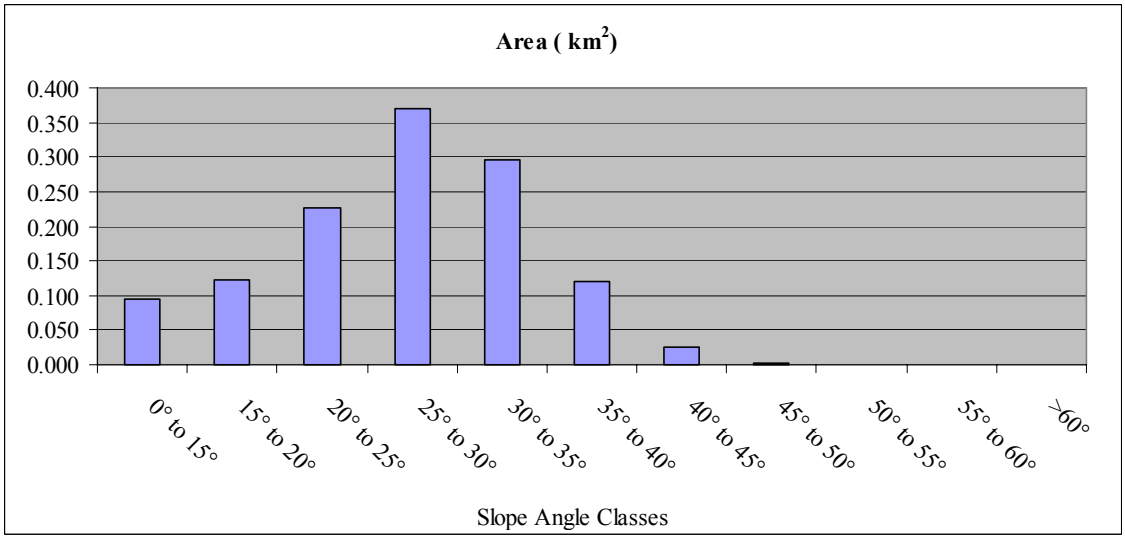

Table of Contents
Table of Contents
Table of Contents
Table of Contents

Table 4 – NE Quadrant - Landslide Densities and Slope Angle Areas for Each Slope Angle Class

Slope angle class	Area (m^2)	Area (km^2)	No. of landslide	Landslide Densities (per km^2)
0° to 15°	67317.14	0.067	0	0.00
15° to 20°	82575.03	0.083	1	12.11
20° to 25°	154733.83	0.155	12	77.55
25° to 30°	246670.84	0.247	42	170.27
30° to 35°	105503.62	0.106	36	341.22
35° to 40°	15545.16	0.016	5	321.64
40° to 45°	823.07	0.001	0	0.00
45° to 50°	0.00	0.000	0	0.00
50° to 55°	0.00	0.000	0	0.00
55° to 60°	0.00	0.000	0	0.00
>60°	0.00	0.000	0	0.00

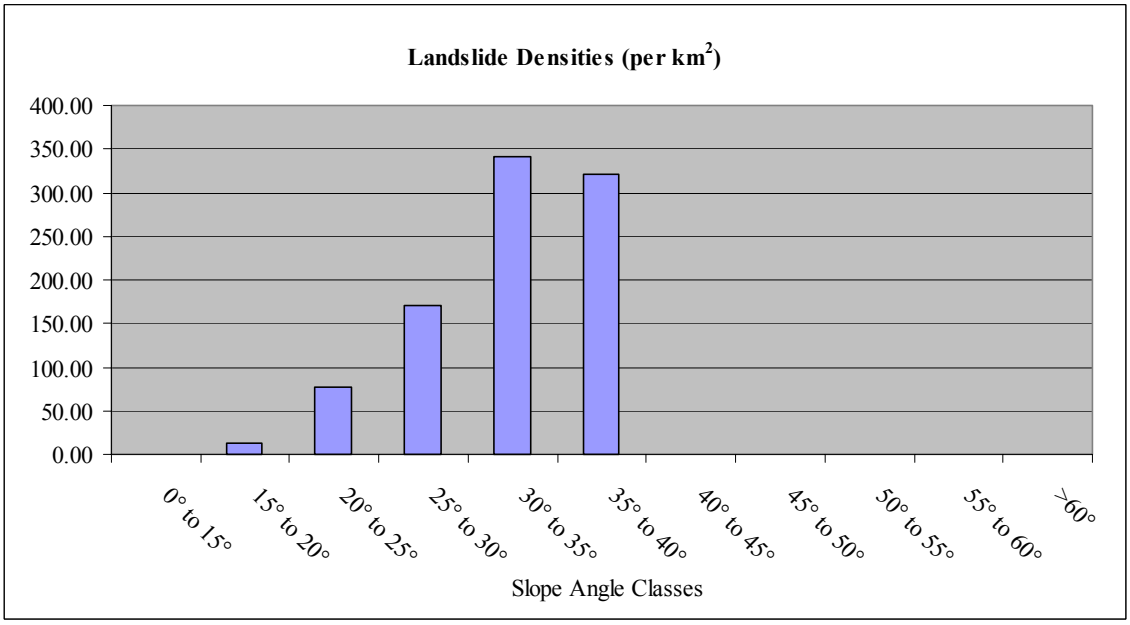

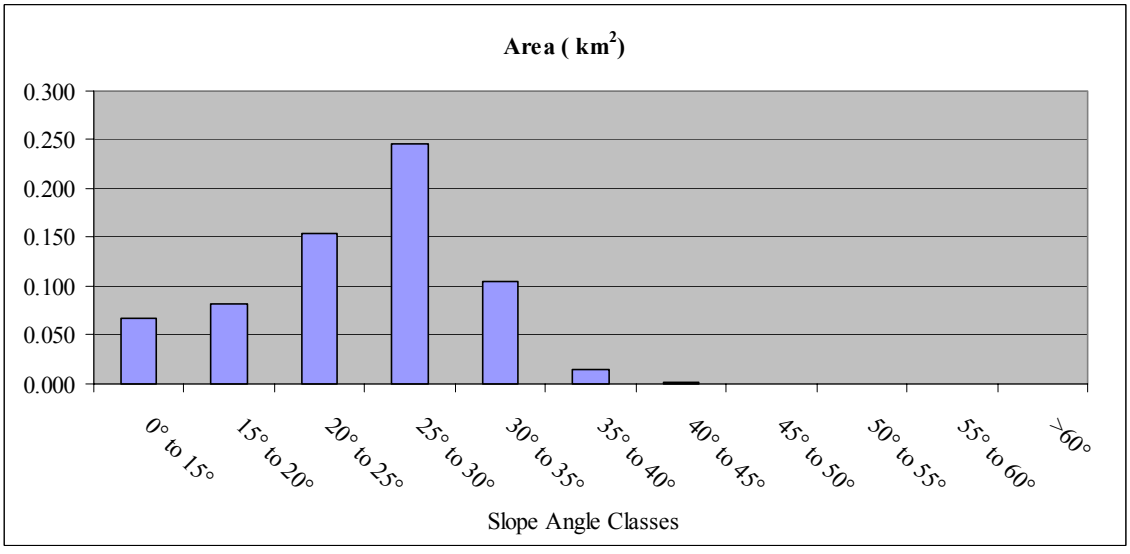

Table of Contents
Table of Contents
Table of Contents
Table of Contents

Table 5 – All Quadrants - Landslide Densities and Slope Angle Areas for Each Slope Angle Class

Slope angle class	Area (m^2)	Area (km^2)	No. of landslide	Landslide Densities (per km^2)
0° to 15°	359715.04	0.360	2	5.56
15° to 20°	361739.02	0.362	10	27.64
20° to 25°	637469.06	0.637	49	76.87
25° to 30°	1010395.85	1.010	137	135.59
30° to 35°	767643.51	0.768	216	281.38
35° to 40°	393322.38	0.393	141	358.48
40° to 45°	162890.09	0.163	93	570.94
45° to 50°	56693.82	0.057	40	705.54
50° to 55°	15076.07	0.015	5	331.65
55° to 60°	3116.42	0.003	0	0.00
>60°	1286.10	0.001	0	0.00

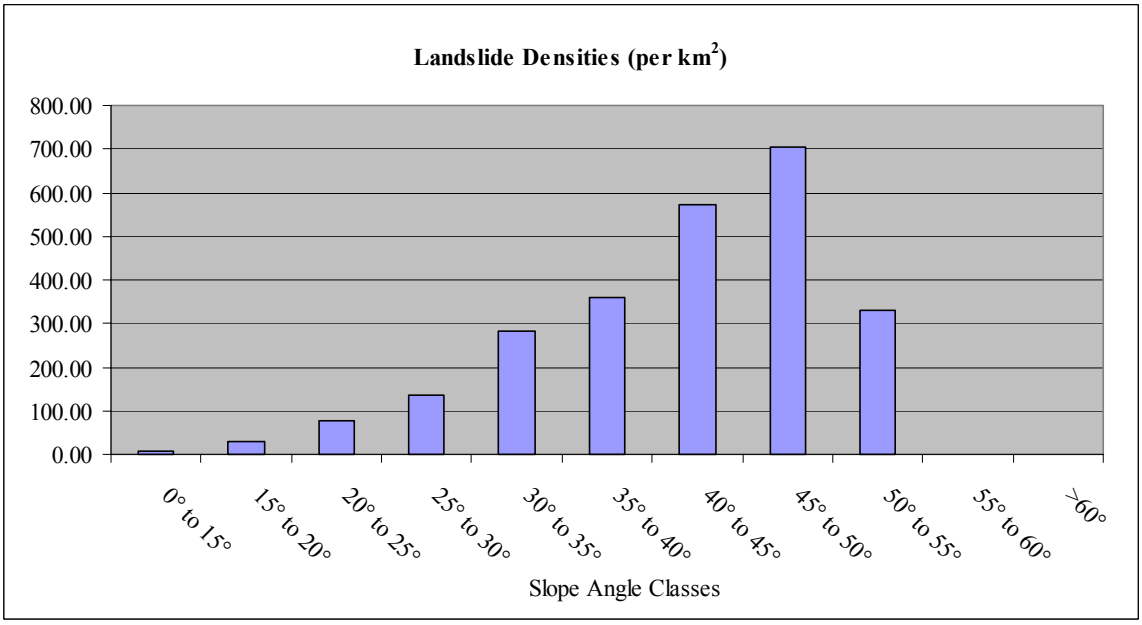

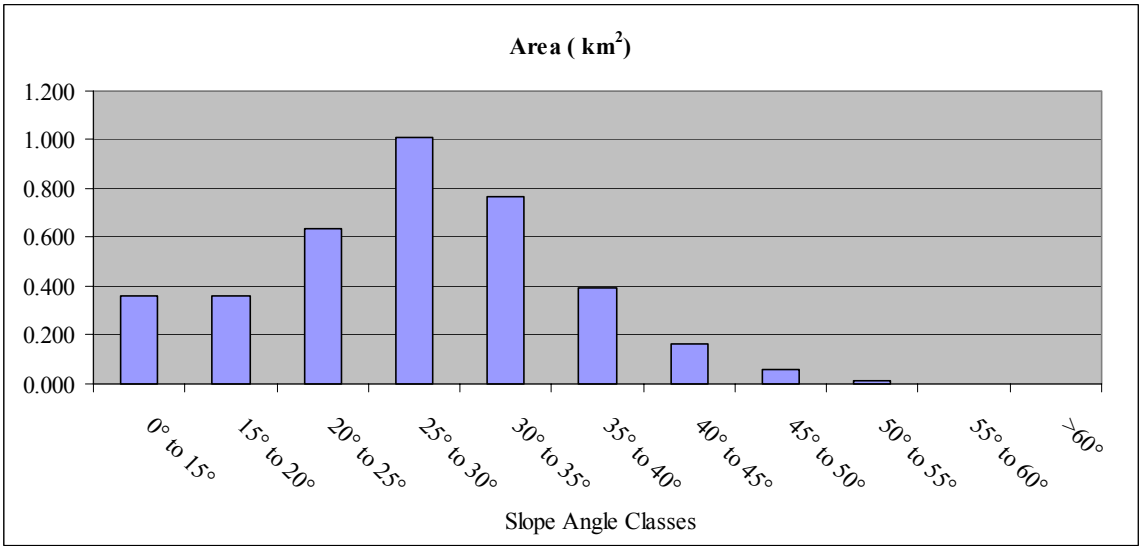

Table of Contents
Table of Contents
Table of Contents
Table of Contents

Table 6 – SE Quadrant - Regolith Susceptibility

Slope angle class	Area (m^2)	Area (km^2)	No. of landslides	Landslide Densities (per km^2)	Susceptibilty Class (This study)
Al	7947	0.008	0	0.00	VL
Rv	28691	0.029	22	766.79	VH
Bv	99	0.000	0	0.00	VL
Cd	95415	0.095	58	607.87	VH
Cr	121476	0.121	18	148.18	M
Crf	1740	0.002	1	574.71	H
Cv	70322	0.070	3	42.66	L
Cla	8513	0.009	1	117.47	M
Clb	18965	0.019	2	105.46	M
Sv(dw)	18496	0.018	3	162.20	M
Sv	150189	0.150	68	452.76	H
Sv+B	23480	0.023	11	468.48	H
Sv+	287134	0.287	138	480.61	H

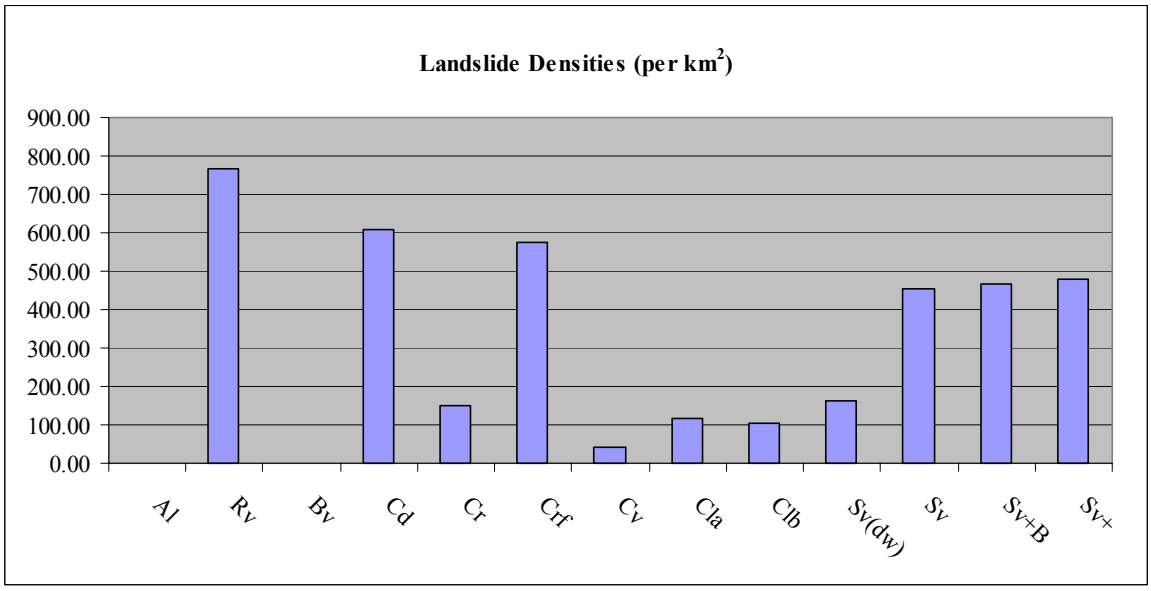

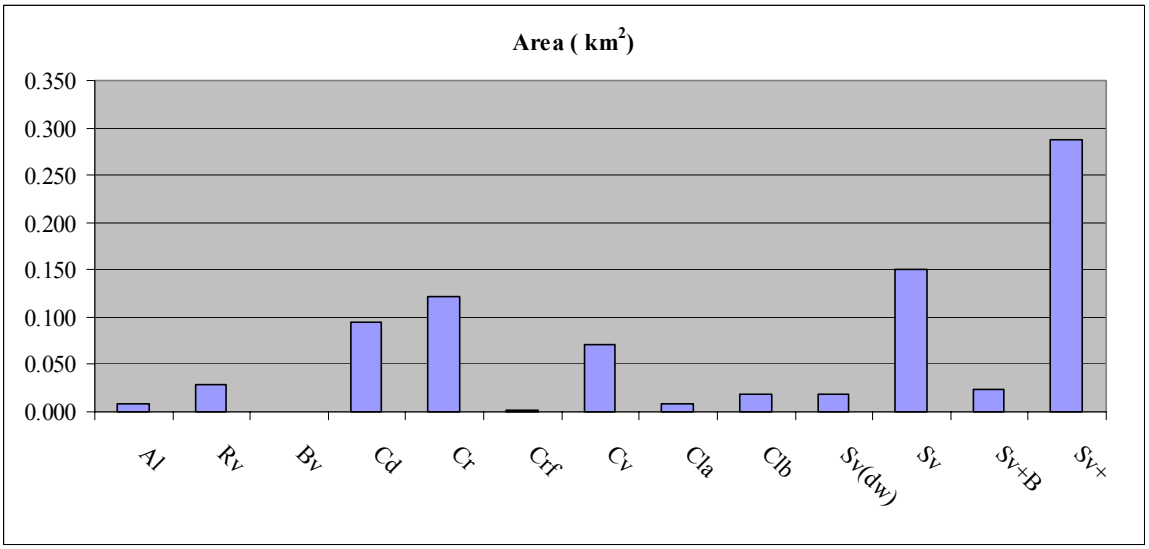

Table of Contents
Table of Contents
Table of Contents
Table of Contents

Table 7 - Summary of Landslide Characteristics of Inspected Landslides (Sheet 1 of 2)

Landslide No.	Gradient (Degree)	Slope Aspect	Length L (m)	Width W (m)	Depth D (m)	Volume V (m^3)	Run-out (m)	Travel Angle (^{o})	Landslide Type	Regolith Type	Remarks
93C	36	273	24	8	1.5	144	320	28	I	Sv	Possible debris flow
99A	31	200	12	10	0.5	30	95	33	II	Sv+/Cd	
00A	37	135	15	12.5	0.8	75	105	42	II	Sv+	
00B	40	200	55	25	0.8	550	152	38	I	Sv+	Detailed fieldsheet in Appendix B
00C	35	144	18.2	12.5	1	114	250	42	II	Cd	Detailed fieldsheet in Appendix B
00C2	32	255	10	18	0.8	90	86	33	II	Sv	
00D2	29	200	14	10	0.5	35	104	31	II	Sv	
00E2	28	197	14	10	0.5	35	90	30	II	Sv	
00F1	38	220	8	6	0.5	12	40	31	I	Sv+	
01A	31	170	20	8	2	160	60	29	II	Sv+	
01B	35	195	27	16	1.5	360	120	34	I	Sv	Detailed fieldsheet in Appendix B
01C	36	210	12	7	0.5	21	50	30	I	Sv	
01D	42	222	15	8	0.8	48	60	30	II	Sv+	
01G	32	235	17	12	0.5	51	40	29	I	Sv	
01H1	35	208	22	8	1	88	60	30	II	Cd	Detailed fieldsheet in Appendix B
01H2	35	210	8	6	0.5	12	50	40	II	Cd	
01I	35	265	10	5	0.8	20	30	32	II	Sv+	
01J	34	134	20	16	0.8	128	60	22	II	Cd/Sv+	
01K	34	138	8	7	0.8	22	40	28	I	Sv+	
01L	35	165	8	5	1	20	20	30	I	Sv+	
01M	25	170	30	5	2	150	60	25	I	Sv(dw)	Detailed fieldsheet in Appendix B
01Na	35	227	12	5	0.8	24	30	25	II	Cd	

Table 7 - Summary of Landslide Characteristics of Inspected Landslides (Sheet 2 of 2)

Landslide No.	Gradient (Degree)	Slope Aspect	Length L (m)	Width W (m)	Depth D (m)	Volume V (m^3)	Run-out (m)	Travel Angle (^{o})	Landslide Type	Regolith Type	Remarks
01N	24	210	20	42	1.5	630	100	20	Misc.	Sv+	Detailed fieldsheet in Appendix B
01Q	35	265	10	8	0.5	20	30	18	II	Cd	
01S	38	120	15	10	0.8	60	80	28	II	Cd	
01Sa	40	100	15	11	1	82.5	50	24	II	Cd	
01Sb	36	085	15	8	1	60	50	32	II	Cd	
01W	40	325	30	15	1	225	100	35	II	Cd	Detailed fieldsheet in Appendix B
01X	34	325	20	12	1	120	80	23	II	Cd/Sv+	
01Y	30	206	8	14	1	56	10	28	II	Sv+	
01CC	35	320	8	5	0.8	16	-	-	I	Sv	
01DD	35	225	15	7.4	0.3	16.65	60	28	II	Sv+/Cd	Minor tension crack
01DDa	40	050	12	8	0.5	24	-	-	I	Sv	
01EE	35	000	22	12	1	90	125	12	II	Sv+/Cd	Detailed fieldsheet in Appendix B

Table of Contents Table of Contents Table of Contents Table of Contents

Table 8 – Maximum Rolling Rainfall at GEO Raingauge No. N05 and Estimated Return Periods for Different Durations Preceding the Landslides around 9 June 2001

Duration	Maximum Rolling Rainfall (mm)	End of Period (Hours)	Estimated Return Period (Years)
5 minutes	11.5	09:35 hours on 9 June 2001	1.5
15 minutes	30.5	09:35 hours on 9 June 2001	3
1 hour	85.5	09:35 hours on 9 June 2001	4
2 hours	145	09:35 hours on 9 June 2001	9
4 hours	225.5	11:00 hours on 9 June 2001	22
12 hours	312	14:00 hours on 9 June 2001	14
24 hours	315	14:00 hours on 9 June 2001	5
2 days	379	14:00 hours on 9 June 2001	5
4 days	552	14:00 hours on 9 June 2001	12
7 days	556	14:00 hours on 9 June 2001	8
15 days	598	14:00 hours on 9 June 2001	4
31 days	721	14:00 hours on 9 June 2001	3

Notes:
(1) Return periods were derived from Table 3 of Lam & Leung (1994).
(2) Maximum rolling rainfall was calculated from 5-minute data.
(3) The use of 5-minute data for durations between 4 hours and 31 days results in better data resolution, but may slightly over-estimate the return periods using Lam & Leung's (1994) data, which are based on hourly rainfall for these durations.
(4) Maximum rolling rainfall was calculated from 5-minute data.

LIST OF FIGURES

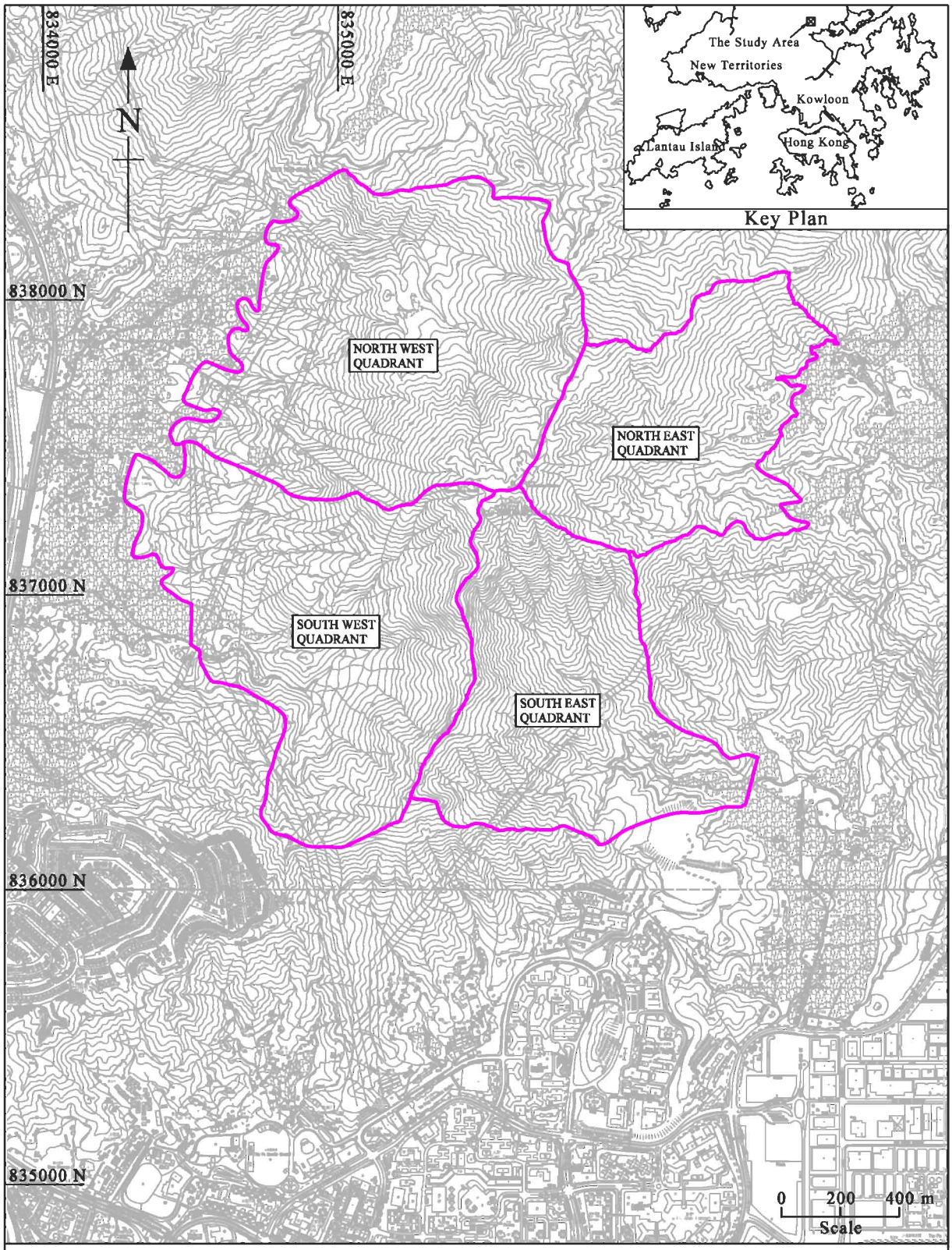

Figure 1 - Location Plan

Table of Contents
Table of Contents
Table of Contents
Table of Contents

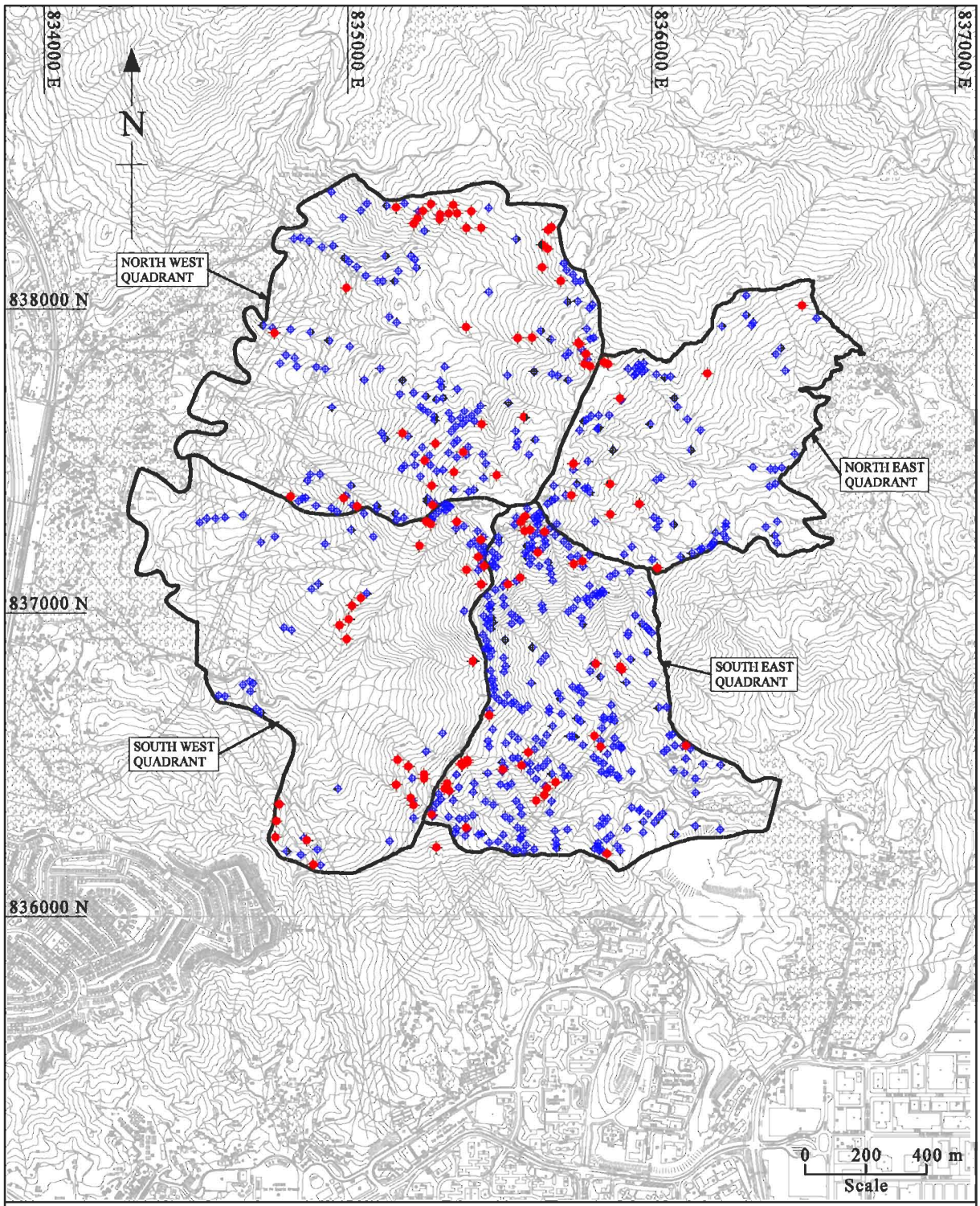

Legend : Quadrant boundary Recent landslide Relict landslide

Note :
(1) Base map is extracted from Survey Sheet Nos. 3SW-D and 7NW-B.
(2) Relict landslide is defined as a scar observed either from API or in the field on which vegetation has re-established.
(3) Recent landslide is defined as a scar observed either from API or in the field which is generally bare of vegetation.

Figure 2 - Location Plan of All Identified Landslide

Table of Contents
Table of Contents
Table of Contents
Table of Contents

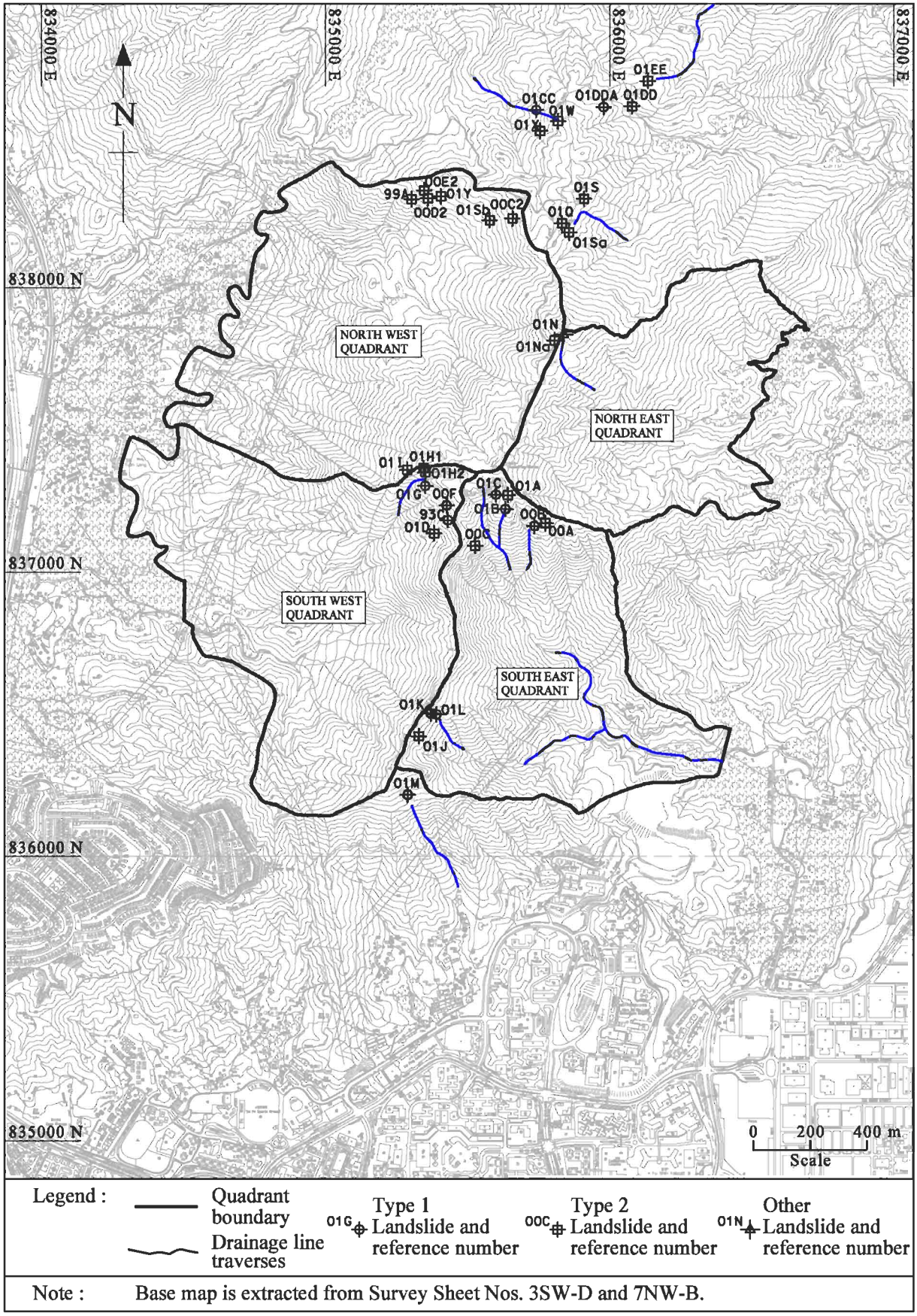

Legend :

- Quadrant boundary
- Drainage line traverses
- 01G — Type 1 Landslide and reference number
- 00C — Type 2 Landslide and reference number
- 01N — Other Landslide and reference number

Note : Base map is extracted from Survey Sheet Nos. 3SW-D and 7NW-B.

Figure 3 - Location Plan of Inspected Recent Landslides

Table of Contents
Table of Contents
Table of Contents
Table of Contents

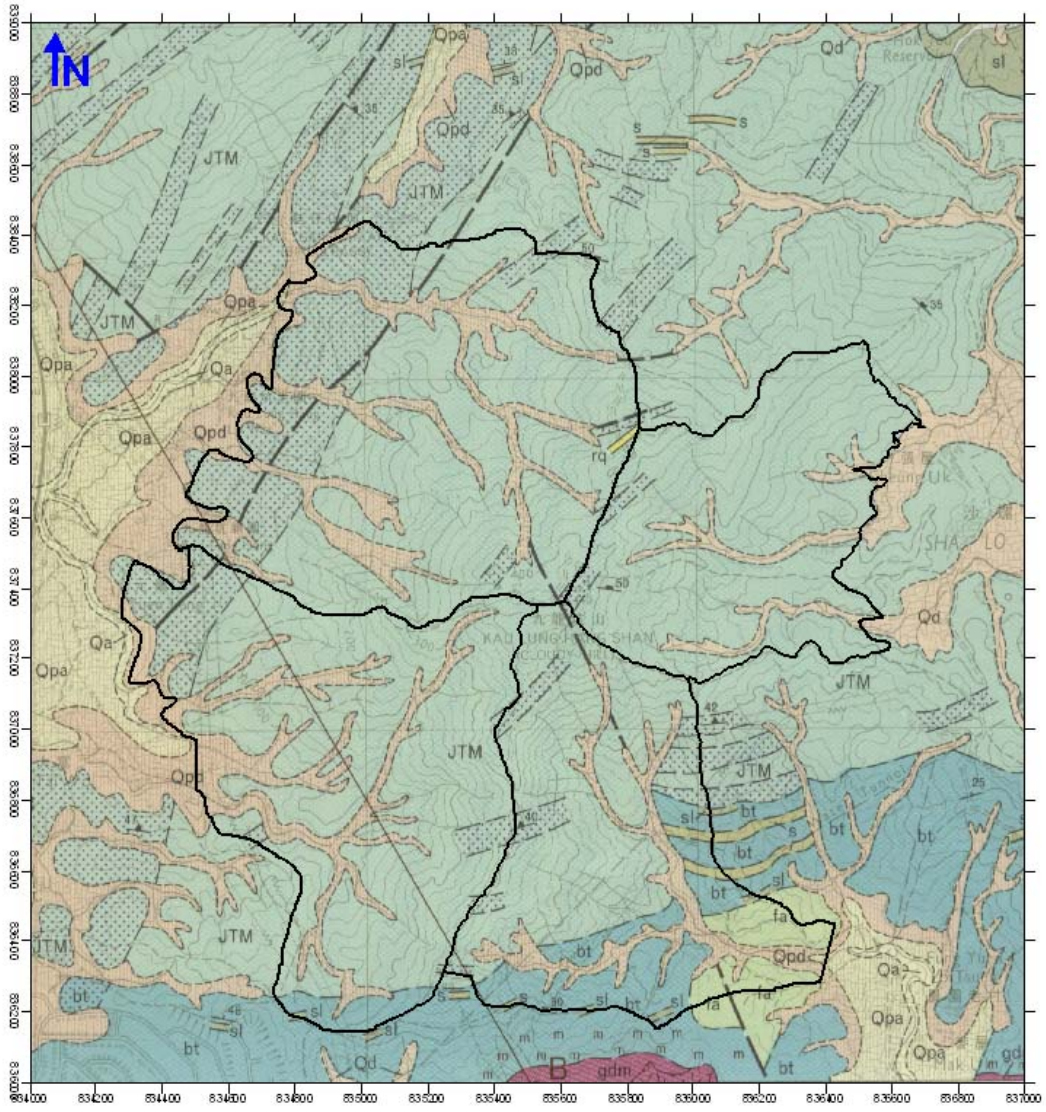

Note: Extract from Sheet 3 of Hong Kong Geological Survey 1:20,000 Scale Map Series HGM20 (GCO, 1988)

Figure 4 – Regional Geology

Table of Contents
Table of Contents
Table of Contents
Table of Contents

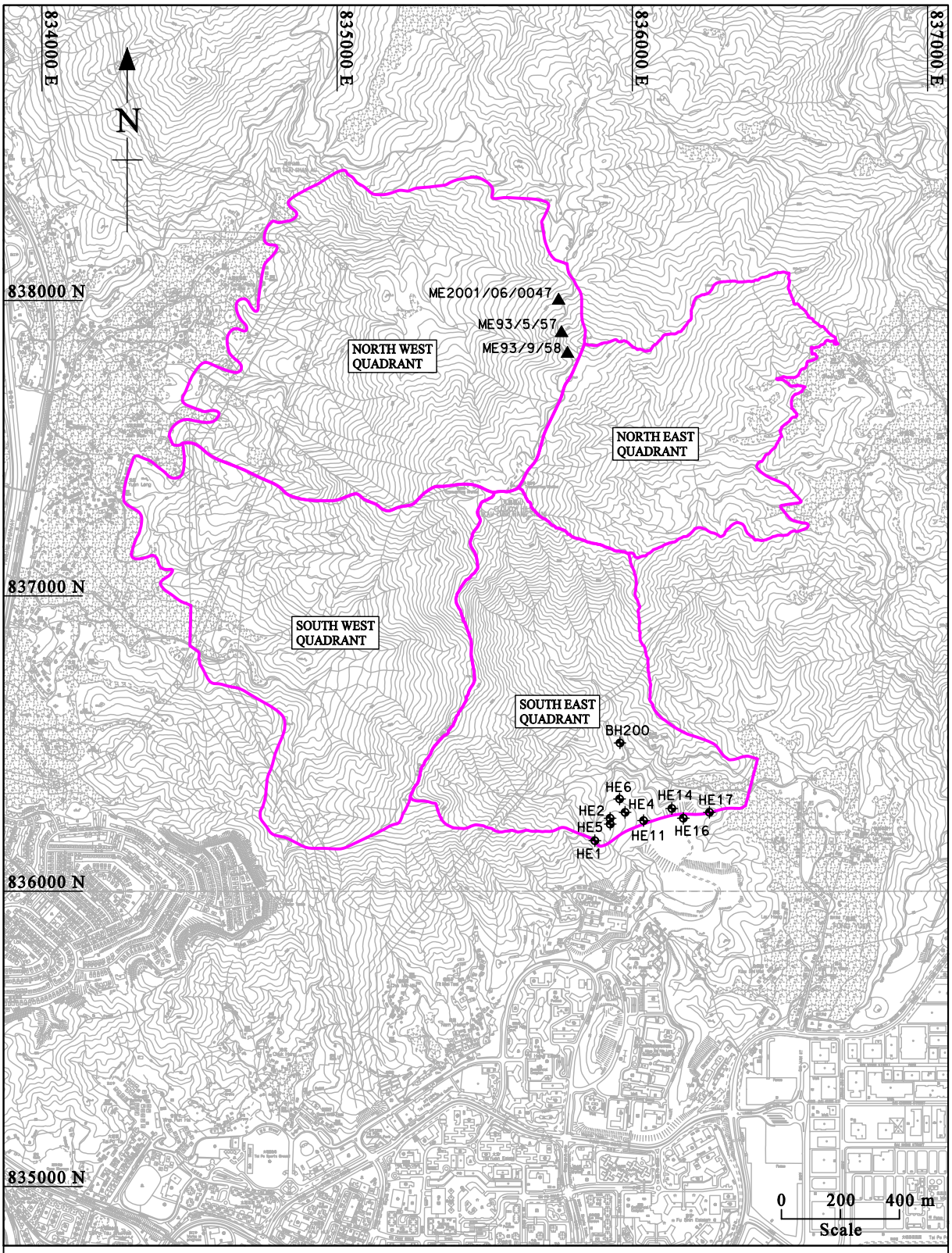

Legend : Quadrant boundary ▲ GEO Incident No. ⌖ Borehole

Note : (1) Base map is extracted from Survey Sheet Nos. 3SW-D and 7NW-B.
(2) Location of GI taken from GIU Report Nos. 4416A and 22009.

Figure 5 - Location Plan of Previous Ground Investigation and Recorded GEO Incidents

Table of Contents
Table of Contents
Table of Contents
Table of Contents

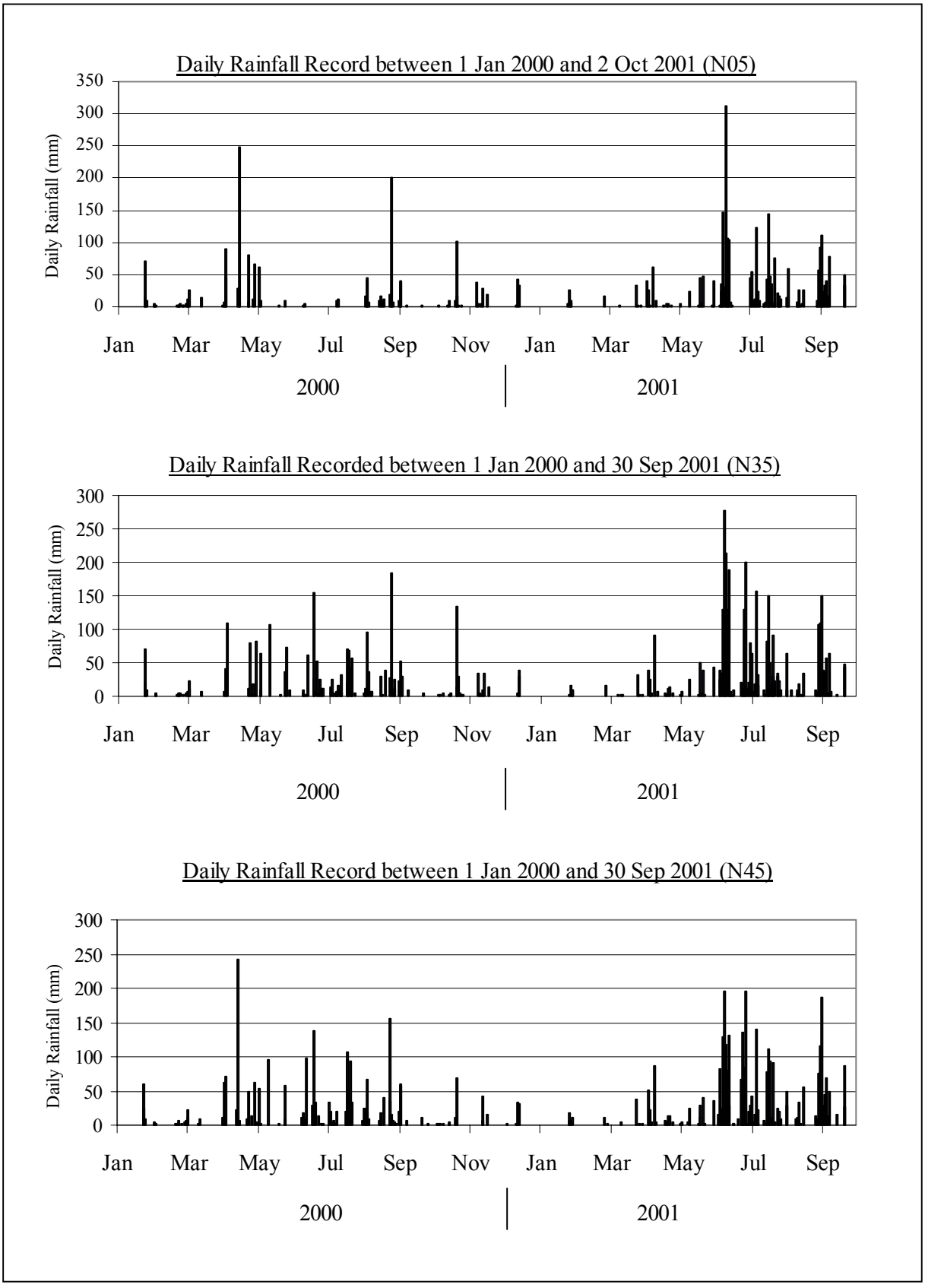

Figure 6 – Daily Rainfall Recorded at GEO Raingauges Nos. N05, N35 & N45 between 1 January 2000 and 30 October 2001

Table of Contents
Table of Contents
Table of Contents
Table of Contents

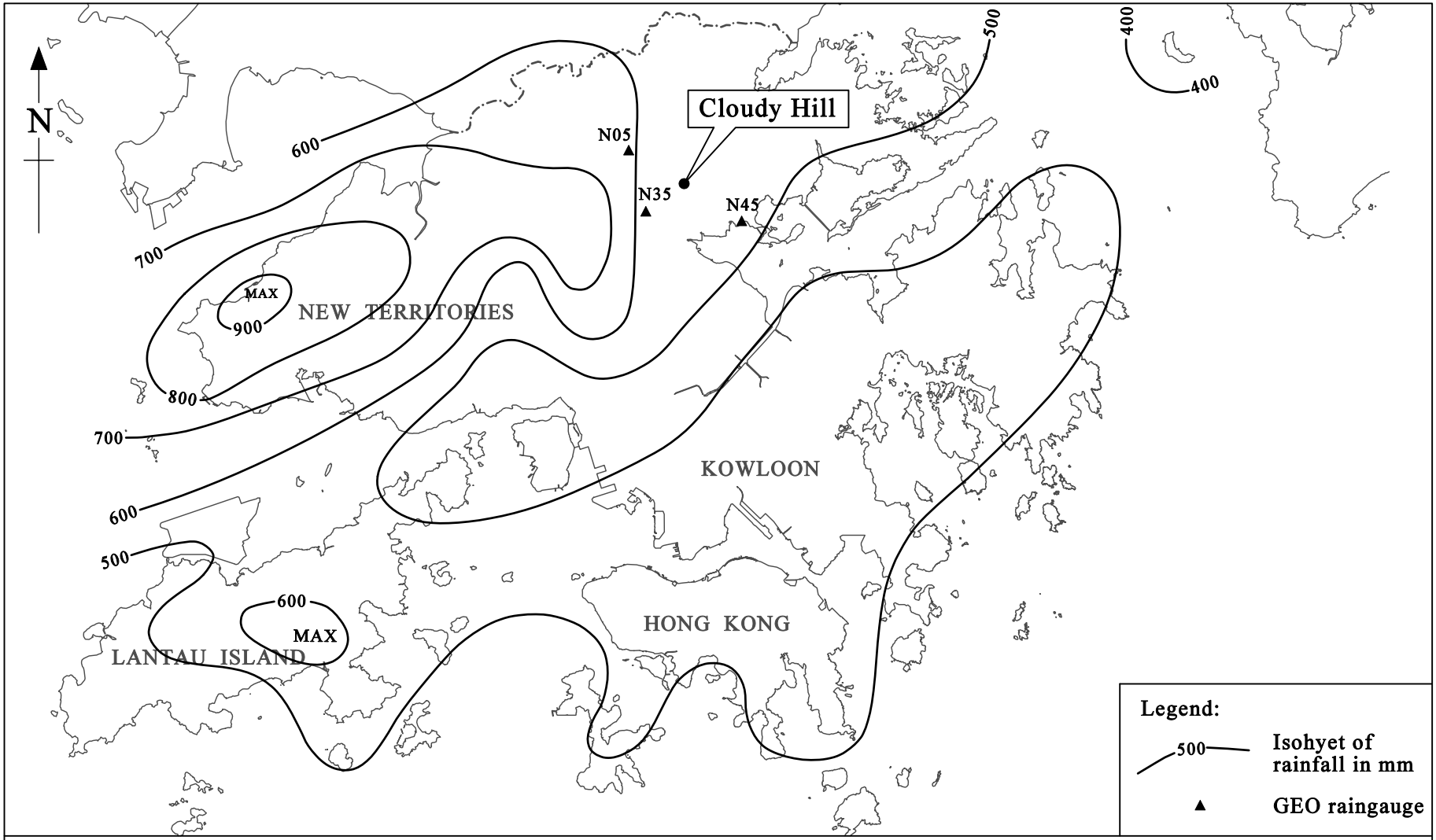

Note : Isohyets prepared by the Hong Kong observatory.

Figure 7 - Rainfall Distribution for April 2000

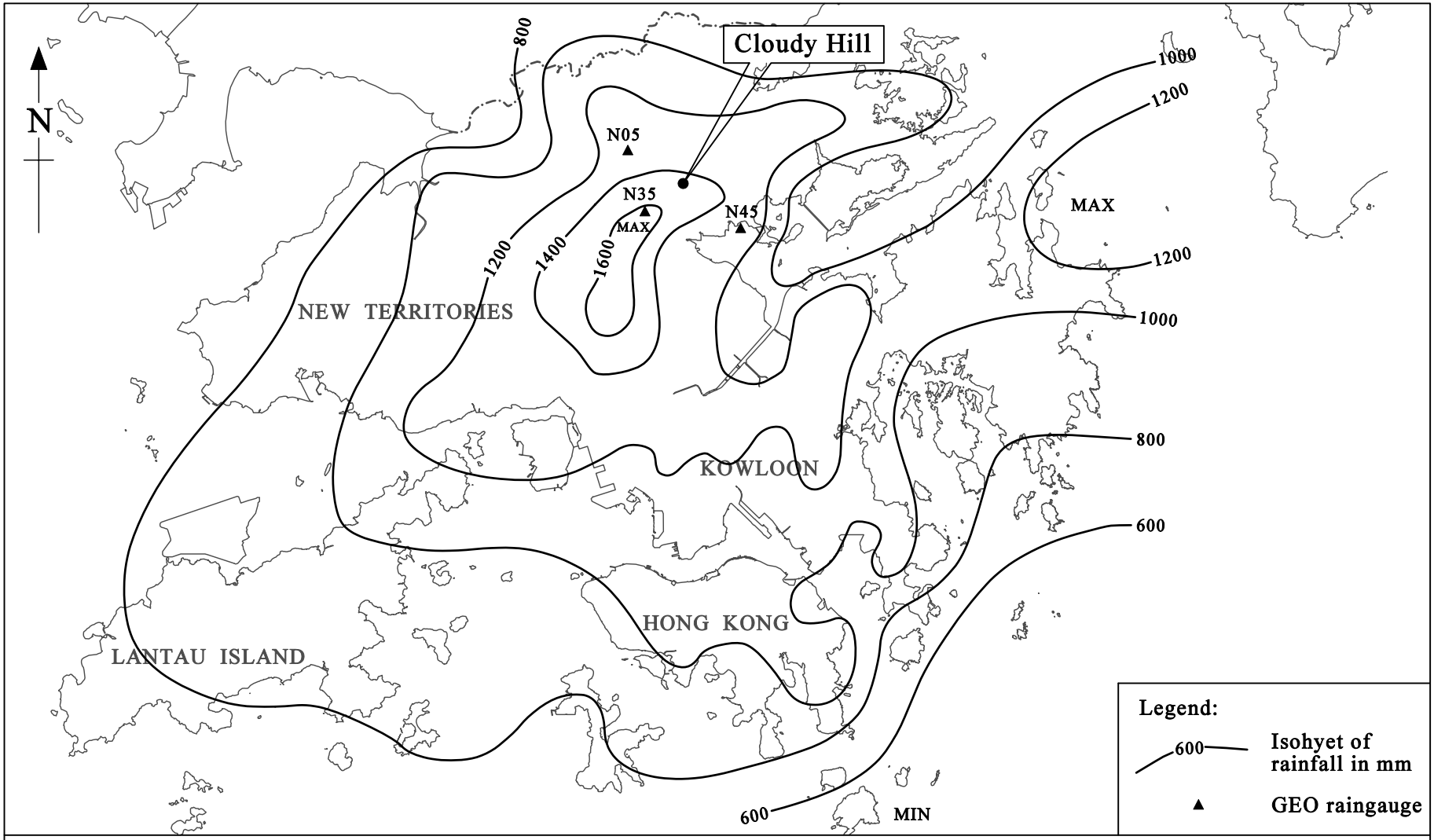

Note : Isohyets prepared by the Hong Kong observatory.

Figure 8 - Rainfall Distribution for June 2001

Table of Contents
Table of Contents
Table of Contents
Table of Contents
Table of Contents

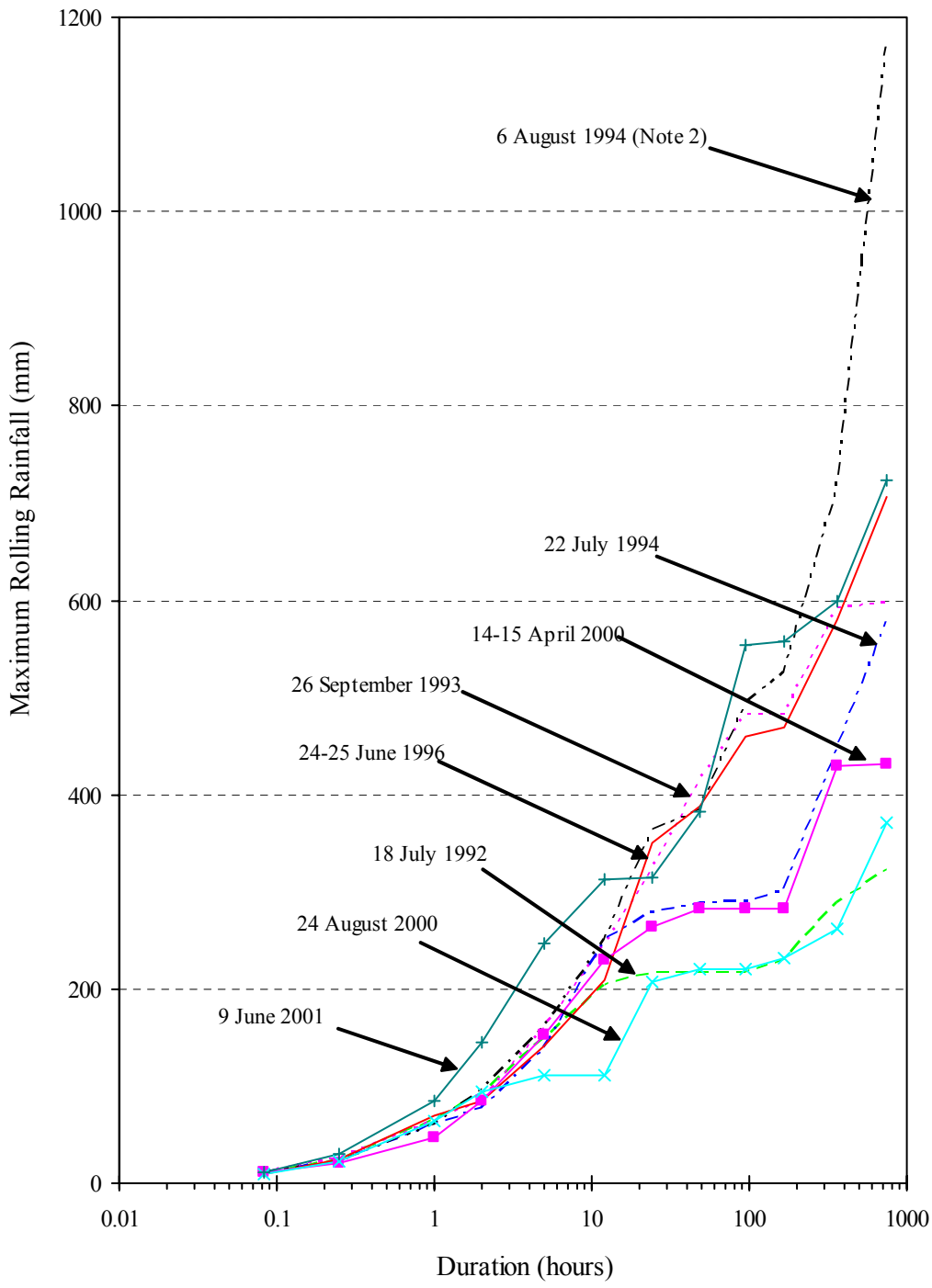

Notes: (1) Rainfall data are 5-minute statistics from GEO raingauge No. N05.

(2) The rainstorm on 22 July 1994 results in a high value for the Maximum Rolling Rainfall for 6 August 1994.

Figure 9 – Maximum Rolling Rainfall at GEO Raingauge No. N05 for Major Rainstorms between 1 January 1987 and 30 September 2002

Table of Contents
Table of Contents
Table of Contents
Table of Contents

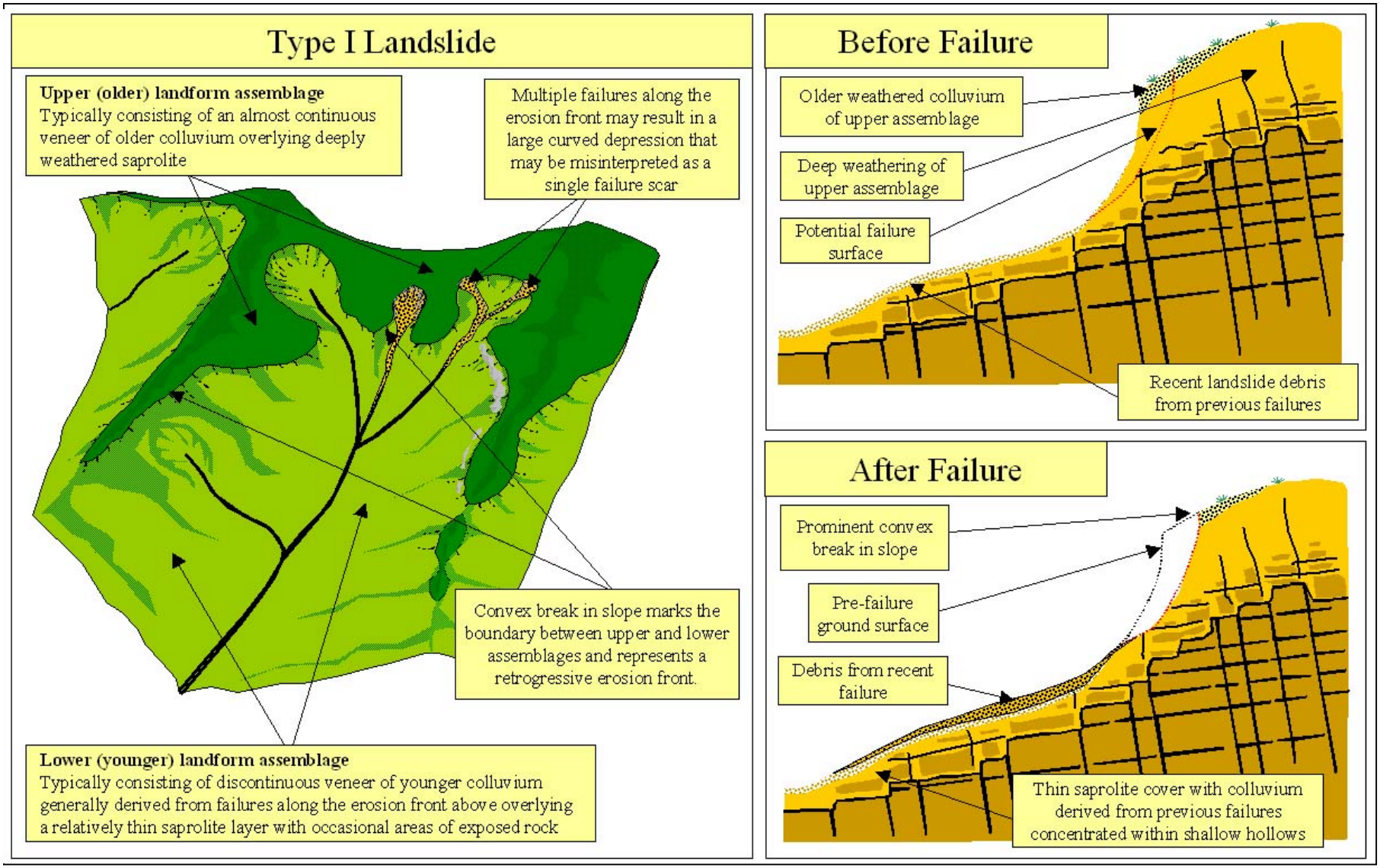

Figure 10 - Setting and Mechanism of a Type I Landslide

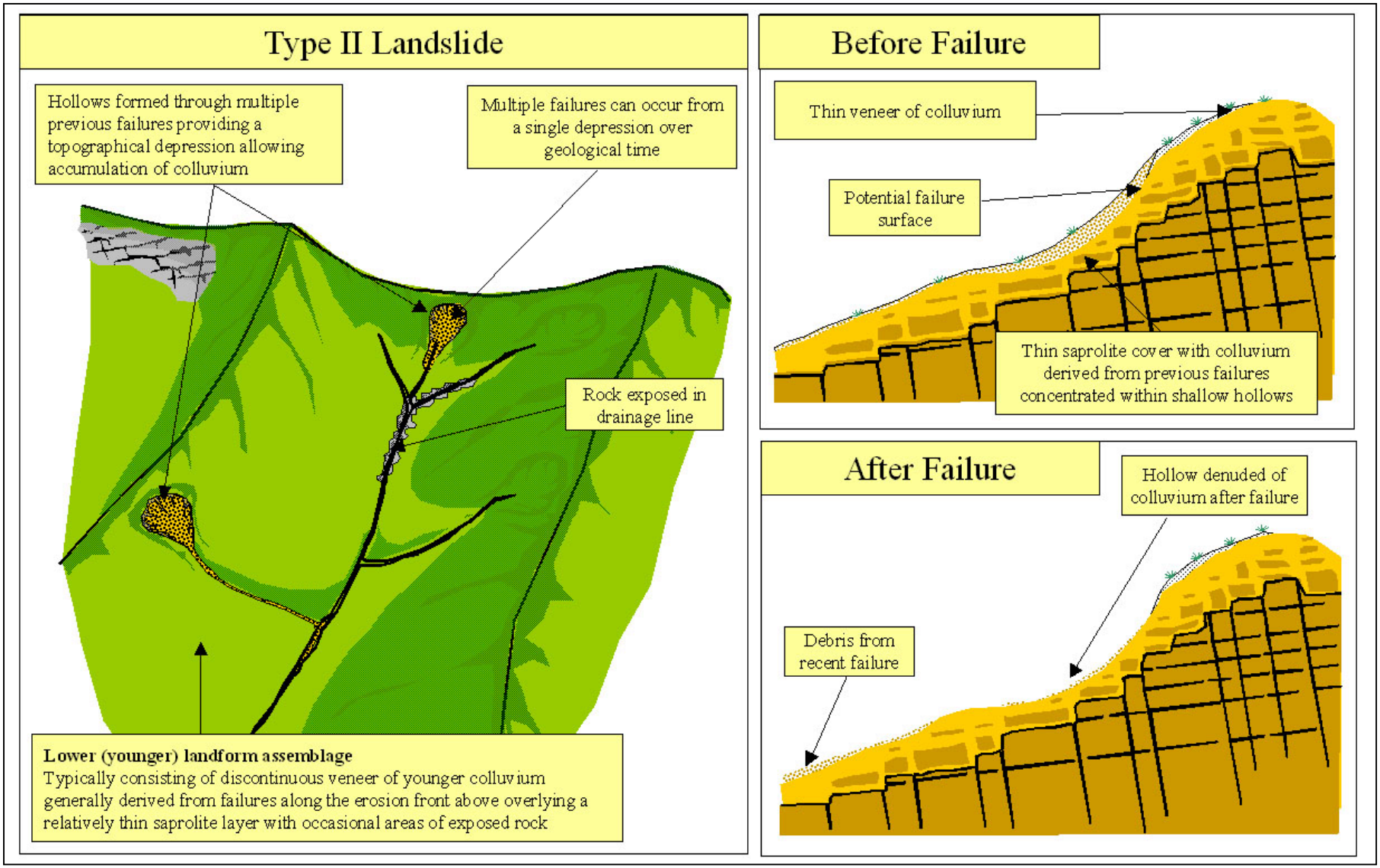

Figure 11 - Setting and Mechanism of a Type II Landslide

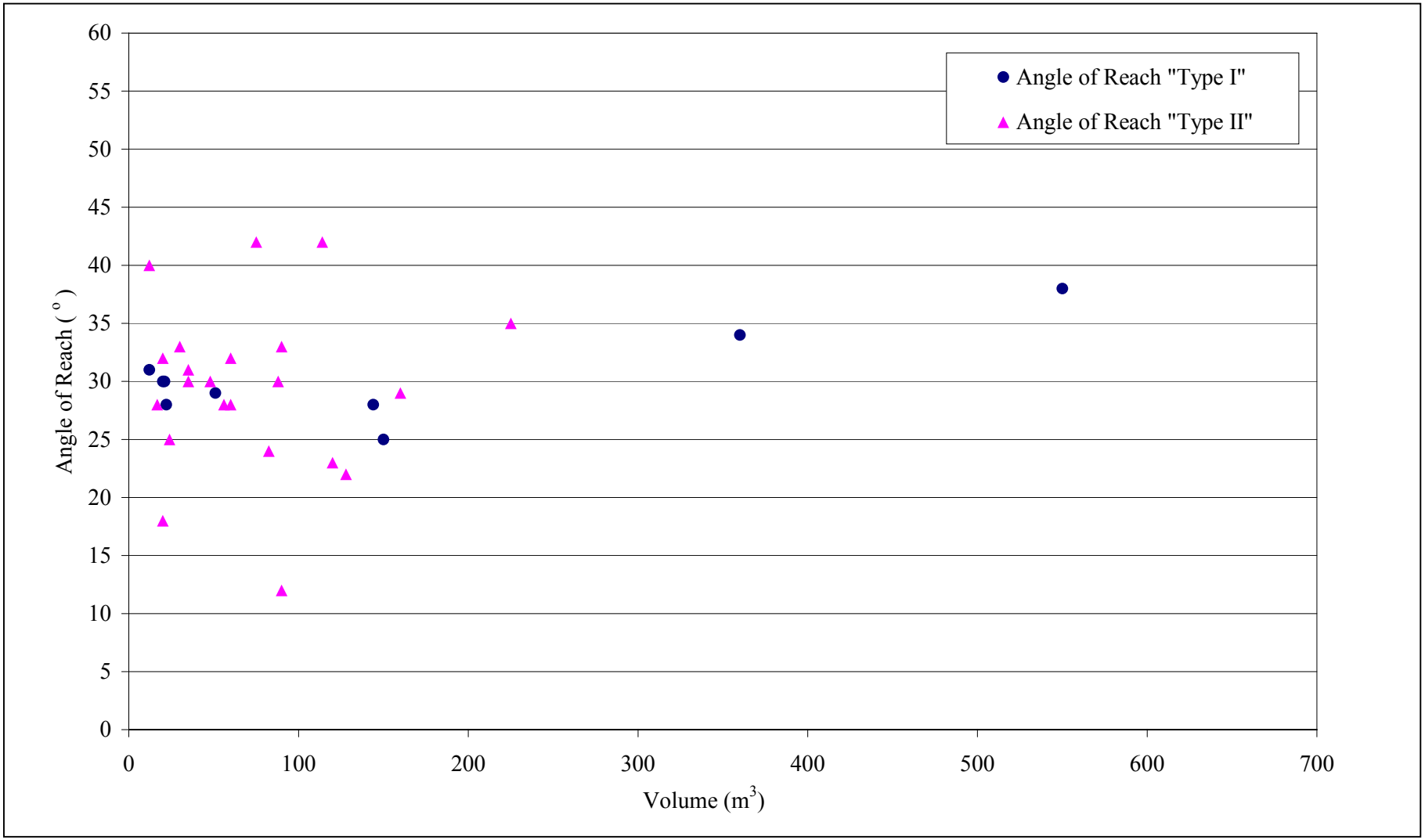

Figure 12 – Mobility of Inspected Recent Landslides

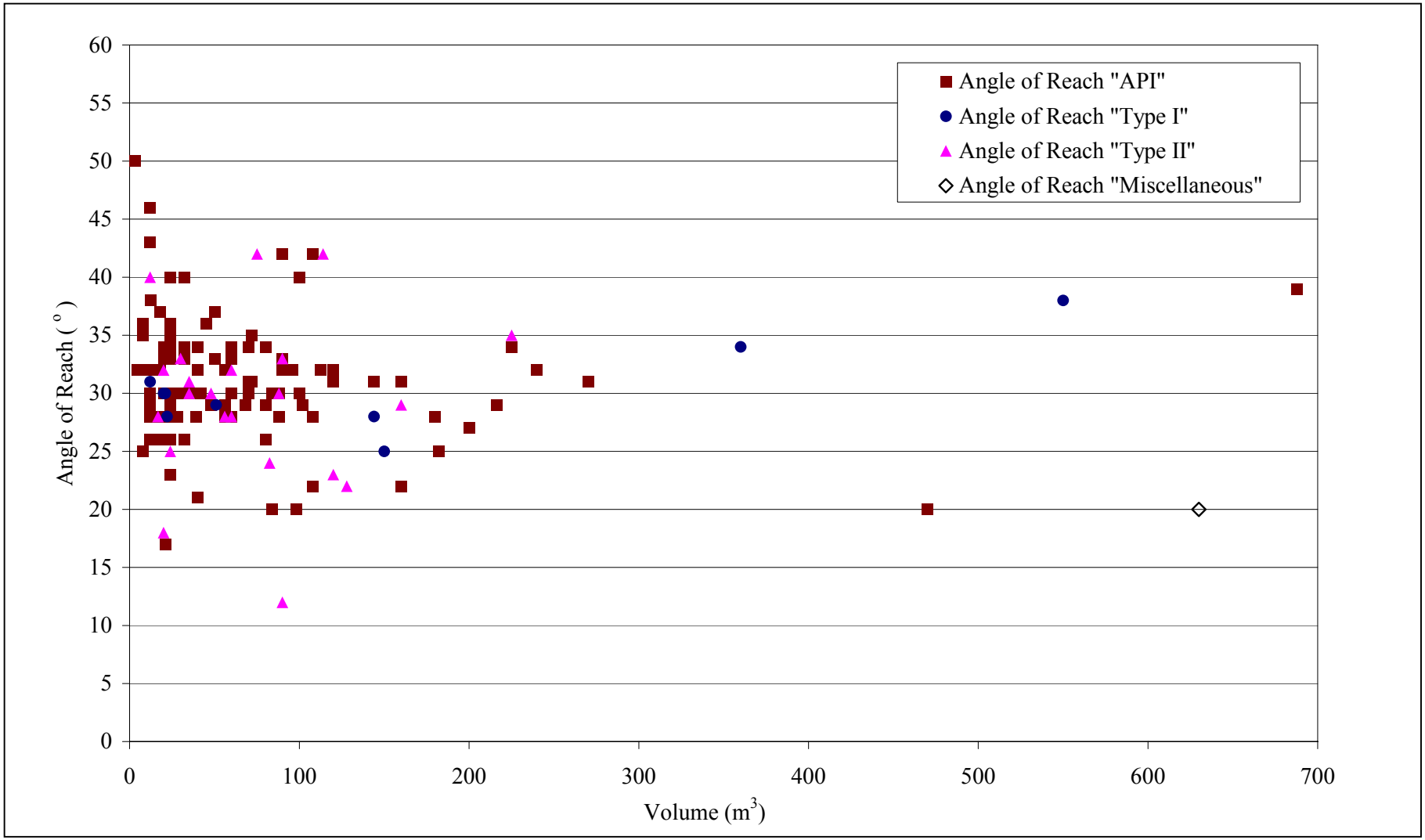

Figure 13 – Mobility of Inspected Landslides and Landslides Identified from Aerial Photograph Interpretation

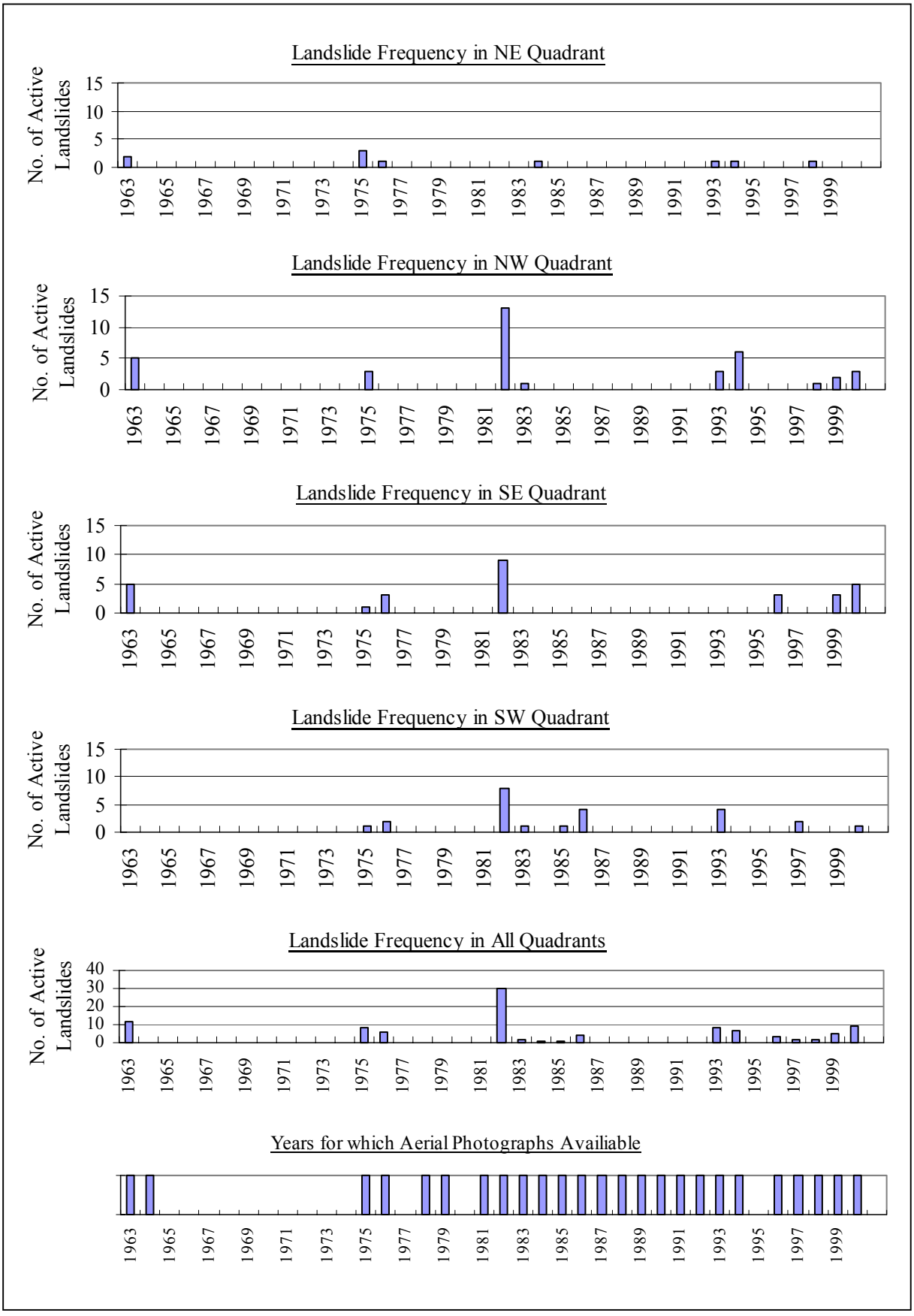

Figure 14 – Temporal Distribution of Landslides and Aerial Photographs

Table of Contents
Table of Contents
Table of Contents
Table of Contents

LIST OF PLATES

Plate 1 – Oblique Aerial View of the Landslides on Cloudy Hill
(Photograph Taken on 9 July 2001)

Plate 2 – General Aerial View of the Landslides on Cloudy Hill
(Photograph Taken on 9 August 2001)

Table of Contents
Table of Contents
Table of Contents
Table of Contents

Plate 3 – Fine Colluvium in Main Scarp of Landslide 00B
(Photograph Taken on 10 May 2001)

Plate 4 – Bouldery Colluvium in the Main Scarp of Landslide 01N
(Photograph Taken on 19 November 2001)

Plate 5 – Surface of Rupture at Landslide 01H
(Photograph Taken on 9 August 2001)

Plate 6 – View of Planar Main Scarp at Landslide 01B
(Photograph Taken on 30 November 2001)

Table of Contents
Table of Contents
Table of Contents
Table of Contents

Plate 7 – View of Concave Surface of Rupture at Landslide 00C
(Photograph Taken on 10 May 2001)

Plate 8 – Planar Surface of Rupture at Landslide 01K
(Photograph Taken on 14 August 2002)

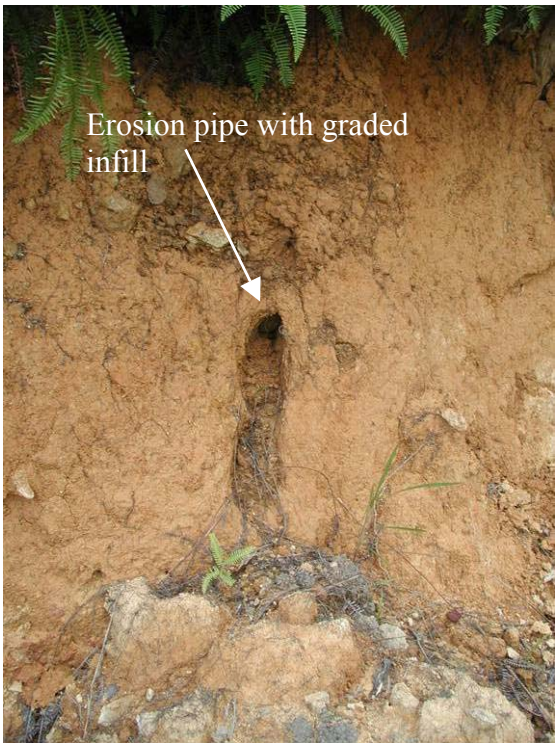

Plate 9 – Erosion Pipe with Partial Graded Infill at Landslide 01W
(Photograph Taken on 22 August 2001)

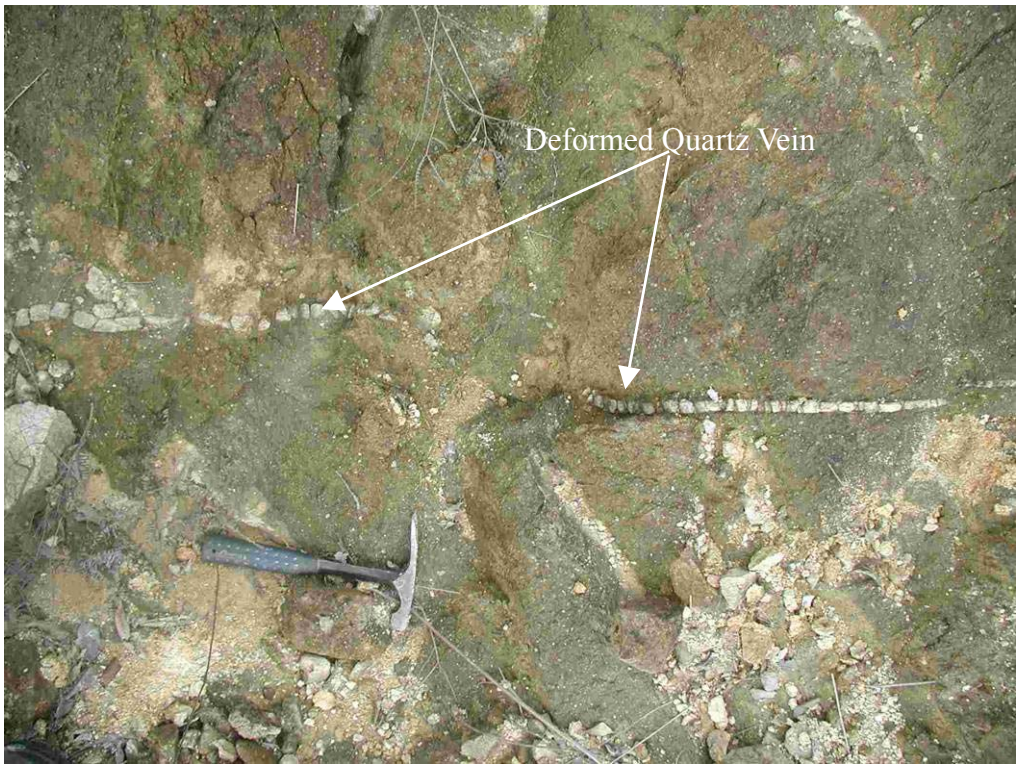

Plate 10 – Offset Quartz Vein in Source floor of Landslide 00C
(Photograph Taken on 12 June 2001)

Table of Contents
Table of Contents
Table of Contents
Table of Contents

Plate 11 – Quartz Vein Parallel to Floor of Landslide 01H1
(Photograph Taken on 29 November 2001)

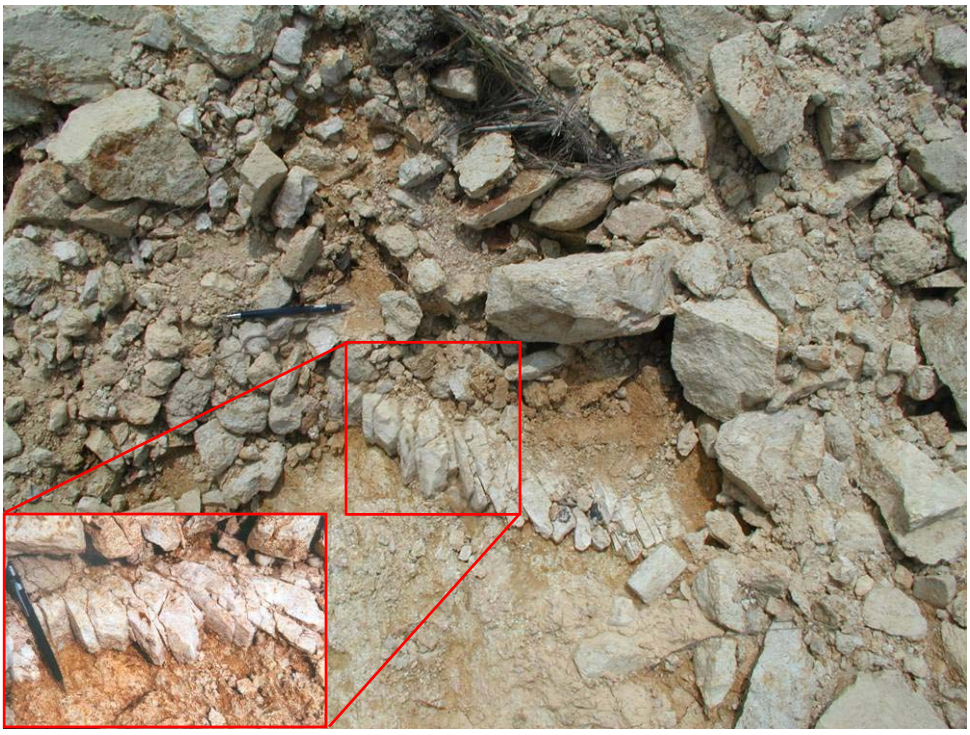

Plate 12 – Quartz Vein Parallel to Surface of Rupture of Landslide 01N
(Photograph Taken on 18 October 2001)

Plate 13 – Planar Persistent Joint along Western Flank of Landslide 01EE
(Photograph Taken on 28 November 2001)

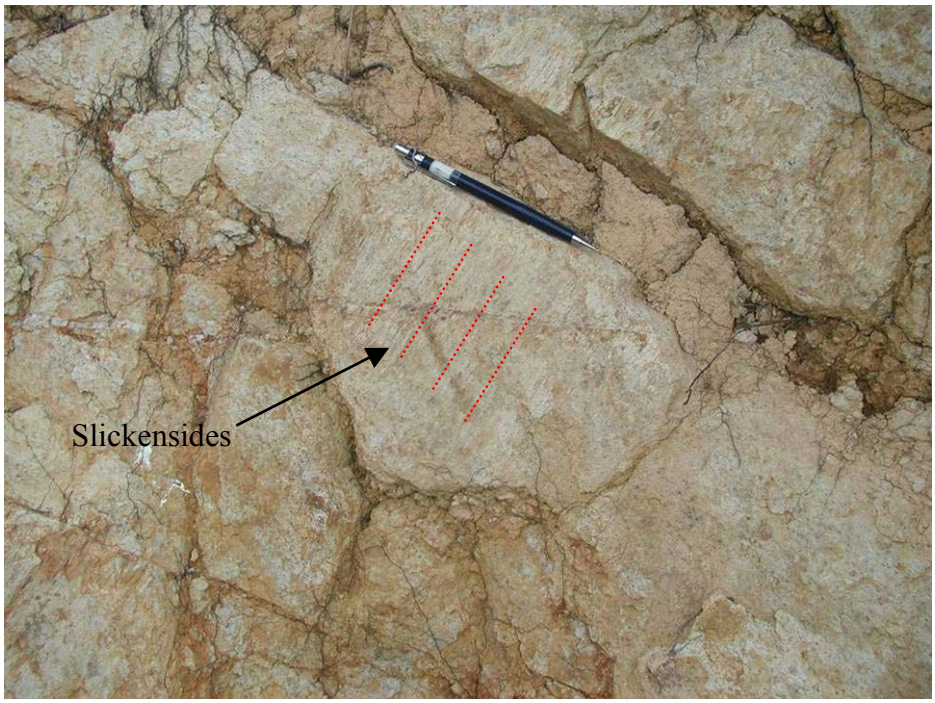

Plate 14 – Clay Infilled Joint in Moderately Decomposed Tuff at Landslide 01EE
(Photograph Taken on 18 August 2001)

Table of Contents
Table of Contents
Table of Contents
Table of Contents

Plate 15 – Tension Crack at Landslide 01DD
(Photograph Taken on 7 September 2001)

Plate 16 – View of Tension Crack at Landslide 01N
(Photograph Taken on 9 August 2001)

Table of Contents
Table of Contents
Table of Contents
Table of Contents

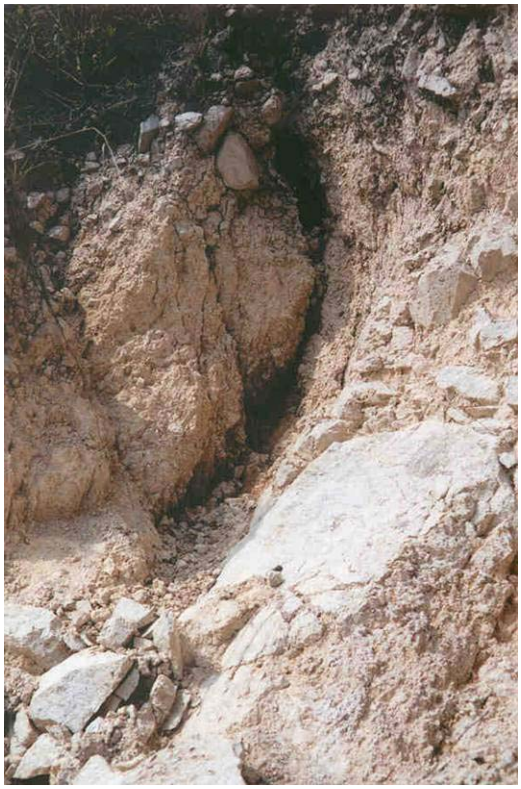

Plate 17 – Partially Displaced Mass Below Tension Crack at Landslide 01N
(Photograph Taken on 18 October 2001)

Plate 18 – Colluvium in the Upper part of the Drainage line in the Southeast Catchment
(Photograph Taken on 11 July 2002)

Table of Contents
Table of Contents
Table of Contents
Table of Contents

Plate 19 – Alluvium at Mouth of Drainage Line
(Photograph Taken on 22 August 2002)

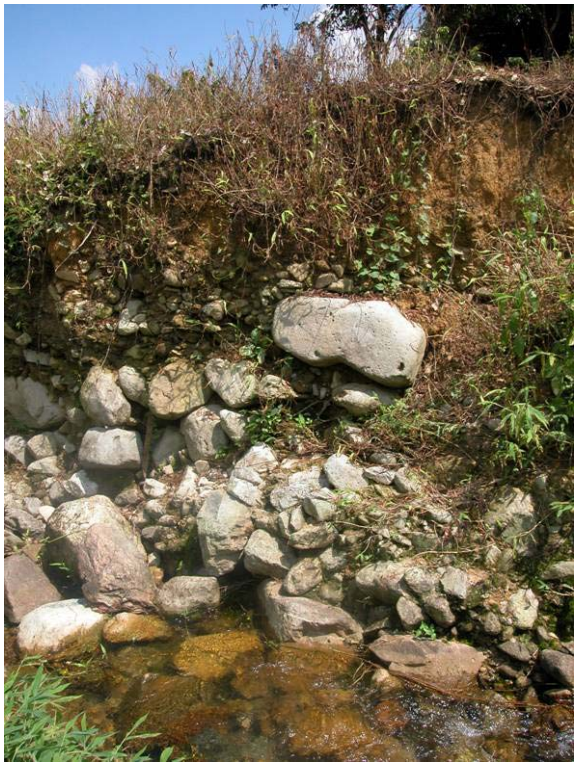

Plate 20 – Possible Layering within the Colluvium
(Photograph Taken on 22 August 2002)

Table of Contents
Table of Contents
Table of Contents
Table of Contents

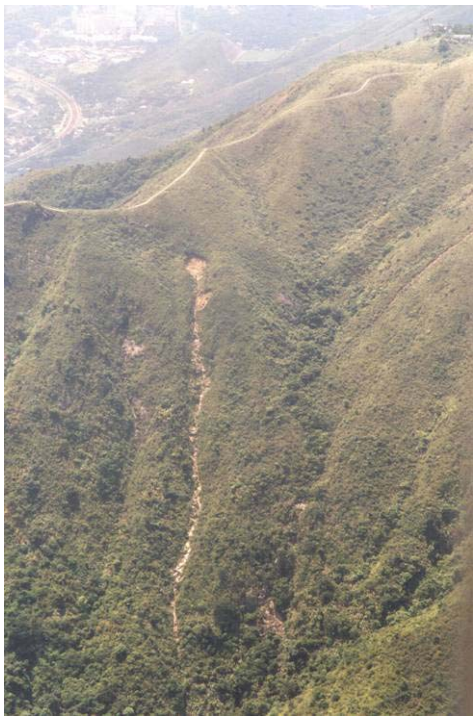

Plate 21 – View of Scar of Landslide 00CSE
(Photograph Taken on 9 July 2001)

Plate 22 – Aerial View of Landslide 01M
(Photograph Taken on 19 October 2001)

Table of Contents
Table of Contents
Table of Contents
Table of Contents

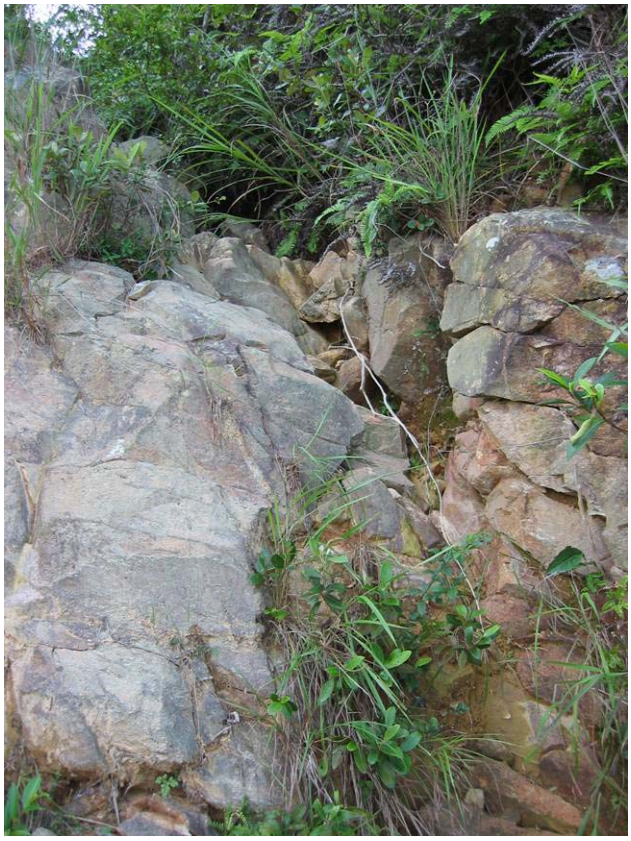

Plate 23 – View of Narrow Drainage Line below Landslide 01M
(Photograph Taken on 19 October 2001)

Plate 24 – Aerial Photograph from 1987 Showing the Convex Break In Slope Separating the Upper and Lower Landforms in the Southeast Quadrant.

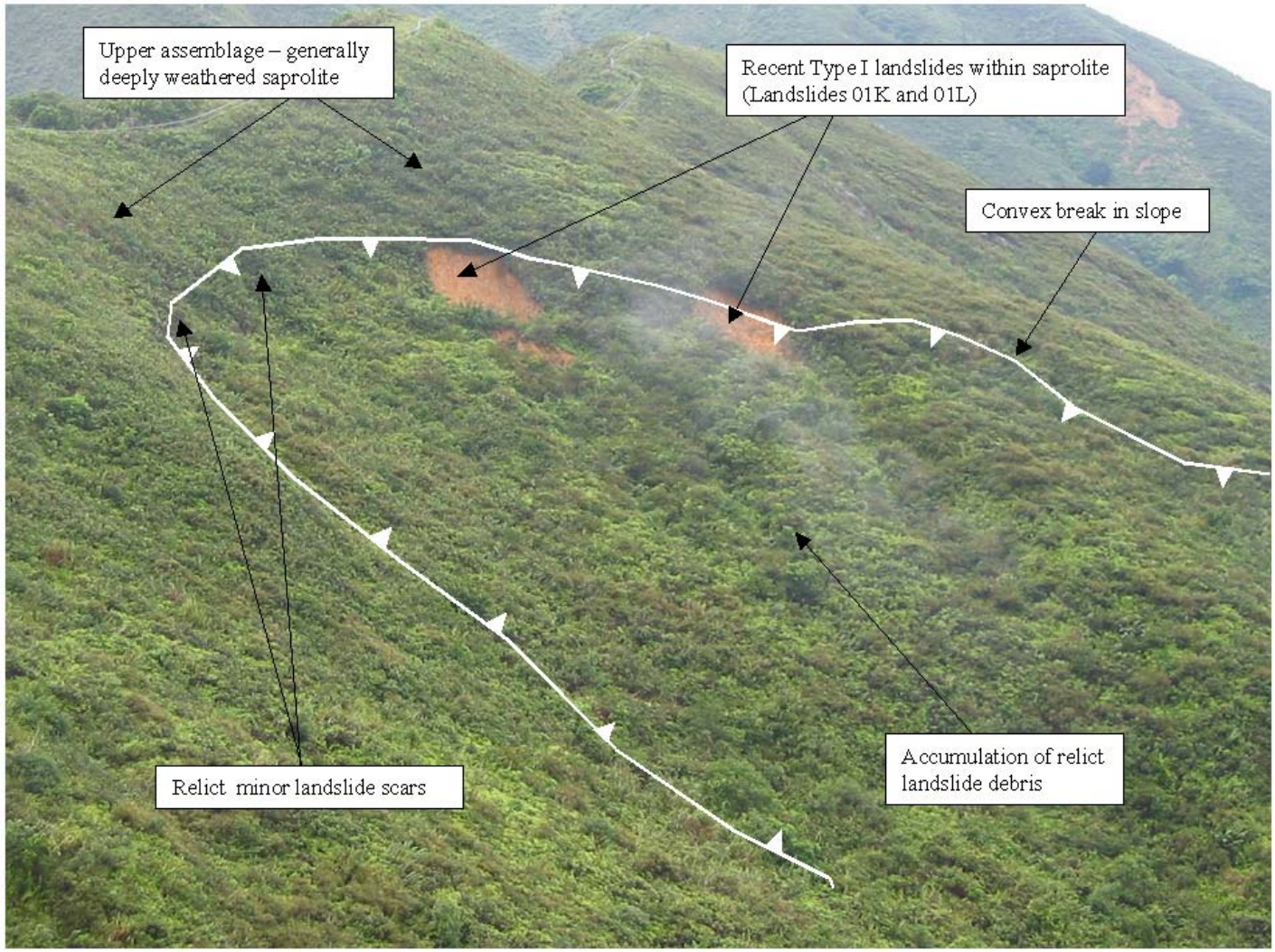

Plate 25 – Geomorphological Setting of Type I Landslide

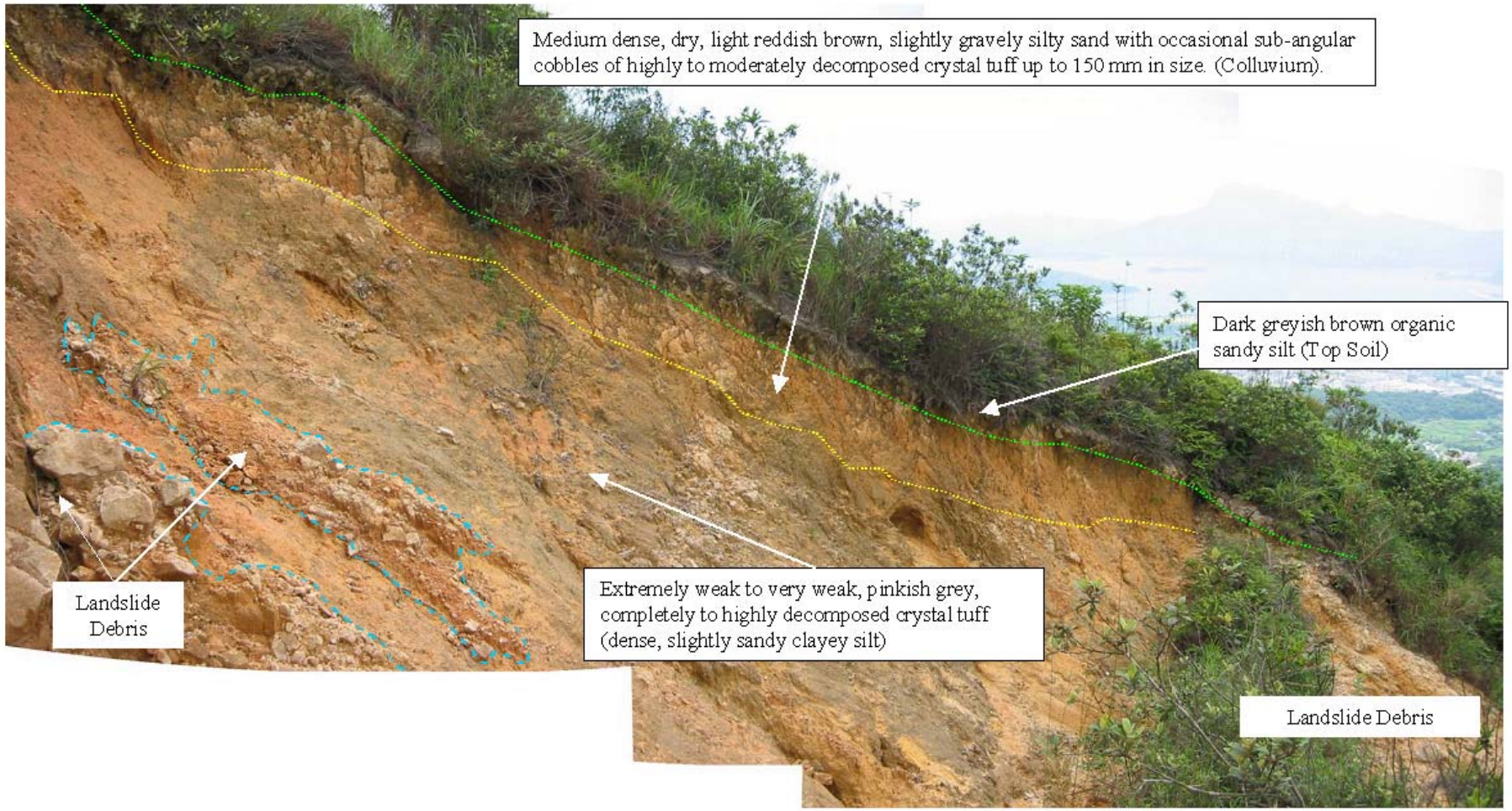

Plate 26 – Detailed View of the Main Scarp of a Type I Landslide (01B) in Sv+

Plate 27 – General View Landslide 01B
(Photograph Taken on 30 November 2001)

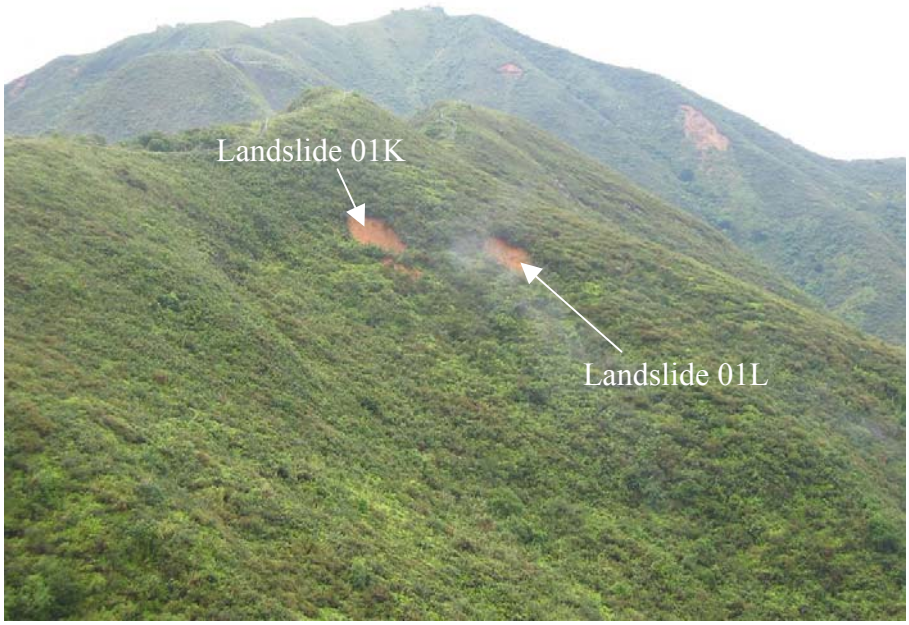

Plate 28 – View of Landslides 01K and 01L
(Photograph Taken on 31 July 2002)

Table of Contents
Table of Contents
Table of Contents
Table of Contents

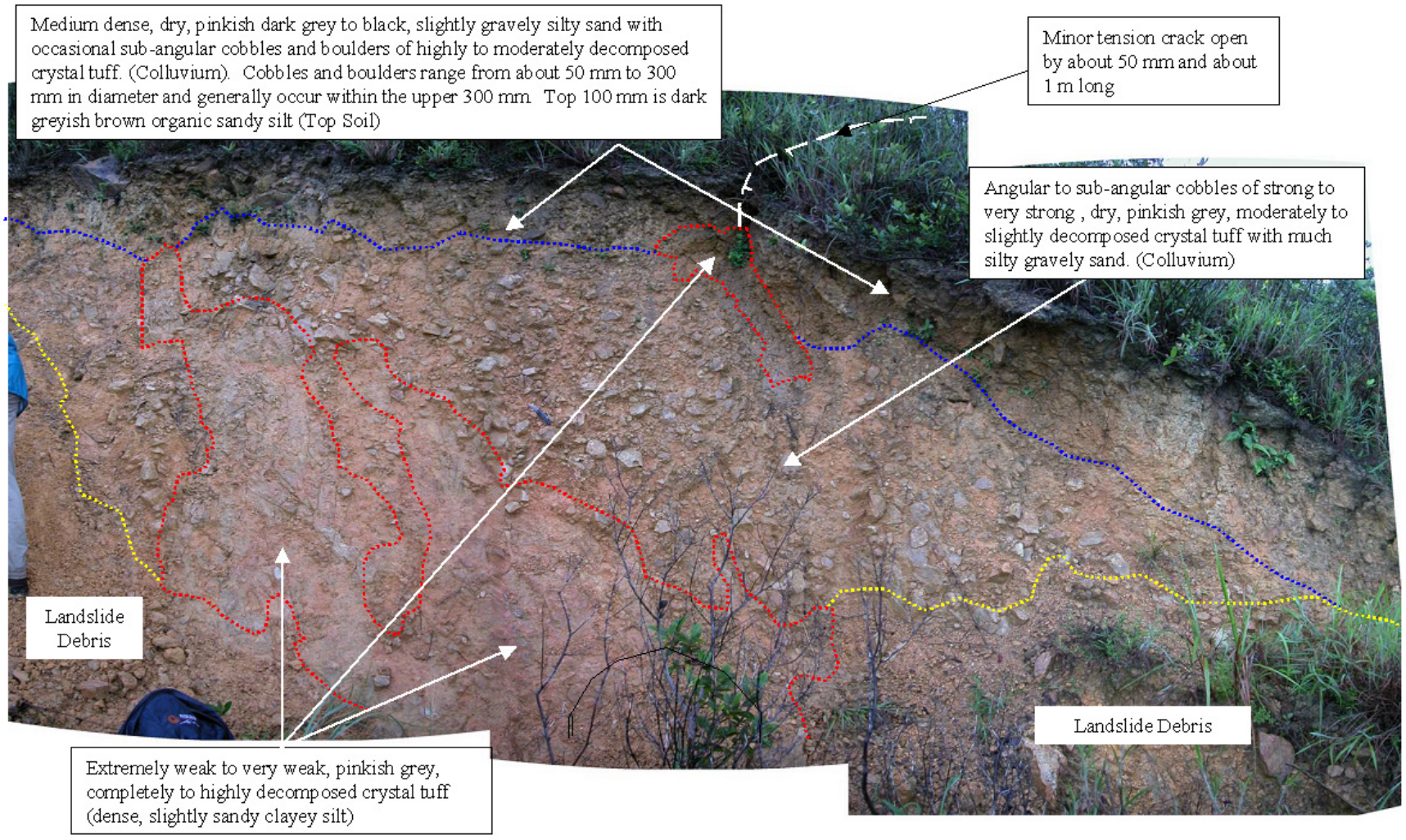

Plate 29 – Detailed View of the Main Scarp of a Type II landslide (01J)

Table of Contents
Table of Contents
Table of Contents

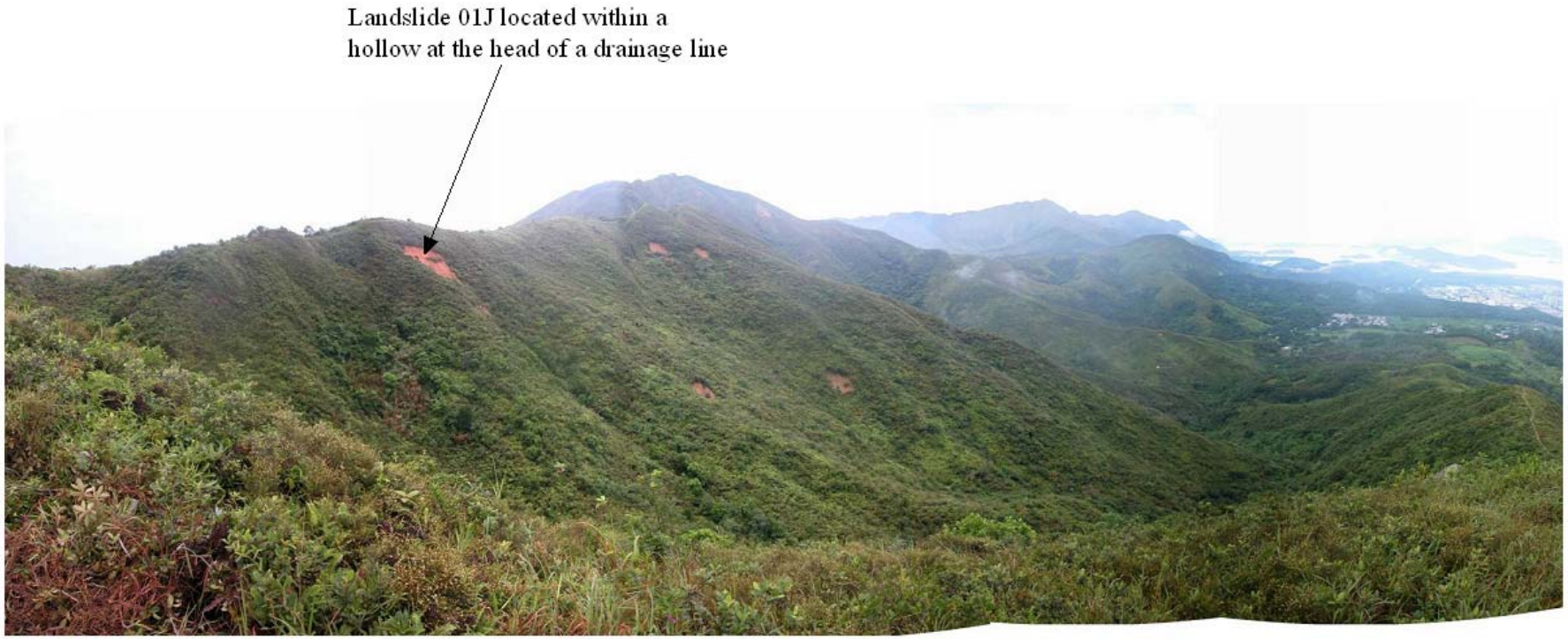

Plate 30 – Geomorphological Setting of a Type II Landslide (01J)

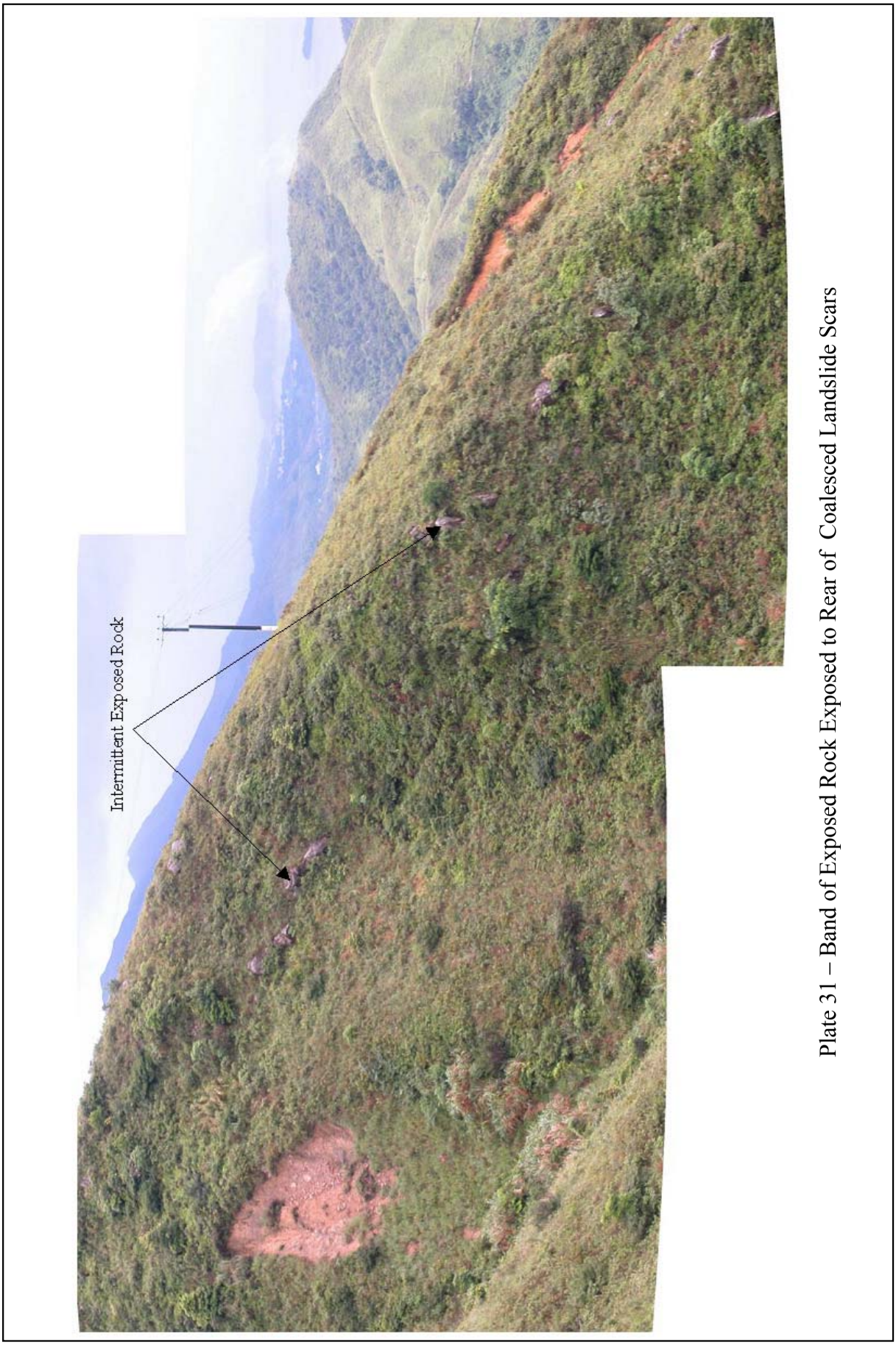

Plate 31 – Band of Exposed Rock Exposed to Rear of Coalesced Landslide Scars